Aus der Klinik für Psychiatrie und Psychotherapie
des Zentralinstituts für Seelische Gesundheit Mannheim
der Medizinischen Fakultät Mannheim
(Direktor: Prof. Dr. med. Andreas Meyer-Lindenberg)

The effect of repetitive transcranial magnetic stimulation and the brain-derived neurotrophic factor genotype on resting-state functional network connectivity.

Inauguraldissertation
zur Erlangung des medizinischen Doktorgrades
der
Medizinischen Fakultät Mannheim
der Ruprecht-Karls-Universität
zu
Heidelberg

vorgelegt von

Philip Post

aus

Heidelberg

2020

Dekan: Herr Prof. Dr. med. Sergij Goerdt
Referent: Herr Prof. Dr. med. Andreas Meyer-Lindenberg

TABLE OF CONTENTS

Page

GLOSSARY

aDMN – anterior default-mode network
ANOVA – analysis of variance
BDNF – brain-derived neurotrophic factor
BOLD – blood-oxygen-level-dependent
DMN – default-mode network
DLPFC – dorsolateral prefrontal cortex
DRD3 - dopaminergic D3 receptors
ECN – executive-control network
EEG – electroencephalogram
EPI – echo-planar imaging
fMRI – functional magnetic resonance imaging
FOV – field of view
IC(s) – independent component(s)
ICA – Independent component analysis
ipDMN – inferior posterior DMN
lECN – left executive control network
met - methionine
PET – positron emission tomography
rECN – right executive control network
RSFC- resting-state functional connectivity
rTMS – repetitive transcranial magnetic stimulation
SLN – salience network
spDMN- superior posterior DMN
TE – echo time
TR – repetition time
val – valine

1. INTRODUCTION

1.1. Functional connectivity

In neuroimaging, functional connectivity refers to the “temporal correlation between spatially remote neurophysiological events” (Friston, Frith, Liddle, & Frackowiak, 1993). Functional connectivity does not necessarily describe anatomical connections of neurons and synapses, which would be referred to as effective or structural connectivity, but rather relates to the fact that certain regions of the brain show correlations in their activity over time and are thus assumed to act in concert (Friston, 1994). It should be noted, that while the synaptic transmissions responsible for effective connectivity usually take place within milliseconds, the fluctuations in neural activity referred to as functional connectivity are observed over timespans of seconds (Friston, 1994). With respect to functional magnetic resonance imaging (fMRI), activation is usually measured via hemodynamic changes, most commonly blood-oxygen-level-dependent (BOLD) signals. Low-frequency co-activations in BOLD-weighted sequences, both at rest and during task performance, have been shown to reflect functional connectivity between spatially independent cortical brain regions (Biswal, Kylen, & Hyde, 1997; Cordes et al., 2001; Damoiseaux et al., 2006; Lowe, Dzemidzic, Lurito, Mathews, & Phillips, 2000). High-frequency co-activations may reflect noise resulting from heart-rate and respiration and must be excluded from functional connectivity analysis (Cordes et al., 2001).

1.1.1. Resting-state functional connectivity

During resting-state fMRI a subject is instructed to lie still, with eyes open or closed, while refraining from any directed cognitive effort. Spontaneous BOLD signal fluctuations in different brain regions observed during resting-state fMRI were initially interpreted as random noise. Biswal and colleagues were the first to demonstrate that the time-series of BOLD activation in the primary motor cortices of subjects during resting-state show a high degree of correlation between the right and left hemispheres (Biswal et al., 1997; Biswal, Yetkin, Haughton, & Hyde, 1995). This observation, coupled with the fact that such networks of baseline connectivity were found to be reproducible and consistent across subjects, hinted at an underlying functional connectivity even between brain regions not currently challenged by a specific task (Damoiseaux et al., 2006; De Luca, Beckmann, De Stefano, Matthews, & Smith, 2006). The networks show a degree of activation and connectivity in the resting-state that is comparable in magnitude to that of task-based activation (S. M. Smith et al., 2009). The correlation in the baseline activity of regions implicated in the same functional networks has been shown to increase when the respective networks are challenged by an appropriate task (Lowe et al., 2000). Similar patterns of neuronal activation have been observed across a variety of different mental states, such as during sleep (Fukunaga et al., 2006; Horovitz et al., 2008), anesthesia (Kiviniemi, Kantola, Jauhiainen, Hyvarinen, & Tervonen, 2003; Peltier et al., 2005; Vincent et al., 2007) and task performance (Arfanakis et al., 2000; Fransson, 2006; Greicius & Menon, 2004) suggesting that these networks of BOLD activation are not merely the result of spontaneous undirected behavior of resting subjects, but rather reflect intrinsic brain activity (Fox & Raichle, 2007). Resting-state functional connectivity may serve as an underlying mechanism for mental processes that are

not directly associated with immediate behavior, such as memory consolidation and rehearsal (Buckner & Vincent, 2007). A key advantage of collecting data in the resting-state is that research or potential diagnostic applications can be extended to patients that are unable to correctly perform mental tasks due to neuropsychiatric disorders such as dementia or acute psychosis (Greicius, 2008). The study of resting-state functional connectivity represents a valuable avenue towards further understanding of the human brain.

1.1.2. Resting-state functional connectivity networks

As described above, the resting brain, unchallenged by specific goal-directed tasks, does not exhibit random activity, but rather reproducible patterns, or networks, of correlating activation and deactivation. These functional connectivity networks have been reproduced in samples of more than 1000 subjects in multiple centers (Biswal et al., 2010). These networks are detectable in infants as young as three years of age and develop with increasing age (C. L. Li, Deng, He, Zhai, & Jia, 2019; Supekar, Musen, & Menon, 2009; Supekar et al., 2010). Spatial characteristics of resting-state networks do not fundamentally differ between male and female individuals (Weissman-Fogel, Moayedi, Taylor, Pope, & Davis, 2010), while age and sex-specific effects on intra- and inter-network connectivity are observable (Allen et al., 2011; Biswal et al., 2010).
A stable set of networks, reproducible in large populations of healthy and mentally ill individuals has become a focus of research into functional connectivity. The specific networks that are most commonly observed during fMRI of resting-state brains have been named in line with their assumed function, based on the tasks and mental states during which increased or decreased intra-network functional connectivity is observed.

Default-mode network (DMN)

Task-related increases in cortical activity, as measured via fMRI or positron emission tomography (PET), have been a focus of functional neuroimaging as they serve as an indicator of the degree to which certain brain regions are involved in specific behaviors and cognitive processes (Raichle, 1998). It has also been observed that certain areas of the brain show decreases in cortical activity during a wide variety of mental tasks (Fox et al., 2005; Fransson, 2006; Gusnard, Raichle, & Raichle, 2001; McKiernan, Kaufman, Kucera-Thompson, & Binder, 2003; Shulman et al., 1997). The consistency with which task-based deactivation occurs in these areas has led to their implication in an organized baseline of brain function, i.e. a default mode, which is suspended during task-directed activity (Raichle et al., 2001).
The default-mode network (DMN) commonly includes the posterior cingulate cortex and the precuneus, the ventral anterior cingulate cortex, the medial prefrontal cortex, the medial temporal lobe, the retrosplenial cortex as well as the hippocampus (Buckner, Andrews-Hanna, & Schacter, 2008; Fox et al., 2005; Greicius, Krasnow, Reiss, & Menon, 2003; Greicius & Menon, 2004; Greicius, Supekar, Menon, & Dougherty, 2009). In a comparative study of fMRI and diffusion tensor imaging, it was found that functional connectivity in the DMN matches structural connectivity (Greicius et al., 2009). Self-referential mental activity and processing of emotions were suggested as core functions of the DMN, due to increased activity in regions belonging to the network during these states (Gusnard, Akbudak, Shulman, &

Raichle, 2001). The DMN has also been implicated in the occurrence of task-unrelated thoughts, which represent intrusive thoughts and unintended cognitions that are a feature of regular cognition as well as a factor in psychiatric disorders such as psychosis and depression (Giambra, 1995). The fact that the occurrence of such stimulus-independent thoughts is reduced by task intensity in a manner similar to the task-based deactivation of the DMN has led to the assumption that the two features are interrelated (Fox et al., 2005).
The theory that the default-mode network of functional connectivity represents a default functional state of the resting brain is supported by various observations: The DMN displays downregulation of activity during the performance of tasks while showing increased activity during resting-state (Greicius et al., 2003; Zuo et al., 2019). The DMN persists during passive sensory processing (Greicius et al., 2003), as well as during executive tasks that are not very challenging (Greicius & Menon, 2004). The degree of DMN-deactivation has been shown to predict performance measurements during working memory tasks, with greater deactivation corresponding to better performance measurements (Anticevic, Repovs, Shulman, & Barch, 2010; White, Jansen, et al., 2013). The DMN does not deactivate homogeneously during task-performance (Leech, Kamourieh, Beckmann, & Sharp, 2011; Piccoli et al., 2015). Some core areas show deactivation irrespective of active task performance, while other areas show a variable degree of deactivation depending on task demands (Mayer, Roebroeck, Maurer, & Linden, 2010).

The feature of the DMN to show decreased activity during active mental tasks has led to it being referred to as a task-negative network. Conversely, networks that show increased activation during mental tasks are referred to as task-positive networks (Fox et al., 2005).

Executive control network (ECN)

The executive control network (ECN), frequently also referred to as the central executive network or frontoparietal control network, is a network displaying increased activity during challenging, attention-related mental tasks, such as working memory, response selection and suppression (Seeley et al., 2007), and goal-directed behavior involving decision making (Menon, 2011).
Consequently, the ECN is referred to as a task-positive network. The ECN consists primarily of regions of the frontal cortex and the parietal neocortex, with key nodes in the dorsolateral prefrontal cortex (DLPFC), the lateral parietal cortex, the dorsomedial frontal cortex and the ventrolateral frontal cortex (Seeley et al., 2007). Connections from the neocerebellum crus I & II to the right and left executive control networks have been described (Habas et al., 2009). Increased activity in these regions during active cognitive tasks has been demonstrated via PET (Mazoyer et al., 2001) as well as fMRI. Performance in executive tasks was found to correlate with the degree of activity in lateral parietal nodes within the ECN (Seeley et al., 2007) and the degree of overall ECN activation (Brown, Schmitt, Smith, & Gold, 2019).

Salience network (SLN)

The salience network (SLN) is represented by correlating activity in the bilateral orbital frontoinsular cortex, the anterior insula, the dorsal anterior cingulate cortex, the paracingulate cortex, and the superior temporal lobe, with connectivity to

subcortical and limbic structures such as the amygdala, the ventral striatum and the ventral tegmental area of the substantia nigra (Seeley et al., 2007). The anterior insula and dorsal anterior cingulate cortex, amongst other regions, have been shown to display increased activity during interoceptive as compared to exteroceptive tasks (Critchley, Wiens, Rotshtein, Ohman, & Dolan, 2004) and in response to the detection of salient stimuli (Sridharan, Levitin, & Menon, 2008). Across studies, the SLN shows increased activity when the subject is concerned with identifying the most homeostatic relevant sensory data, whether they are emotional, cognitive or homeostatic (Seeley et al., 2007). Correspondingly, the SLN is hypothesized to mediate brain functions related to salience, i.e. direction of attention to relevant stimuli (Menon & Uddin, 2010). A positive correlation between SLN functional connectivity in the dorsal anterior cingulate cortex and anxiety measurements before an MRI scan has been shown, while executive function in a cognitive task showed no influence on SLN connectivity (Seeley et al., 2007). Increased activity in the SLN has also been associated with moral cognition (Sevinc, Gurvit, & Spreng, 2017).

The DMN, the ECN, and the SLN are considered as core neurocognitive networks, due to their importance for higher cognitive function (Menon, 2011).
Synchronous BOLD signal fluctuations have also been detected in brain areas associated with sensorimotor and language functions (Cordes et al., 2000). Corresponding resting-state functional connectivity networks have been identified and include visual networks, consisting primarily of areas of the occipital cortex, auditory networks, including parts of the lateral lobes, and sensorimotor networks, with key areas in the pre-and postcentral gyri (Allen et al., 2011; Beckmann, DeLuca, Devlin, & Smith, 2005; Calhoun, Adali, Pearlson, & Pekar, 2001; Damoiseaux et al., 2006).

1.1.3. Inter-network functional connectivity

Further research has demonstrated that functional connectivity networks interact with each other - increased activity in certain networks is consistently matched by either increased or decreased activity in other networks (Fox et al., 2005; Fransson, 2006). This concept is referred to as inter-network connectivity as it relates to effects between different connectivity networks, as opposed to intra-network connectivity which pertains to effects that occur within a specific network. While the former relates to connectivity between entire networks or between nodes belonging to different networks, the latter relates to connectivity between different nodes belonging to the same network. Overall, the correlation between networks or sub-networks associated with similar functional domains, such as default-mode, vision or motor functions, is stronger than the correlation between those associated with different domains (Allen et al., 2011). Dynamic interaction between functional connectivity networks has been demonstrated to vary across individuals and to be behaviorally relevant for attention performance (Kelly, Uddin, Biswal, Castellanos, & Milham, 2008).
The ECN has been shown to anti-correlate with the DMN; the greater the engagement in an active cognitive task, the stronger is the activation of the ECN, while the activation of the DMN decreases (Fox & Raichle, 2007; Fox, Zhang, Snyder, & Raichle, 2009). This anti-correlation, however, is not static and to some degree dependent on the specific mental task, so that co-activation of both networks is possible (Piccoli et al., 2015). Especially tasks that simultaneously involve attention and working-memory functions associated with the ECN and self-referential cognition linked to the DMN require the activation of both networks (Menon, 2011). In fact,

distinct sub-networks of the DMN show characteristic patterns of inter-network connectivity (S. M. Smith et al., 2012), and some sub-networks of the DMN and the ECN are positively correlated during resting-state (Allen et al., 2011; Manoliu et al., 2013; Manoliu et al., 2014).
Finally, the SLN has been shown to be involved in switching between the DMN and the ECN in response to changes in task demands and stimulus modalities (Goulden et al., 2014; Sridharan et al., 2008). Thus, the SLN is thought to be involved in the generation of behavioral responses to salient stimuli by engaging the ECN and disengaging the DMN if the detected stimulus requires externally oriented attention (Menon, 2011).

1.1.4. Analysis of functional connectivity via independent component analysis

Beckmann and colleagues were the first to use probabilistic independent component analysis (ICA) to identify connectivity networks from spontaneous BOLD fluctuations (Beckmann et al., 2005). ICA is a technique for data analysis that allows separating a time-series of a dependent variable; in this case, the time-series of signal intensities in a set of voxels into underlying components consisting of independent spatial maps with associated time-courses (Bell & Sejnowski, 1995). This method in its basic form is not an ideal approach for drawing group inferences from fMRI data; as ICA decomposes each data set into the components that are best suited to explain the observed variance, components may vary across subjects, which impede direct comparisons between subjects. Calhoun and colleagues have developed a modified ICA process for drawing group inferences resulting in one set of independent components across all subjects in a sample (Calhoun et al., 2001). This method is the basis of the analysis software used in this thesis.
For fMRI data, ICA is a robust and effective tool for the identification of low-frequency activity patterns, such as functional connectivity networks (Beckmann et al., 2005; De Luca et al., 2006). ICA is a “data-driven” rather than “hypothesis-driven” method for data analysis. It allows for the detection of multiple networks instead of showing only those correlations that are specifically searched for, as is the case for seed-based methods (De Luca et al., 2006). Seed-based analysis requires the hypothesis-based a-priori selection of regions of interest, as the individual analysis of the thousands of voxels constituting an fMRI scan would result in a prohibitively large number of possible effects. Changes in connectivity can then only be detected between the seeds, while effects outside of the regions of interest remain hidden. ICA allows for the discovery of effects not specifically searched for, by including all voxels from the dataset when generating the ICs.
A further advantage of ICA is that a large proportion of noise signals are routinely grouped as separate components, which can easily be excluded from further statistical analysis (Beckmann et al., 2005). This is mainly because head movements, vascular processes, and respiratory and cardiac artifacts show frequency spectra that are sufficiently different from those of the BOLD signal and are therefore easily detected by the ICA algorithm. It has been demonstrated that ICA can detect functional connectivity networks at least as well as standard seed-based analysis (Greicius & Menon, 2004).
Common algorithms for ICA require the a-priori definition of the number of independent components (ICs) that should be assumed to underlie the observed variation in the data set. For example, it is possible to decompose the spontaneous BOLD fluctuations of a given data set into 20 ICs, 50 ICs or 70 ICs. Low numbers of ICs may result in the grouping of multiple functional connectivity networks, or

functional connectivity networks and unrelated noise signals, into a single IC. In this case, information is lost, as relevant interactions between different networks may remain hidden. Conversely, the selection of a large number of ICs may result in coherent networks being subdivided into multiple ICs, which could obscure information on the interaction between and within extensive functional connectivity networks.
The decomposition of resting-state fMRI data into 70 ICs has, for example, resulted in the detection of as many as two (S. M. Smith et al., 2009) or four (Allen et al., 2011) DMNs and six different attentional networks (Allen et al., 2011), each encompassing parts of the overall network. It has been shown that the decomposition into 20 ICs as compared to 70 ICs resulted in the detection of 3 and 8 visual networks, respectively, with the latter networks representing either left-right-hemisphere subdivisions or, more commonly, divisions into sub-functions (Allen et al., 2011). The heterogeneity of numbers of ICs across studies reduces the comparability of results.
The need for a large number of IC for detection of all networks and noise components, therefore, has to be balanced with the aim of identifying all relevant functional connectivity networks.
ICA serves as a valuable method in the analysis of inter-network connectivity. Jafri and colleagues were the first to evaluate inter-network connectivity via correlation analysis of IC time-courses (Jafri, Pearlson, Stevens, & Calhoun, 2008). The temporal relationships of connectivity fluctuations within resting-state networks can be considered as a measure of the degree of connectivity between the networks. This approach has been utilized in several publications (Doll, Holzel, Boucard, Wohlschlager, & Sorg, 2015; Manoliu et al., 2013; Manoliu et al., 2014; Oldehinkel et al., 2019) and serves as the basis for the analysis of inter-network connectivity in this investigation.

1.1.5. Resting-state functional connectivity networks in schizophrenia and depression

Abnormalities in intra- and inter-network functional connectivity observed in patients suffering from psychiatric disorders have been synthesized into models of psychopathology following the presumed function of the networks. Aberrant network connectivity, especially within and between the DMN, SLN, and ECN, has been identified as a tool to gain insight into dysfunctional brain architecture underlying psychiatric disorders (Menon, 2011).

In line with the DMNs role in self-referential cognition, an aberrant increase in DMN connectivity has been linked to increased interoception and dysfunctional negative cognitions in affective disorders (Kaiser, Andrews-Hanna, Wager, & Pizzagalli, 2015; Sheline et al., 2009) as well as preoccupation with internally generated stimuli, such as hallucinations, and impaired information processing in psychosis (Anticevic et al., 2012; Buckner et al., 2008; Zhou et al., 2007). Individuals suffering from schizophrenia have repeatedly been shown to display increased connectivity in the DMN (Harrison, Yucel, Pujol, & Pantelis, 2007; Salvador et al., 2010; Whitfield-Gabrieli et al., 2009; Zhou et al., 2007), a finding which extends to their unaffected siblings (Liu et al., 2012). Overactivity of the DMN has been shown to correlate with the intensity of positive clinical symptoms, such as hallucinations and delusions (Garrity et al., 2007). Insufficient DMN suppression during cognitive tasks has also

been observed in patients with schizophrenia (Anticevic, Repovs, & Barch, 2013) and their unaffected siblings (de Leeuw, Kahn, Zandbelt, Widschwendter, & Vink, 2013).
A meta-analysis performed in 2015 identified hyperconnectivity within the DMN as a characteristic resting-state network dysfunction in major depressive disorder (Kaiser et al., 2015). Functional connectivity between nodes of the DMN has consistently been found to be significantly increased in patients suffering from depression (Greicius et al., 2007; Liston et al., 2014). These changes in intra-network connectivity within the DMN are associated with a stronger presentation of depressive cognitions (Zhu et al., 2012) and become more pronounced during tasks involving emotional processing (Grimm et al., 2009).
Increased connectivity within the DMN represents a common characteristic of schizophrenia and major depressive disorder and is linked to symptom severity in both.

Dysfunction of the ECN has been associated with psychiatric disorders that show altered cognitive control. Deficits in executive cognitive functions, especially concerning attention and planning performance, are a central symptom in schizophrenia already detectable in patients at first onset of the disorder (Chan, Chen, & Law, 2006). Reduced connectivity within the ECN has indeed been described in patients suffering from schizophrenia both at rest (Baker et al., 2014; Tu, Lee, Chen, Li, & Su, 2013) and during working-memory task performance (Anticevic et al., 2013). Connectivity between nodes of the ECN is also reduced in patients suffering from major depressive disorder (Kaiser et al., 2015; Liston et al., 2014). Hypoactivity of the DLFPC within the left ECN was found to correlate negatively with the severity of depressive symptoms (Dong et al., 2019).
In contrast to the previously outlined hyperconnectivity of the DMN, within the ECN, hypoconnectivity represents a commonality between schizophrenia and depression and has been associated with aggravated symptoms in both disorders.

Dysfunction within the SLN and altered connectivity of the SLN to the DMN have been associated with the inability to shift attention away from pathological cognitive processes (Hare et al., 2019), resulting in anxiety (Geng, Li, Chen, Li, & Gu, 2015) and increased rumination (R. Zhang & Volkow, 2019). Decreased connectivity within the SLN is associated with increased severity of hallucinations in schizophrenia (Manoliu et al., 2014) and has been linked to depressed mood and reduced quality of life (Ohta et al., 2018). Dysregulation of the SLN in patients with schizophrenia during a task featuring high- and low-salience stimuli has also been reported, with SLN activity not being influenced by the level of salience, contrary to findings in healthy individuals (White, Gilleen, & Shergill, 2013).
For major depressive disorder, decreased connectivity of the right insula within the SLN was associated with greater severity of depressive symptoms (Manoliu et al., 2013).
Similar to the observations reported for the ECN, the SLN also features reduced connectivity in both schizophrenia and major depressive disorder.

Findings of altered connectivity concerning the DMN, the ECN and the SLN in psychiatric disorders have not only been observed within each network but also extend to the way whole networks interact with each other. While observations regarding intra-network connectivity generally point in the same direction in both disorders, i.e. hyperconnectivity within the DMN and hypoconnectivity within the ECN

and the SLN, substantial differences can be observed regarding inter-network connectivity.
In patients with schizophrenia, connectivity between nodes of the DMN and the ECN was found to be increased (Salvador et al., 2010) and the severity of hallucinations in schizophrenic patients with psychosis has been shown to relate to increased connectivity between the ECN and the DMN (Manoliu et al., 2014). In contrast, decreased connectivity between the DMN and the ECN has been reported in major depressive disorder (Manoliu et al., 2013) and has been discovered to be state-independent, present in both current and remitted patients (Dong et al., 2019). Findings in late-life depression differ somewhat, with patients displaying decreased connectivity between the ECN and subcortical components of the DMN, while connectivity between the left ECN and posterior components of the DMN was found to be increased (W. Li et al., 2017). A meta-analysis performed in 2015 reported hyperconnectivity between some nodes of the ECN and the DMN as characteristic in major depressive disorder (Kaiser et al., 2015).
Reduced connectivity between the DMN and the SLN has been linked to the intensity of both positive and negative symptoms in schizophrenia (Hare et al., 2019), while increased connectivity between the SLN and the DMN has been observed in major depressive disorder (Manoliu et al., 2013). Increased connectivity between the SLN and the right ECN may reliably differentiate healthy individuals from patients with major depressive disorder (Dong et al., 2019).
The study of inter-network connectivity offers complementary insights that allow differentiating between these two major psychiatric disorders.

Even before the analysis of functional connectivity was broadly applied, the field has launched first attempts to directly modulate neuronal activity. The discovery of stable functional networks that are implicated in a multitude of physiological and pathological cognitive processes opened a wide array of potential targets where the selective modulation of connectivity could yield considerable therapeutic effects. One established and extensively studied approach is transcranial magnetic stimulation, outlined in detail below.

1.2. Repetitive transcranial magnetic stimulation (rTMS)

1.2.1. Mechanism of action of rTMS and its effects on neuronal plasticity

Magnetic stimulation was introduced in 1985 as a pain-free, non-invasive and easy-to-use procedure, allowing for transcranial application of stimuli to the human motor cortex (Barker, Jalinous, & Freeston, 1985). By application of a rapidly changing electric current to a coiled wire, a magnetic field can be produced. This magnetic field can be used to indirectly activate corticospinal neurons, via modulation of synaptic inputs (Hallett, 2000). This stimulation can be used to selectively target brain areas associated with specific functions: A stimulus to the occipital lobe results in a temporary scotoma (Amassian et al., 1989) and a stimulus to the V5 area of the visual cortex can cause impairment of motion perception (Beckers & Zeki, 1995). Stimulation of the motor cortex results in a motor evoked potential in the associated peripheral muscle. Single-pulse TMS is routinely used in neurology for diagnostic applications, such as measuring central motor conduction time in spinal pathologies (Brunholzl & Claus, 1994).
Transcranial magnetic stimulation with a train of pulses is known as repetitive TMS or rTMS. If pulse frequencies above 1Hz are utilized, it is usually referred to as high-

frequency rTMS. rTMS can cause increases in cortical excitability which can last for minutes and can cause epileptic seizures in healthy individuals, especially when applied during long stimulation periods with high pulse frequencies and intensities above the threshold for evoking motor potentials (Wassermann, 1998). Guidelines for maximum stimulation duration at certain frequencies and intensities have been published, as the risk for epileptic seizures is considered lower in association with sub-threshold stimulation intensities (Wassermann, 1998). As with single-pulse TMS, rTMS can be employed to selectively target brain areas associated with different neurological functions and to impair associated performance. This effect has been demonstrated for 15-20Hz rTMS of the motor cortex, which results in accuracy errors in finger movement sequences (Gerloff, Corwell, Chen, Hallett, & Cohen, 1997), and for 25Hz rTMS of the left inferior frontal region which causes speech arrest (Pascual-Leone, Gates, & Dhuna, 1991).
However, rTMS not only produces temporary “lesions” during stimulation in the affected cortical regions but also longer-lasting effects directly related to neuronal plasticity. Neuronal plasticity refers to lasting changes in synaptic strength in response to experience or injury and involves processes such as long-term potentiation and long-term depression, which represent increases and decreases in synaptic efficacy, respectively. rTMS with frequencies of 5Hz and above are associated with an increase in cortical excitability and a decrease in cortical inhibition (Fitzgerald, Fountain, & Daskalakis, 2006; Lee, Siebner, & Bestmann, 2006), and frequencies of 1Hz result in inhibitory effects on cortical neurons (Lee et al., 2006). As effects of rTMS on cortical excitability have been shown to outlast the stimulation period by at least 30 minutes (Peinemann et al., 2004), long-term potentiation and long-term depression have been advanced as plausible underlying mechanisms (Huerta & Volpe, 2009; H. Wang, Wang, & Scheich, 1996). However, interindividual differences up to opposite effects on cortical excitability in response to identical rTMS protocols have been reported (Gangitano et al., 2002).

1.2.2. Therapeutic applications of rTMS over the DLPFC

The ability of rTMS to modulate brain function in a non-invasive and low-risk manner has led to medical trials to study its potential therapeutic application in psychiatric and neurological disorders. The greatest amount of research has been dedicated to its effect in depressive disorders where the therapeutic potential of rTMS was first demonstrated. High-frequency rTMS of the left DLPFC on five consecutive days resulted in a significant amelioration of symptoms for at least two weeks in a majority of patients without significant side-effects (Pascual-Leone, Rubio, Pallardo, & Catala, 1996). Both high frequency (>5Hz) rTMS of the left DLPFC and low frequency (<5Hz) rTMS of the right DLPFC have shown similar antidepressant effects in patients with major depressive episodes (Cao, Deng, Su, & Guo, 2018). Cognitive enhancing effects of DLPFC rTMS have also been demonstrated in these patients (Iimori et al., 2019; Martin, McClintock, Forster, Lo, & Loo, 2017). rTMS is a more cost-effective therapy than electroconvulsive therapy for treatment-resistant depression (Zhao et al., 2018) In the United States, FDA approval for rTMS as a treatment of major depressive episodes has been granted in 2011 (Food and Drug Administration, 2011).
rTMS has also been evaluated as a treatment for patients with schizophrenia. A meta-analysis of rTMS effects on symptom dimensions in schizophrenia found a positive treatment effect for auditory hallucinations and negative symptoms, but also some evidence for possible adverse effects involving worsening of positive

symptoms, especially after stimulation of the right DLPFC (Kennedy, Lee, & Frangou, 2018). A meta-analysis from 2018 reported the superiority of rTMS over sham treatment for the amelioration of negative symptoms in patients with schizophrenia (Osoegawa et al., 2018). Concerning cognitive deficits in schizophrenia, a recent meta-analysis showed that rTMS of the DLPFC produces long-lasting improvements in working-memory and language function (Jiang et al., 2019). Evidence for positive rTMS effects in clozapine-resistant schizophrenia has also been reported (Wagner et al., 2019). However, a recent meta-analysis of rTMS effects in treatment-resistant schizophrenia does not support an effect on total, positive or negative symptoms in this population (Siskind et al., 2019).
There is also some evidence that rTMS might serve as a treatment option for other psychiatric disorders, such as post-traumatic stress disorder and generalized anxiety disorder (Cirillo et al., 2019), substance abuse and eating disorders (Song, Zilverstand, Gui, Li, & Zhou, 2019), autism spectrum disorder (Barahona-Correa, Velosa, Chainho, Lopes, & Oliveira-Maia, 2018), obsessive-compulsive disorder (Rehn, Eslick, & Brakoulias, 2018) as well as Tourette syndrome (Hsu, Wang, & Lin, 2018). In addition, potential therapeutic applications of rTMS extend to neurological disorders such as chronic pain, Parkinson's disease, focal epilepsy, and to aiding recovery after strokes (Fregni & Pascual-Leone, 2007; Hallett, 2000; Seminowicz, de Martino, Schabrun, & Graven-Nielsen, 2018).
Overall, rTMS represents a non-pharmaceutical, non-invasive approach to the modulation of brain function with reliable evidence for therapeutic effects in a variety of psychiatric and neurological disorders (Hauer et al., 2019). The mechanisms of action underlying the therapeutic effects of rTMS are however still a subject of active research. One area of interest is the modulation of functional connectivity via rTMS.

1.2.3. The influence of rTMS over the DLPFC on functional connectivity

As outlined above, the DLPFC represents a key network node of the ECN and is involved in executive cognitive processes. Furthermore, rTMS over the DLPFC has been shown to produce a variety of pro-cognitive effects in patients suffering from depression and schizophrenia. The DLPFC is easily accessible on the scalp for stimulation, and the duration of specific rTMS effects was estimated to last up to 30 minutes post-stimulation (Tik et al., 2017). In several studies, the DLPFC was successfully stimulated at a location 5 cm anterior to the hot spot for motoric effects of stimulation (Dang, Avery, & Russo, 2007; Esslinger et al., 2014; Pascual-Leone et al., 1996). Superior effects were reported for individually adjusted locations of the DLPFC using fMRI based neuronavigation (Fitzgerald et al., 2009). The combination of rTMS and neuroimaging techniques has enabled the investigation of stimulation effects on network dynamics by studying local and remote changes in functional connectivity (Reithler, Peters, & Sack, 2011).
Regarding local effects, 5 Hz rTMS stimulation of the DLPFC at intensities below the active motor threshold did not lead to changes in DLPFC activation (Esslinger et al., 2014; Rounis et al., 2006). 1Hz rTMS at higher intensities, i.e. intensities at the level of the motor threshold, produced mixed effects (X. Li et al., 2004; Nahas et al., 2001; van der Werf, Sanz-Arigita, Menning, & van den Heuvel, 2010). In contrast, there is ample evidence that DLPFC stimulation leads to changes in the connectivity of the DLPFC with other areas involved in the ECN as wells as with nodes of other resting-state networks. Low-frequency 1Hz rTMS of the left DLPFC has been found to reduce connectivity within the DMN in healthy subjects (van der Werf et al., 2010). Normalization of hyperconnectivity within the DMN has also been observed following

10Hz rTMS over the left DLPFC in patients with depression (Liston et al., 2014). 10Hz rTMS of the right DLPFC led to an increase in connectivity within the SLN, while stimulation of the left DLPFC produced an opposite effect (Schluter, Jansen, van Holst, van den Brink, & Goudriaan, 2018). In a combined task- and resting-state fMRI study, the application of 5Hz high-frequency rTMS of the right DLPFC resulted in decreased functional connectivity between the right DLPFC and the left hippocampus, which is part of the DMN, during a working-memory task, but no rTMS effects on resting-state functional connectivity (Bilek et al., 2013). Inhibitory continuous theta-burst rTMS over the left DLPFC has also been shown to reduce resting-state functional connectivity between the left DLPFC and brain regions involved in the DMN without directly changing activity in these areas (Shang et al., 2019). 5Hz rTMS of the left DLPFC has been found to decrease connectivity between nodes of the DMN and the SLN in patients suffering from major depressive disorder and posttraumatic stress disorder and this change was associated with symptom reduction (Philip et al., 2018). 10Hz excitatory rTMS over the left DLPFC has been shown to induce anticorrelated activity, i.e. segregation, between the DMN and the ECN, while not directly affecting connectivity within the ECN (Liston et al., 2014), and to increase connectivity between nodes of the ECN and the SLN (Tik et al., 2017).
rTMS of the DLPFC has been reported to influence inter-network connectivity between the ECN, DMN, and SLN as well as intra-network connectivity in the DMN and SLN in healthy subjects. These effects add to the findings of the therapeutic effects of rTMS in patients with depression (Liston et al., 2014; Philip et al., 2018; Tik et al., 2017). However, differences in stimulation protocols impair the comparability of results and could explain discrepancies in the observed effects on functional connectivity.
Regarding 5Hz rTMS of the right DLPFC, only one study has investigated changes in functional connectivity between nodes of different networks and found no stimulation effects on connectivity during the resting-state (Bilek et al., 2013).
Further research is needed to enable a better understanding of the effect of rTMS on functional connectivity and to identify factors that are involved in interindividual differences with respect to therapeutic response to rTMS. As rTMS has been shown to influence neuronal plasticity, other elements that impact this mechanism are relevant targets for further research. The genotype for the brain-derived neurotrophic factor represents one such element. A common polymorphism of this genotype has been shown to influence neuronal plasticity, presentation of psychiatric disorders, functional connectivity, and therapeutic response to rTMS.

1.3. The Brain-Derived Neurotrophic Factor (BDNF)

1.3.1. Biological structure and function

The Brain-Derived Neurotrophic Factor (BDNF) is a protein from the neurotrophin family of growth factors. It was first isolated and described as a protein involved in the survival and growth of neurons by Barde, Edgar and Thoenen in 1982 (Barde, Edgar, & Thoenen, 1982). BDNF binds to the p57 neurotrophin receptor, as do all members of the neurotrophin family, as well as the TrkB [Tropomyosin-related kinase B] receptor (Barbacid, 1995; Soppet et al., 1991; Squinto et al., 1991).
Analysis of BDNF mRNA expression in the brain of adult rats has shown that the BDNF gene is expressed in the entire brain with the highest concentrations of the corresponding mRNA in the hippocampus followed by the cerebral cortex (Hofer, Pagliusi, Hohn, Leibrock, & Barde, 1990). BDNF expression was found to be higher

in adult rat brains compared to developing brains with levels being lowest in embryonal rat brains (Maisonpierre et al., 1990). The levels of BDNF have also been shown to vary during brain development across different brain regions (Katoh-Semba, Takeuchi, Semba, & Kato, 1997). In humans, regional BDNF mRNA expression was reported to change over the lifespan (Webster, Herman, Kleinman, & Shannon Weickert, 2006; Webster, Weickert, Herman, & Kleinman, 2002).
BDNF expression is influenced by neuronal stimuli, such as osmotic stimulation of the hypothalamus (Castren, Thoenen, & Lindholm, 1995), optical stimulation of the visual cortex (Castren, Zafra, Thoenen, & Lindholm, 1992), electrical stimulation of the hippocampus (Castren et al., 1993; Patterson, Grover, Schwartzkroin, & Bothwell, 1992) as well as in response to neuronal damage (Ballarin, Ernfors, Lindefors, & Persson, 1991; Lindvall et al., 1992), epileptic seizures (Dugich-Djordjevic et al., 1992; Ernfors, Bengzon, Kokaia, Persson, & Lindvall, 1991), immobilization stress (M. A. Smith, Makino, Kvetnansky, & Post, 1995) and physical exercise (Neeper, Gomez-Pinilla, Choi, & Cotman, 1995).
Moreover, it has been demonstrated that BDNF is involved in regulating the proliferation and survival of cells and influences synaptic growth in mammals, including humans (Hariri et al., 2003). In rats, BDNF infused in the brain supports the survival of axotomized neurons (Morse et al., 1993). Long-term potentiation, a mechanism of synaptic plasticity resulting in increased synaptic strength, is impaired in BDNF knock-out mice (Korte et al., 1995), with the administration of recombinant BDNF being able to repair this deficit (Patterson et al., 1996). Levels of BDNF in brain tissue decrease with increasing age in humans, especially in the hippocampus (Hattiangady, Rao, Shetty, & Shetty, 2005) which could be linked to age-related cognitive impairment (Mattson & Magnus, 2006).
These findings have led to the hypothesis that BDNF plays a role in directing growth, differentiation and survival of neurons, especially of peripheral sensory and brain neurons (Hong, Liou, & Tsai, 2011; Jones, Fariñas, Backus, & Reichardt, 1994; Webster et al., 2006).

1.3.2. The val^{66}met polymorphism in the gene for BDNF

The gene for BDNF in humans is located on chromosome 11p13 and contains 11 exons (Pruunsild, Kazantseva, Aid, Palm, & Timmusk, 2007). The most frequent and most extensively-studied nonconservative single nucleotide polymorphism mutation in the BDNF gene in humans is located at nucleotide 196 and consists of a substitution of methionine for valine in codon 66 (Egan et al., 2003). As the polymorphism occurs in the pro-region of the BDNF-gene, it is unlikely to directly influence the biological function of the BDNF polypeptide since the structure of the protein is not altered. However, the mutation has been found to influence secretion and intracellular trafficking of BDNF (Chen et al., 2004; Egan et al., 2003).
In vitro, the val^{66}met substitution influences the release of BDNF in response to neuronal activity with the methionine variant resulting in reduced secretion. At the same time, secretion in the absence of neuronal activity is not influenced by the substitution (Egan et al., 2003). In rats, a met^{66}met genotype is associated with a reduction in the activity-dependent secretion of BDNF, while baseline expression of the gene is not changed (Chen et al., 2006). In adult mice, the met^{66}met genotype is related to significantly lower concentrations of BDNF in hippocampal tissue (Bath et al., 2012).
The val^{66}met polymorphism has been shown to influence hippocampal synaptic activity in humans (Egan et al., 2003). The presence of a methionine allele is

associated with poorer episodic memory (Cathomas, Vogler, Euler-Sigmund, de Quervain, & Papassotiropoulos, 2010; Egan et al., 2003), and a stronger rate of decline in skilled task performance (Sanchez et al., 2011). Methionine allele carriers were also found to display reduced corticospinal output and reduced size of motor map areas in response to a period of motor training compared to val^{66}val homozygotes (Kleim et al., 2006).
The distribution of the BDNF val^{66}met genotype varies across populations of different ethnicity. The frequency of the met^{66} allele is estimated as 41.1% in Japanese (Itoh, Hashimoto, Kumakiri, Shimizu, & Iyo, 2004), 29.7% in Italian (Ventriglia et al., 2002) and 18.0% in US-American (Egan et al., 2003).

1.3.3. The influence of BDNF genotypes in psychiatric disorders

The role of BDNF in neural plasticity has led to the assumption that the BDNF val^{66}met genotype might represent a risk factor for the development of psychiatric disorders, especially for psychotic and affective symptoms, but findings are mixed. However, a substantial number of studies suggest an effect of the BDNF genotype on the presentation and course of a variety of psychiatric disorders, including schizophrenia and major depressive disorder.

A causal connection between the BDNF genotype and susceptibility for schizophrenia could not be established as the evidence so far has been mixed:
A meta-analysis performed in 2007 reported an association between the val^{66}met genotype and schizophrenia, in particular, an increase in risk of 19% in the homozygous carriers (Gratacos et al., 2007). Conversely, another meta-analysis performed in 2007 reported a lack of an association between the genotype for the val^{66}met polymorphism and schizophrenia (Kanazawa, Glatt, Kia-Keating, Yoneda, & Tsuang, 2007). A lack of linkage or linkage disequilibrium between BDNF genotype and schizophrenia has been reported in an Irish population (Hawi et al., 1998) and a Japanese population (Sasaki et al., 1997).
Multiple, although heterogeneous findings of an effect of the BDNF genotype on clinical characteristics of schizophrenia have been reported:
While the BDNF genotype does not seem to influence age at onset in schizophrenia by itself, an interaction between the genotype for BDNF and the ser^{9}gly polymorphism in the gene for dopaminergic D3 receptors [DRD3] has been reported, with an earlier age at onset by 3 years in patients that were met^{66} carriers for BDNF and ser^{9}ser homozygotes for DRD3 (Gourion et al., 2005). In a sample of patients suffering from schizophrenia, their siblings and healthy controls, met^{66}met homozygous carriers scored lower on a verbal episodic memory test than val^{66}met and val^{66}val carriers, independent of diagnostic status (Egan et al., 2003). In another study involving patients with schizophrenia and healthy subjects, met^{66} carriers showed poorer verbal memory performance independent of diagnostic status, while visuospatial abilities were impaired only in met^{66}-carrying patients (Ho et al., 2006). On the other hand, in a sample of patients with schizophrenia and their relatives, met^{66} carriers were found to score higher on some domains of an IQ test than val^{66}val homozygotes (Vyas & Puri, 2012). Performance in a prefrontal cognition task was not related to the BDNF val^{66}met genotype in patients with schizophrenia, while performance in an n-back task was better in val^{66}val homozygotes (Rybakowski, Borkowska, Skibinska, Szczepankiewicz, et al., 2006). Executive functioning in patients with schizophrenia was described to be impaired in met^{66} carrier; however, this finding only applied to male individuals (Lu et al., 2012). In female patients, the

presence of the valine allele was associated with more severe psychopathology and poorer scores in some measures of neurocognitive functioning, while no such effects were observed in males (Kim et al., 2016). Another study observed no influence of the BDNF genotype on cognitive factor scores in patients with schizophrenia, but an increased severity of negative symptoms was detected in met^{66} carriers (Mezquida et al., 2016). Deficits in performance on attentional tasks were also noted in patients with schizophrenia that were met^{66} carriers (X. Y. Zhang et al., 2012).
A meta-analysis performed in 2015 on the relationship between the BDNF genotype and neurocognitive functioning in patients with schizophrenia discovered no significant effect of the genotype on most neurocognitive domains; however, significant correlations between peripheral serum levels of BDNF and ability for reasoning as well as problem-solving were reported, with higher peripheral BDNF levels corresponding to better performance (Ahmed, Mantini, Fridberg, & Buckley, 2015).
Concerning treatment response, val^{66}val homozygote patients with schizophrenia exhibit a better response to treatment with the antipsychotic agent Olanzapine (Nikolac Perkovic et al., 2014) and met^{66}met homozygotes were at least four times as likely as val^{66} carriers to exhibit treatment resistance to antipsychotic pharmacotherapy (J. P. Zhang et al., 2013).

The BDNF val^{66}met genotype has also been found to influence the clinical presentation of affective disorders.
A meta-analysis performed in 2010 on the effects of the BDNF genotype on the susceptibility for depression reported no genotype effect in women, while the presence of a met^{66} allele in men was associated with a significantly increased risk for major depressive episodes (Verhagen et al., 2010). Overall, major depressive disorder was not linked with the val^{66}met polymorphism in European and Asian populations in a meta-analysis performed in 2016 (M. Li, Chang, & Xiao, 2016).
In bipolar disorder, the val^{66}val genotype is associated with both an earlier age of onset of the disease and better performance in a prefrontal cognition test, compared to the val^{66}met genotype (Rybakowski, Borkowska, Czerski, Skibinska, & Hauser, 2003; Rybakowski, Borkowska, Skibinska, Szczepankiewicz, et al., 2006). Studies in individuals with bipolar disorder have also shown a preferential transmission of the val^{66} allele in adults (Neves-Pereira et al., 2002; Sklar et al., 2002), as well as children and adolescents (Geller et al., 2004). However, these findings were described in Caucasian populations and two studies of Asian populations failed to replicate the association between BDNF genotype and bipolar disorder (Kunugi et al., 2004; Nakata et al., 2003). There is evidence of an association between the val^{66} allele and a lower age of onset and impaired neurocognitive function in patients with bipolar disorder (Rybakowski, Borkowska, Skibinska, & Hauser, 2006).
A meta-analysis performed in 2007 did not suggest a relationship between the val66met genotype and the susceptibility for bipolar disorder (Kanazawa et al., 2007), a finding which was also reported in a meta-analysis from 2014 (Z. Wang, Li, Gao, & Fang, 2014). However, a more recent meta-analysis showed a significant association of the val^{66} allele with bipolar disorder in populations of European but not those of Asian descents (M. Li et al., 2016).

1.3.4. The influence of BDNF genotypes on functional connectivity

The BDNF gene polymorphism val^{66}met has also been associated with changes in functional connectivity. Since studies involving resting-state functional connectivity

are scare, the overview given below includes results from studies featuring active mental tasks.
Met^{66} carriers showed increased functional connectivity between key nodes of the ECN and the SLN, both in the resting-state (C. Wang, Zhang, et al., 2014) as well as during a task involving executive functions (Schweiger et al., 2019). In contrast, met^{66} carriers showed decreased connectivity between areas belonging to the SLN and the DMN in a task on facial emotion recognition (Mukherjee et al., 2011). Likewise, resting-state functional connectivity was reduced within the ECN and the DMN in children and adolescents carrying the met^{66} allele, while functional connectivity was increased in a paralimbic network incorporating key nodes of the SLN (Thomason, Yoo, Glover, & Gotlib, 2009). Connectivity between central nodes of the DMN during an episodic memory task was greater for val^{66} homozygotes, compared to met^{66} carriers (Fera et al., 2013). Resting-state connectivity between the hippocampus and the cerebellum was reduced in healthy met^{66} carriers, while met^{66} carriers suffering from late-onset depression showed decreased connectivity between the hippocampus and the temporal cortex (Yin, Hou, Wang, Sui, & Yuan, 2015).
Met^{66} carriers also showed reduced hippocampal involvement during both encoding and retrieval of memories (Hariri et al., 2003) as well as poorer episodic memory (Egan et al., 2003). Others reported a corresponding reduction of hippocampal grey matter volume (Pezawas et al., 2004) as well as abnormal hippocampal activity in fMRI (Egan et al., 2003).
These findings suggest an effect of BDNF polymorphism on functional connectivity networks. Interestingly, the pattern of alterations observed in met^{66} carriers seems to be directly opposite to that observed in patients suffering from schizophrenia and major depressive disorder.
Since both BDNF genotype and rTMS are directly involved in the modulation of neuronal plasticity, further knowledge about their direct interaction is warranted.

1.3.5. The influence of BDNF genotype on the effects of rTMS

Considering the therapeutic effects of rTMS in a variety of psychiatric disorders and the evidence linking the BDNF genotype with certain characteristics of these disorders, research into the influence of the BDNF genotype of the effects of rTMS has been performed.
The aftereffect of both inhibitory and faciliatory 1Hz rTMS of the dominant motor cortex on corticospinal excitability, as measured via amplitudes of motor evoked potentials, was found to be lower in met^{66} carriers, suggesting that these individuals are less susceptible to the effects of rTMS (Cheeran et al., 2008). Influence of the BDNF genotype on motor-evoked potentials after rTMS of the non-dominant primary motor cortex has been reported, with val^{66}val homozygotes differing from met^{66} carriers in their response to sub- and supra-threshold 10Hz rTMS (Hwang, Kim, Yoon, Uhm, & Chang, 2015).
The response to left DLPFC 1Hz and 17Hz rTMS in patients suffering from depression is significantly greater in individuals with the val^{66}val homozygote genotype for the BDNF gene (Bocchio-Chiavetto et al., 2008). A better clinical outcome in val^{66}val homozygous patients with treatment-resistant major depression, receiving a combined treatment consisting of right dorsolateral prefrontal cortex 1Hz rTMS and therapeutic sleep deprivation, has been reported (Krstic et al., 2014).

While interactions between BDNF genotype and rTMS effects have been demonstrated, and while both are known to influence functional connectivity, their

interactive effects on functional connectivity have not yet been investigated. This study seeks to fill this gap in knowledge.

1.4. Objectives

This investigation seeks to determine the effect of repetitive transcranial magnetic stimulation (rTMS) of the right dorsolateral prefrontal cortex (DLPFC) on resting-state functional connectivity networks, as observed via independent component analysis (ICA) of functional magnetic resonance imaging (fMRI) data, and the degree to which the val^{66}met polymorphism in the gene for the brain-derived neurotrophic factor (BDNF) influences rTMS effects. Changes in functional connectivity are evaluated between the default-mode network (DMN), the salience network (SLN) and the executive control network (ECN). These networks were selected based on their well-documented role in higher cognitive functioning and their implication in altered inter-network functional connectivity in major psychiatric disorders. Individual effects for rTMS and the BDNF genotype on inter-network functional connectivity and interaction effects of rTMS and BDNF genotype with respect to therapeutic effectiveness have previously been reported.

This investigation tests the following hypotheses:

1. 5Hz rTMS over the right DLPFC influences resting-state inter-network functional connectivity between the DMN, the ECN and the SLN
2. The val^{66}met polymorphism in the gene for BDNF influences resting-state inter-network functional connectivity between the DMN, the ECN, and the SLN
3. The val^{66}met polymorphism in the gene for BDNF influences effects of 5Hz rTMS over the right DLPFC on resting-state inter-network functional connectivity between the DMN, the ECN, and the SLN

2. MATERIAL & METHODS

2.1. Subjects

2.1.1. Sample characteristics

The local ethics committee of the University of Heidelberg approved this study (reference number: 0270.4-MA).
The study was performed on 107 healthy, right-handed subjects. All subjects lived in the Rhine-Neckar-Area in Germany. Subjects were recruited via newspaper listings and adverts on notice boards at universities or other public institutions. Subjects that had expressed interest in participating in further trials during earlier studies were also called upon.
40 subjects had to be excluded during the data analysis process because of poor imaging quality due to excessive head movements with translation in excess of 3mm and rotation in excess of 3°, missing fMRI scan data for either session, missing genotype data, because the subject fell asleep during resting-state image acquisition or because the subject did not complete the study.
The remaining sample consisted of 67 individuals. The average fluid level of intelligence, as measured by the Culture Fair Intelligence Test (CFT-20 R; Weiß, 2008), was 122. All subjects had achieved a level of education of at least a high school degree ([Abitur]). Table 1 gives an overview of the sample characteristics.
No subject fulfilled any criteria in the short form of the Diagnostic Interview for Mental Disorders ([diagnostisches Interview für psychische Störungen]) (Mini-DIPS; Margraf, 1994) or in the Schizotypical Personality Questionnaire (SPQ; Raine, 1991).

Table 1: Sample characteristics: The minimum (Min), maximum (Max) and mean values, as well as standard deviation (SD), are shown. Level of education scaled ordinally (1=no degree; 2=middle school [Hauptschule]; 3=junior high school [Realschule]; 4=high school [Abitur]). Abbreviations: CFT, Culture Fair Intelligence Test.

	Min	Max	Mean	SD
Age in years	19	49	24.9	5.1
Level of Education	4	4	4	0
CFT, IQ-score	96	140	122	8.9

2.1.2. Inclusion & exclusion criteria

The first step in subject recruitment consisted of a standardized interview in which the individuals were informed about the study and their medical history was evaluated regarding exclusion criteria:
Subjects with a history of abuse of alcohol or illegal drugs or known neurological or psychiatric disorders such as migraines, epilepsy, depression, and schizophrenia were excluded from the study. Subjects who had first-degree relatives suffering from any of the above were also excluded. Furthermore, subjects taking psychotropic medication or drugs that lower the threshold for seizures or influence the motor

threshold were not allowed to participate. Subjects who had suffered an accident with loss of consciousness or had received heart or brain surgery, as well as those suffering from chronic medical conditions, were also not included in the study sample. For female participants, the possibility of an existing pregnancy had to be excluded. MRI exclusion criteria encompassed permanent tattoos and ferromagnetic implants.

2.1.3. Preliminary examinations

As part of the standardized interview, subjects gave written informed consent on the study design after receiving thorough information on the procedure on the two examination days, the possible side effects of the magnetic stimulation, magnetic resonance imaging, and the blood-draw procedure as well as the associated genotyping. On this occasion, a physician obtained the blood sample for the genetic analysis.
Written informed consent for the MRI scan was gathered again on each of the days of scanning.
Additionally, a battery of psychological interviews and tests was performed: among these, the diagnostic short examination Mini-DIPS is most relevant to the design of this study due to its ability to detect possible psychiatric disorders and a short overview will be given in the following.

- The short form Diagnostic Interview for Mental Disorders (Mini-DIPS; Margraf, 1994) is designed for screening for the psychiatric disorders according to the criteria set out in the DSM-IV (published by the *American Psychiatric Association*, APA in 1994) and the ICD-10 (published by the *World Health Organization*, WHO in 1991). The test is the short form of the extended Diagnostic Interview for Mental Disorders (DIPS) and served to detect possible psychological or psychiatric abnormalities that constituted exclusion criteria for this study.

2.2. Experimental design

Every subject completed two data collection sessions according to the study design necessitating the administering of a true and a sham rTMS stimulation. Blinding of the study personnel regarding the type of stimulation was not possible due to technical reasons. The subject, however, was unaware as to whether true or sham stimulation was performed, and subjects were randomly assigned the stimulation condition for the first session. Care was taken to avoid more than two weeks between the two sessions and both measurements were performed at approximately the same time of day.

At the first data collection session, the subject's motor threshold was determined using the rTMS coil that was subsequently used for stimulation (see chapter 2.3.1.1). After threshold determination, the subject entered the MRI scanner and a high-resolution structural image of the subject's head was generated. The subject then performed an n-back task during fMRI scanning. This fMRI data served as a localizer for the DLPFC in the T1 scan. The subject was registered for neuronavigation, and the stimulation target, as well as the most suitable position for the TMS coil, were determined and registered (see chapter 2.3.1.3). Stimulation was then performed with the subject lying supine on the bed of the MRI scanner. Immediately after the

stimulation, MRI scanning was started. After a localizer scan and a flanker task, which will not be evaluated in this study, the resting-state BOLD scan was performed. The second data collection session followed a similar schedule and started with the determination of the subject's motor threshold. Since the stimulation target had already been determined during the first session, the second session immediately continued with registration for neuronavigation, rTMS or sham stimulation, and fMRI scanning.
Table 2 shows the procedure that was adhered to during the two measuring sessions

Table 2: Stimulation and data collection procedure adhered to during the two sessions. The stimulation condition for the first session was assigned randomly, with the alternate condition applied during the second session.

1st session:
Determination of the subject's motor threshold
MRI scan: high-res T1 structural image & n-back task fMRI Activation-based selection of right DLPFC from n-back task scan
Registration of surface of subject's head for neuronavigation
Determination and registration of ideal position of TMS coil for stimulation
Stimulation condition: rTMS/sham stimulation
Data collection: localizer scan, flanker task, resting-state scan
2nd session:
Determination of the subject's motor threshold
Registration of surface of subject's head for neuronavigation
Stimulation condition: Sham stimulation/rTMS
Data collection: localizer scan, flanker task, resting-state scan

2.3. Independent variables

2.3.1. Transcranial magnetic stimulation

2.3.1.1. Stimulation protocol

Transcranial magnetic stimulation was performed with a MagPro X100 Stimulator (MagVenture, Farum, Denmark). The coil is a passively cooled, MRI-compatible 70 mm double-ring-coil (MCF-B65). Stimulation was administered with an intensity of 90% of the active motor threshold (see chapter 2.3.1.2) and a frequency of 5 Hz.

After each minute, stimulation was paused for one minute, which resulted in 2100 pulses being administered in 13 minutes. Therefore, the protocol for stimulation represents an extension of the protocol used in two previous studies (Rizzo et al., 2004; Rounis et al., 2006) by 1 and 2 stimulation cycles, respectively, and matches the protocol used in another study (Esslinger et al., 2014). Assisted by neuronavigation, the coil was held to the subject's head tangentially to the point of maximum activation in the right DLPFC, as determined in the preceding fMRI scan during an n-back task. The coil was held at a 45° angle to the sagittal plane with the coil's handle aimed ventrally.
For the sham stimulation, the coil was flipped by 180° resulting in the side of the coil housing the passive cooling aggregates to touch the subject's head. According to the manufacturer, this reduces the strength of the stimulation by at least 80%.

2.3.1.2. Determination of the active motor threshold

The motor threshold represents a measure of the membrane excitability of corticospinal neurons (Ziemann, Lonnecker, Steinhoff, & Paulus, 1996). However, it is not constant for any individual but rather depends on a multitude of neurophysiological factors that may vary across time (Kiers, Cros, Chiappa, & Fang, 1993). The motor threshold was therefore determined independently at the beginning of each data collection session. Using the TMS coil, single magnetic pulses were applied to the right primary motor cortex until a movement of the subject's extended index finger could be observed. The subject was instructed to close his or her eyes and relax. Pulses were applied in an arrhythmical manner to avoid conscious finger movements by the subject. The lowest intensity at which five out of ten stimuli evoke a visible motor response corresponds to the active motor threshold (Rothwell et al., 1999).

2.3.1.3. Functional neuronavigation

For this study, the TMS Navigator LACS 2000, Version 1.7 from the company Localite in St. Augustin was used. The system consists of the Localite software for Microsoft Windows, an infrared camera with an infrared light source able to detect retroflecting markers. The retroflecting markers were mounted on an attachment for the TMS coil and a headband for the subject. The principle is based on the method for neuronavigation described by Ettinger and colleagues (Ettinger et al., 1998).
The retroflecting markers on both the coil and the headband worn by the subject can be detected and localized by the infrared camera and the PC software calculates their respective positions in space via triangulation. The system enables targeted and reproducible stimulation due to real-time visual feedback on the position of the coil in relation to the subject's anatomy.
The subject's head was mapped in the Localite software by registering at least 200 points of the scalp, as well as prominent facial features. The data points were mapped to their counterparts in the T1-weighted structural MRI scans. By overlaying the structural image with the data from the T2* functional scan taken during n-back task performance, the most active region in the DLPFC could be identified. The stimulation target was chosen accordingly, and the target and coil position were kept identical for both the true and the sham stimulation sessions.

2.3.2. Genotype data

Blood samples for genotyping of the subjects were drawn by a licensed physician during the preliminary session. The blood samples were analyzed concerning the rs6265 polymorphism using a TaqMan 5' nuclease assay (Life Technologies, USA) by the Department Genetic Epidemiology in Psychiatry at the Central Institute of Mental Health in Mannheim (Schweiger et al., 2019).
Distribution of the $val^{66}met$ polymorphism in the BDNF gene at codon 66, located at nucleotide 196 on chromosome 11p13, in the study population is shown in table 3.

Table 3: Sample characteristics for the BDNF $val^{66}met$ polymorphism

	$val^{66}val$	$val^{66}met$	$met^{66}met$
Number of subjects	41	24	2

Allele frequencies of 0.791 for Val^{66} and 0.209 for Met^{66}, with a χ^2 of 0.467, indicate that the study population does not deviate significantly from a Hardy-Weinberg Equilibrium for the $val^{66}met$ genotype.
Due to the low number of $met^{66}met$ homozygotes in the sample, these individuals were grouped with the $val^{66}met$ heterozygotes as met^{66} carriers for further analysis, consistent with other neuroimaging studies involving this genotype (Cole et al., 2011; de Araujo et al., 2018; Ho et al., 2006; Tost et al., 2013).

2.4. Dependent variables

2.4.1. Resting-state fMRI

The subject was instructed to lie in the MRI scanner with eyes open for five minutes, allowing for 150 whole-brain scans with a two second repetition time (TR), and instructed to think of nothing in particular. None of the subjects that were included in the data analysis reported to have closed their eyes or fallen asleep during the scan.

2.4.2. Functional magnetic resonance imaging

Scanning was performed using a 3-Tesla-MRI-System (SIEMENS Magnetom Trio; Erlangen, Germany). The subject's head was placed in a SIEMENS 32-channel head coil. Foam pads were used to minimize head movements. Subjects were able to abort the scan at any time using an emergency button. An MRI compatible pulse oximeter and a chest belt were used to monitor pulse and breathing, respectively.
During the first session, a high-resolution T1-sequence with a voxel size of 1x1x1mm and a field of view (FOV) of 256mm in 192 slices was recorded. This sequence was used for the topography for neuronavigation.
Functional MRI data were acquired during the n-back task in the first session as well as during the resting-state scans after stimulation in both sessions, using a T2*-weighted echo-planar imaging (EPI) sequence with the following parameters: 28 slices, repetition time (TR) = 2000ms, echo time (TE) = 30ms, flip angle = 80°, slice thickness = 4mm, gap = 1mm, field of view (FOV) = 192mm; voxel size = 3x3x5mm.

2.5. Data analysis

2.5.1. Preprocessing of fMRI data

Preprocessing of the fMRI data was performed using standard procedures implemented in the Statistical Parametric Mapping software (SPM) version 8 (http://www.fil.ion.ucl.ac.uk/spm/). The first 4 volumes of the time series were discarded to allow for equilibrium magnetization. The following preprocessing steps were performed: realignment to the first image, slice time correction, spatial normalization into standard stereotactic space according to the Montreal Neurological Institute (MNI) template, and smoothing with a 9mm FWHM Gaussian filter.

2.5.2. Functional connectivity analysis

Identification of resting-state functional connectivity networks was performed using the Group ICA/IVA of fMRI Toolbox (GIFT) v4.0b (http://icatb.sourceforge.net) for Matlab 8 ("MATLAB 8.0 and Statistics Toolbox 8.1," 2013).

The number of independent components to be extracted from the data set was determined via dimension estimation using the minimum description length criteria (Y. O. Li, Adali, & Calhoun, 2007), as implemented in GIFT. The ICA was consequently performed for 26 components. A group ICA was run for the fMRI data from all subjects and all sessions. After data concatenation and reduction by two-step principal component analysis, independent component estimation was performed using the Infomax algorithm (Bell & Sejnowski, 1995). For the back-reconstruction of subject-specific spatial maps and time courses, the GICA3 algorithm was used (Erhardt et al., 2011). The ICA step was repeated for a total of 20 ICAs (ICASSO), to ensure the stability of the estimated components (Himberg, Hyvarinen, & Esposito, 2004).
The output of the ICA analysis includes a spatial map of z-scores and an associated time course of BOLD-signal fluctuations for each IC and each subject, as well as average spatial maps and time courses across all subjects and all sessions.

2.5.3. Identification of resting-state functional connectivity networks

Two characteristics of the frequency spectra of independent components obtained by ICA of BOLD fMRI have been established as being able to differentiate between those components that primarily represent intrinsic neuronal activity and those that are constituted of or contaminated by physiological noise (Allen et al., 2011; Robinson et al., 2009). The dynamic range of the frequency spectrum represents the difference in power between the maximum and the minimum of the frequency distribution. The power ratio is obtained by dividing the integral of low-frequency (<0.1Hz, “LF”) by the integral of high-frequency (>0.15Hz, “HF”) signals. Low values for the dynamic range and/or the LF/HF-power ratio indicate components that are significantly contaminated or consist primarily of physiological noise, such as head movements, blood flow artifacts and flow signals of the CSF.

Components with a dynamic range of <0.025 and an LF/HF-power spectrum <4 were excluded from further analysis, representing a conservative approach for the selection of low-contamination components (Allen et al., 2011).
For identification of relevant resting-state networks from the fourteen remaining independent components, an automated and objective method was used, as previously described in multiple publications (Doll et al., 2015; Dong et al., 2019; Manoliu et al., 2013; Manoliu et al., 2014). The independent components generated in this analysis were correlated via multiple spatial correlation with a sample of independent components provided by Allen and colleagues, generated from a dataset of 603 healthy adolescents (Allen et al., 2011), available online from the TReNDS Center for Translational Research in Neuroimaging and Data Science (TReNDS, 2019). Networks of interest for this investigation were selected from the sample provided by Allen and colleagues, namely those belonging to the DMN, the ECN and the SLN. The independent components that showed the highest correlation coefficients with the canonical TReNDS networks of interest were selected for further analysis.
A total of five ICs were found to represent the resting-state networks of interest, with the DMN split into three ICs, the ECN split into two ICs and the SLN represented by a single IC.

2.5.4. Effects of rTMS and genotype on inter-network connectivity

To determine inter-network functional connectivity, the temporal correlation of mean time series of the resting-state networks was analyzed, following an approach first outlined by Jafri and colleagues (Jafri et al., 2008). For each subject, the time course data was extracted from each of the identified components of interest. Pearson correlation analyses, using Matlab 13, were performed on the time course data for five components representing the networks of interest, resulting in a total of 15 correlations per subject. The Pearson correlation coefficients were transformed into z-values using Fisher r-to-z transformation and subjected to statistical analyses in SPSS 26.0. Normal distribution of the subjects' z-values was assessed using the Shapiro-Wilk test ($p>0.05$). Subsequently, the z- transformed correlation coefficients for each network pair were analyzed using a mixed ANOVA with rTMS stimulation as a within-subject factor and BDFN genotype as a between-subject factor. Homogeneity of the error variances was assessed by Levene's test ($p > .05$). Main effects and interactions were followed up in post-hoc t-tests. The p-value threshold for each network-pair ANOVA was set at $p<0.05$ and corrected for multiple comparisons using the Bonferroni correction method, resulting in a corrected p-value threshold of $p<0.003$ for 15 network comparisons. Post-hoc tests were similarly Bonferroni corrected for the number of performed post-hoc comparisons.

A power analysis for the sample (n=67) was performed using the G*Power 3.1 software (Faul, Erdfelder, Buchner, & Lang, 2009) to assess statistical sensitivity to detect an effect of genotype (i.e. between-subject effect) or an effect of rTMS (i.e. within-subject effect) in a mixed-effects ANOVA design. Sensitivity was evaluated for the conventional Type I error rate of $\alpha = .05$ and for the specific Bonferroni corrected Type I error rate of $\alpha_{corr} = .003$. Additional a-priori parameters were set as follows: The correlation among repeated measures was set at a conservative estimate of 0.5 and the nonsphericity correction was set to 1. For effects involving the within-subject factor, the model yielded a power of 80% to detect a standardized effect size of $f \geq .17$ at $\alpha = .05$, and a standardized effect of $f \geq .24$ at $\alpha_{corr} = .003$. For the effect of

genotype, the model yielded a power of 80% to detect a standardized effect size of f ≥ .30 at α = .05, and a standardized effect of f ≥ .42 at α_{corr} = .003. In this context, a standardized effect size of f ≥ 0.10 denotes a small effect, f ≥ 0.25 denotes a medium effect and f ≥ 0.40 denotes a large effect (Cohen, 2013). The current study was therefore sufficiently powered to detect medium to large effects when accounting for correction for multiple comparisons.

3. RESULTS

3.1. Selection of independent components

Values for the dynamic range and the LF/HF-power ratio were determined for all independent components (ICs; table 4). Figure 1 in the appendix shows a scatter plot for dynamic range and power spectrum values for all ICs.

Table 4: Values for dynamic range and LF/HF-power spectrum for all independent components (ICs).

	Dynamic range	LF/HF-power ratio
IC 1	0.023	1.943
IC 2	0.040	13.553
IC 3	0.025	2.533
IC 4	0.042	11.566
IC 5	0.034	6.958
IC 6	0.041	13.589
IC 7	0.041	11.003
IC 8	0.022	2.331
IC 9	0.024	2.919
IC 10	0.027	2.765
IC 11	0.025	1.284
IC 12	0.023	1.658
IC 13	0.045	19.050
IC 14	0.044	12.087
IC 15	0.024	1.515
IC 16	0.040	8.377
IC 17	0.022	1.122
IC 18	0.023	2.075
IC 19	0.047	21.099
IC 20	0.046	15.977
IC 21	0.025	2.090
IC 22	0.023	2.522
IC 23	0.045	13.106
IC 24	0.035	6.053
IC 25	0.046	15.503
IC 26	0.038	7.744

IC 1, 3, 8, 9, 10, 11, 12, 15, 17, 18, 21, 22 were excluded due to a dynamic range <0.025 and a LF/HF-power spectrum <4. Fourteen components were retained for further analysis.

3.2. Identification of resting-state networks

Multiple spatial correlation analysis of the mean spatial z-maps of the remaining independent components (IC 2, 4, 5, 6, 7, 13, 14, 16, 19, 20, 23, 24, 25 and 26) was performed using GIFT v4.0b for SPM8 to identify matches for DMN, ECN and SLN components described by Allen and colleagues (Allen et al., 2011) and made available by the TReNDS Center (TReNDS, 2019).
The ICs 2, 5, 7, 23 and 24 showed the strongest correlation with sensorimotor networks, visual networks, auditory networks, and basal ganglia networks, and are of no further interest for this investigation. ICs 4, 6, 13, 14, 16, 19, 20, 25 and 26 showed the strongest correlation with the published IC templates representing DMN, ECN and SLN networks.
Correlation coefficients between the independent components and the templates are shown in Table 5.

Table 5: Correlation coefficients after multiple spatial regression for independent components (IC) from this analysis and independent components representing DMN, ECN, and SLN from E. A. Allen et al., 2011.

Network from Allen and colleagues, 2011	Correlation coefficient	Independent component
Ventral Default-mode Network	0.479	IC 6
	0.243	IC 4
	0.209	IC 14
Dorsal Default-mode Network	0.494	IC 20
	0.369	IC 16
Left Executive Control Network	0.232	IC 13
Right Executive Control Network	0.297	IC 19
	0.202	IC 26
Anterior Salience Network	0.191	IC 25

These components were then visually inspected to validate the results of the multiple spatial correlation analysis. For each network from the literature sample, the IC with the strongest correlation coefficient was selected, except for the dorsal DMN, where two components were retained after visual inspection.
ICs 6, 16 and 20 were found to represent the anterior DMN (aDMN), inferior posterior (ipDMN) and superior posterior (spDMN), respectively. ICs 13 and 19 corresponded to the left ECN (lECN) and right ECN (rECN), respectively. IC 25 was identified as the best match for the SLN.
The ICs that were ultimately selected to represent the DMN, the ECN and the SLN are shown and described below.

Default-mode network:

IC 6 includes areas primarily in the bilateral posterior cingulate cortices, as well as the bilateral precuneus and cuneus, key nodes of the DMN. See figure 2 for a visual representation of component 6 and its power spectrum.

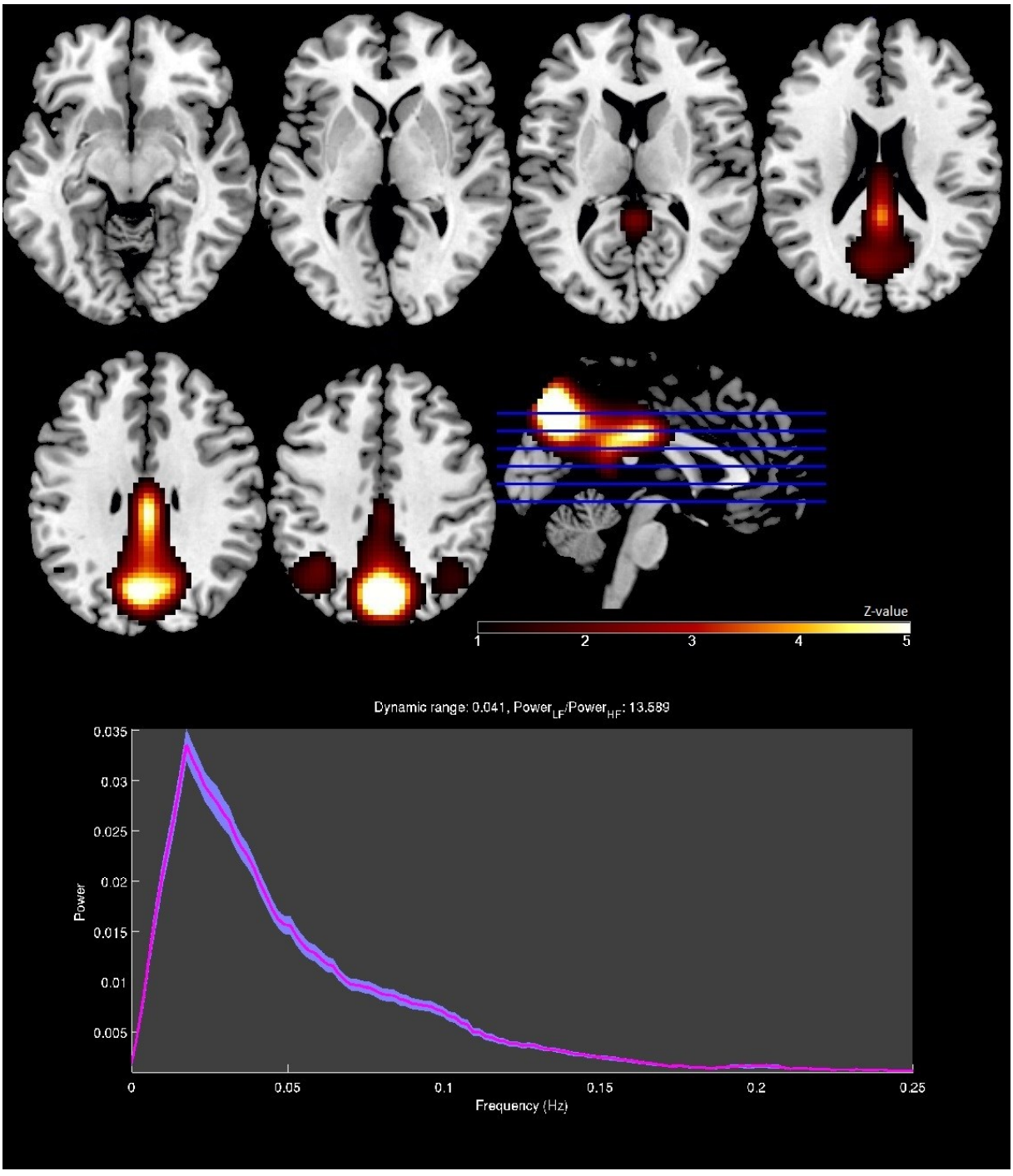

Fig. 2. Top: Mean z-maps for IC 6 superimposed on a high-resolution T1 image (color scale representing z-values from 1 to 5). Bottom: IC 6 power spectrum with power in arbitrary units plotted onto signal frequency in hertz, as well as computed values for the dynamic range of the power spectrum and the low-frequency to high-frequency power ratio.

The key anterior nodes of the DMN missing from component 6 were found to be contained in IC 20, including the medial prefrontal cortex, the bilateral angular gyrus, as well as some additional areas in the precuneus and posterior cingulate cortex. See figure 3 for a visual representation of IC 20 and its power spectrum.

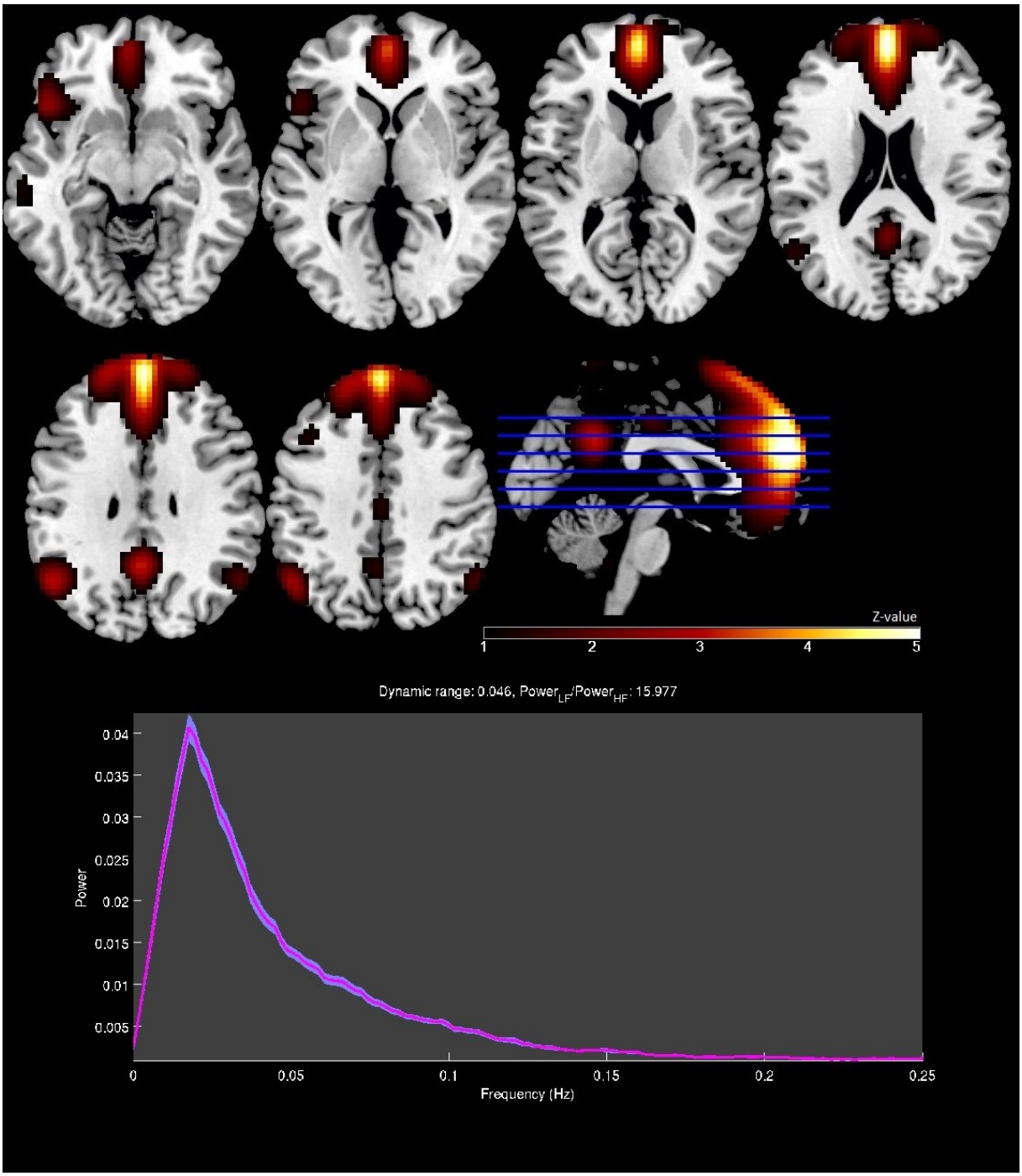

Fig. 3. Top: Mean z-maps for IC 20 superimposed on a high-resolution T1 image (color scale representing z-values from 1 to 5). Bottom: IC 20 power spectrum with power in arbitrary units plotted onto signal frequency in hertz, as well as computed values for the dynamic range of the power spectrum and the low-frequency to high-frequency power ratio.

IC 16 represented an intermediary between IC 6 and IC 20, with foci in the bilateral precuneus as well as the bilateral angular gyrus, the bilateral hippocampus and parahippocampus and areas in the medial prefrontal cortex. See figure 4 for a visual representation of component 16 and its power spectrum.

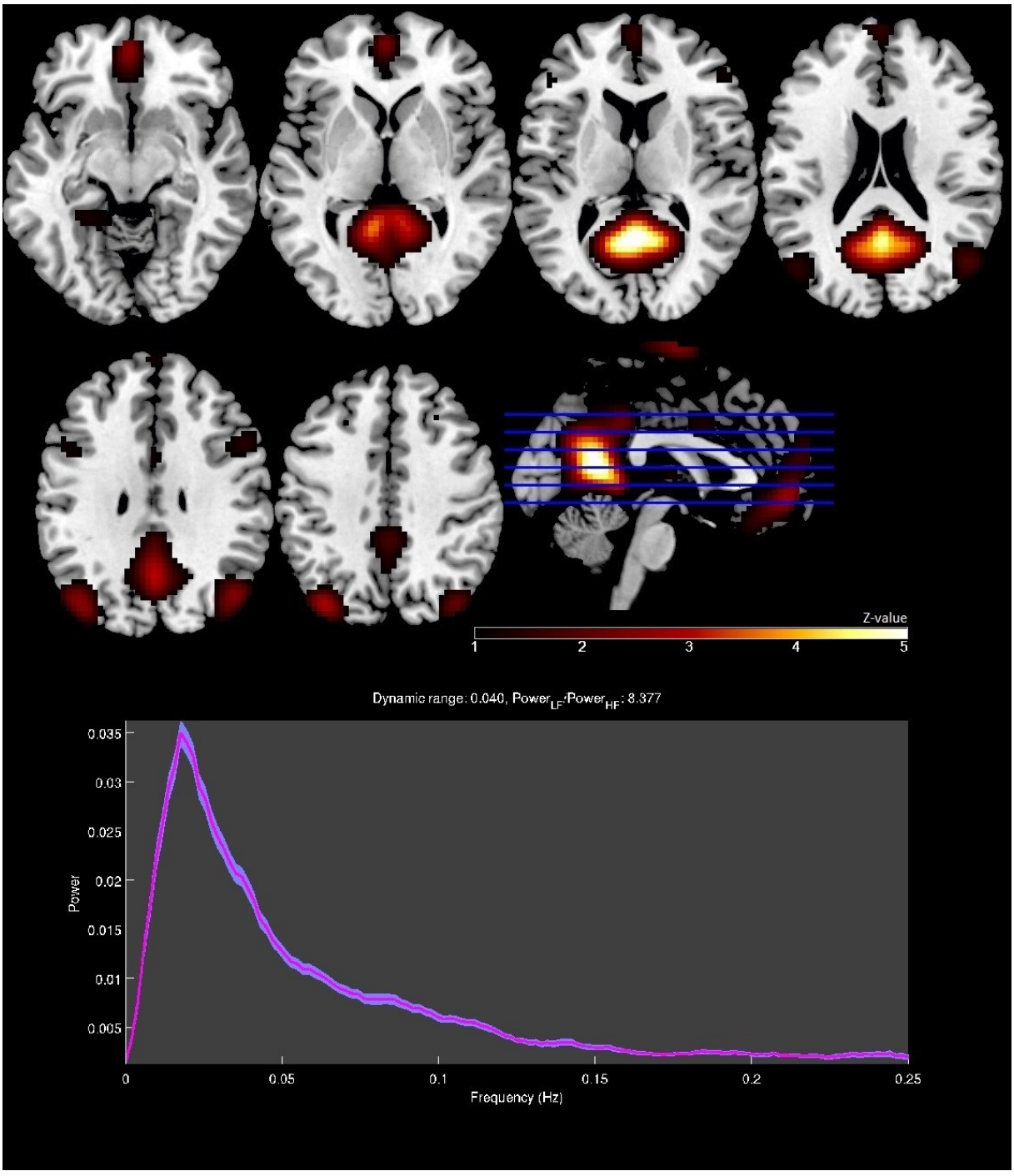

Fig. 4. Top: Mean z-maps for IC 16 superimposed on a high-resolution T1 image (color scale representing z-values from 1 to 5). Bottom: IC 16 power spectrum with power in arbitrary units plotted onto signal frequency in hertz, as well as computed values for the dynamic range of the power spectrum and the low-frequency to high-frequency power ratio.

Executive control network:

IC 19 included primarily the right parietal cortex and the right frontal cortex. These regions match key nodes of the ECN for the right hemisphere. See figure 5 for a visual representation of IC 19 and its power spectrum.

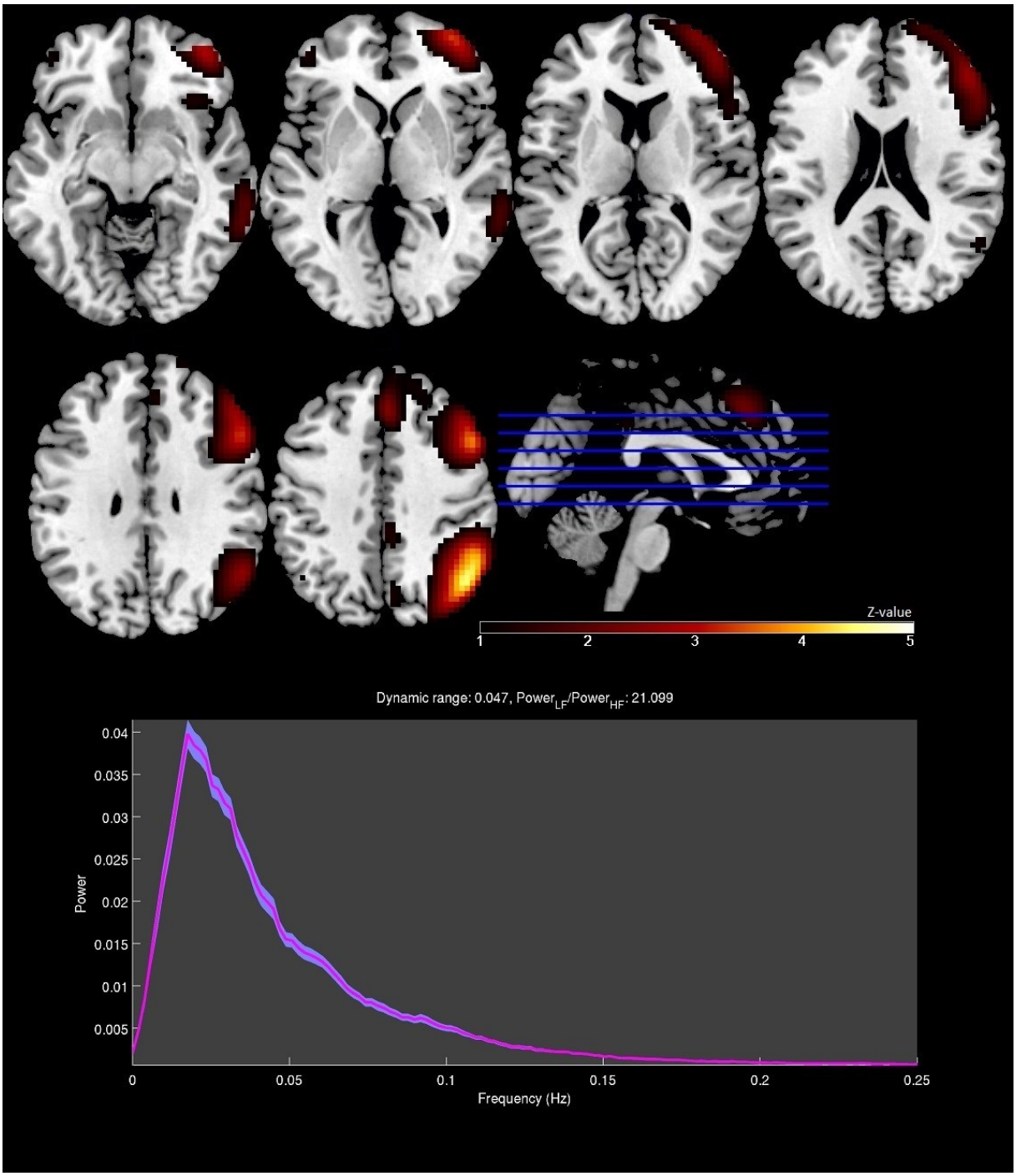

Fig. 5. Top: Mean z-maps for IC 19 superimposed on a high-resolution T1 image (color scale representing z-values from 1 to 5). Bottom: IC 19 power spectrum with power in arbitrary units plotted onto signal frequency in hertz, as well as computed values for the dynamic range of the power spectrum and the low-frequency to high-frequency power ratio.

ECN nodes located in the left hemisphere were found to be contained in IC 13. This component displayed foci in the left parietal cortex, as well as the left frontal cortex. See figure 6 for a visual representation of IC 13 and its power spectrum.

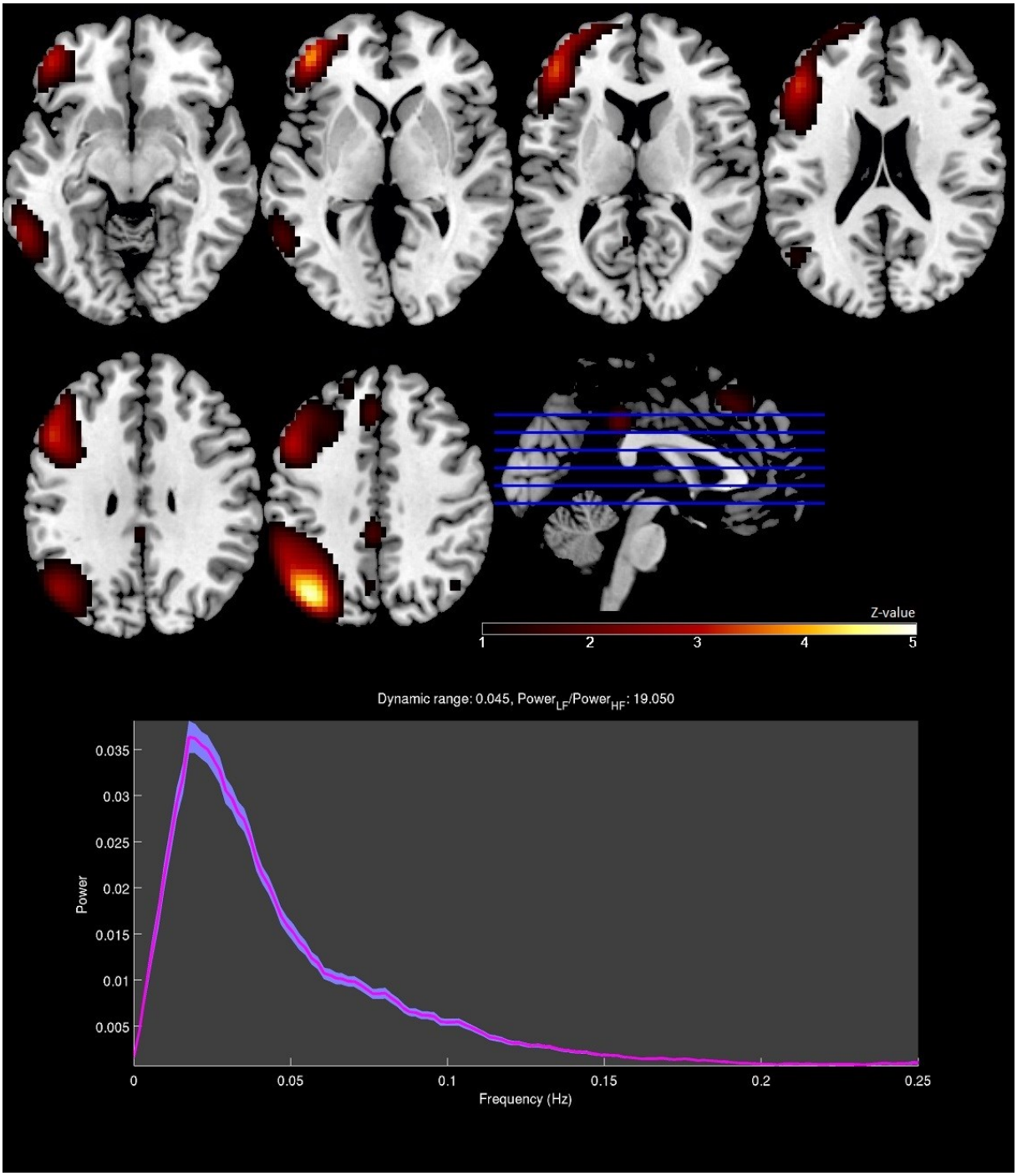

Fig. 6. Top: Mean z-maps for IC 13 superimposed on a high-resolution T1 image (color scale representing z-values from 1 to 5). Bottom: IC 13 power spectrum with power in arbitrary units plotted onto signal frequency in hertz, as well as computed values for the dynamic range of the power spectrum and the low-frequency to high-frequency power ratio.

Salience network:

IC 25 included the bilateral insula and the bilateral anterior cingulate cortex, matching central nodes of the SLN. See figure 7 for a visual representation of IC 25 and its power spectrum.

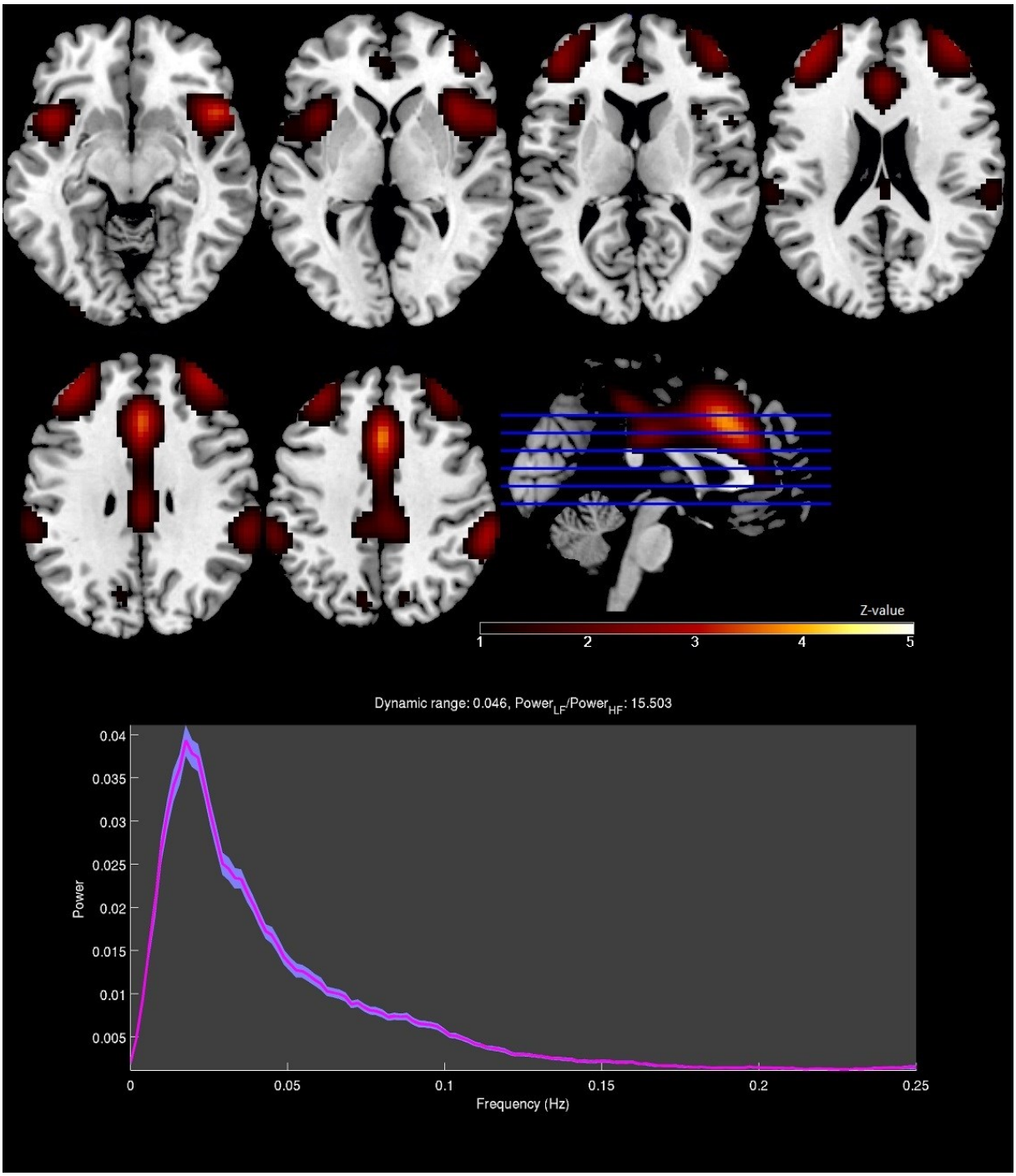

Fig. 7. Top: Mean z-maps for IC 25 superimposed on a high-resolution T1 image (color scale representing z-values from 1 to 5). Bottom: IC 25 power spectrum with power in arbitrary units plotted onto signal frequency in hertz, as well as computed values for the dynamic range of the power spectrum and the low-frequency to high-frequency power ratio.

The DMN was split into three ICs which were studied separately in the analyses on intra- and inter-network connectivity. IC 6 was found to represent predominantly the superior posterior parts of the DMN and will be referred to as the superior posterior DMN (spDMN) in further analysis. IC 16 included primarily inferior posterior parts of the DMN and will be referred to as the inferior posterior DMN (ipDMN). IC 20 was found to contain predominantly the anterior parts of the DMN and will be referred to as the anterior DMN (aDMN). Taken together, the aDMN, the spDMN, and the ipDMN contain all key DMN nodes.
The ECN was split into two ICs, representing a left-right split. IC 19 was found to represent predominantly the right hemisphere parts of the ECN and will be referred to as the right ECN (rECN) in further analysis. IC 13 was found to contain predominantly the left hemisphere parts of the ECN and will be referred to as the left ECN (lECN). Taken together, the rECN and the lECN contain all key ECN nodes.
Given its good match for key SLN nodes, IC 25 will be referred to as the SLN in further analysis.

3.3. Effect of rTMS and genotype on inter-network connectivity

Table 6 shows the mean correlation coefficients for all network pairs from all subjects during both sessions. Table 7 in the appendix shows the mean Pearson correlation coefficients according to stimulation condition and genotype group.

Table 6: Mean and standard deviation (shown in parenthesis) of Pearson correlation coefficients for all networks from all subjects, across both stimulation conditions. Abbreviations: spDMN, superior posterior default-mode network; ipDMN, inferior posterior DMN; aDMN, anterior DMN; lECN, left executive control network; rECN, right executive control network; SLN, salience network.

	spDMN	**ipDMN**	**aDMN**	**lECN**	**rECN**	**SLN**
spDMN		0.347 *(0.178)*	0.322 *(0.166)*	0.161 *(0.209)*	0.211 *(0.187)*	0.020 *(0.231)*
ipDMN	0.347 *(0.178)*		0.164 *(0.167)*	0.049 *(0.190)*	-0.004 *(0.196)*	-0.082 *(0.224)*
aDMN	0.322 *(0.166)*	0.164 *(0.167)*		0.223 *(0.210)*	0.071 *(0.211)*	-0.230 *(0.252)*
lECN	0.161 *(0.209)*	0.049 *(0.190)*	0.223 *(0.210)*		0.359 *(0.175)*	-0.179 *(0.193)*
rECN	0.211 *(0.187)*	-0.004 *(0.196)*	0.071 *(0.211)*	0.359 *(0.175)*		0.098 *(0.201)*
SLN	0.020 *(0.231)*	-0.082 *(0.224)*	-0.230 *(0.252)*	-0.179 *(0.193)*	0.098 *(0.201)*	

There was a statistically significant interaction between stimulus condition and genotype group for the correlation between the time courses of the spDMN and the lECN, $F(1, 65) = 9.331$, $p = .003$, partial $\eta^2 = .126$.
Levene's test confirmed the homogeneity of error variances for the spDMN/lECN correlations ($p>0.5$). There was also a homogeneity of covariances, as assessed by Box's test ($p = .094$).
To determine the simple main effect of genotype on connectivity between the spDMN and the lECN, an independent samples t-test was performed. There was a nominally significant difference between network time series correlation of the genotype groups after rTMS, at $p<0.05$ without correction for multiple comparisons, with mean time series z-values 0.109 (95%-CI[0.002, 0.216]) greater for the met^{66} carriers, t(65) = -2.037, $p = .046$. There was no statistically significant difference between spDMN and lECN time series correlation of the genotype groups after sham stimulation, t(65) = .846, $p = .400$.
To determine the simple main effect of rTMS on connectivity between the spDMN and the lECN for each genotype group, a paired t-test was performed. There was a statistically significant effect of stimulus condition on between network time series correlation in the met^{66} carrier group between sham stimulation; $t(25)= -3.355$, $p= .003$; with mean time series z-values 0.1371 (95%-CI[0.053, 0.221]) greater after rTMS. The effect of stimulus condition in the val^{66}val homozygote group did not reach statistical significance: $t(40) = .788$, p = .435. See figure 10 for a bar chart of mean spDMN and lECN time series correlation for the stimulation condition and the genotype groups.

Figure 10 – spDMN/lECN stimulation condition and genotype group interaction effects

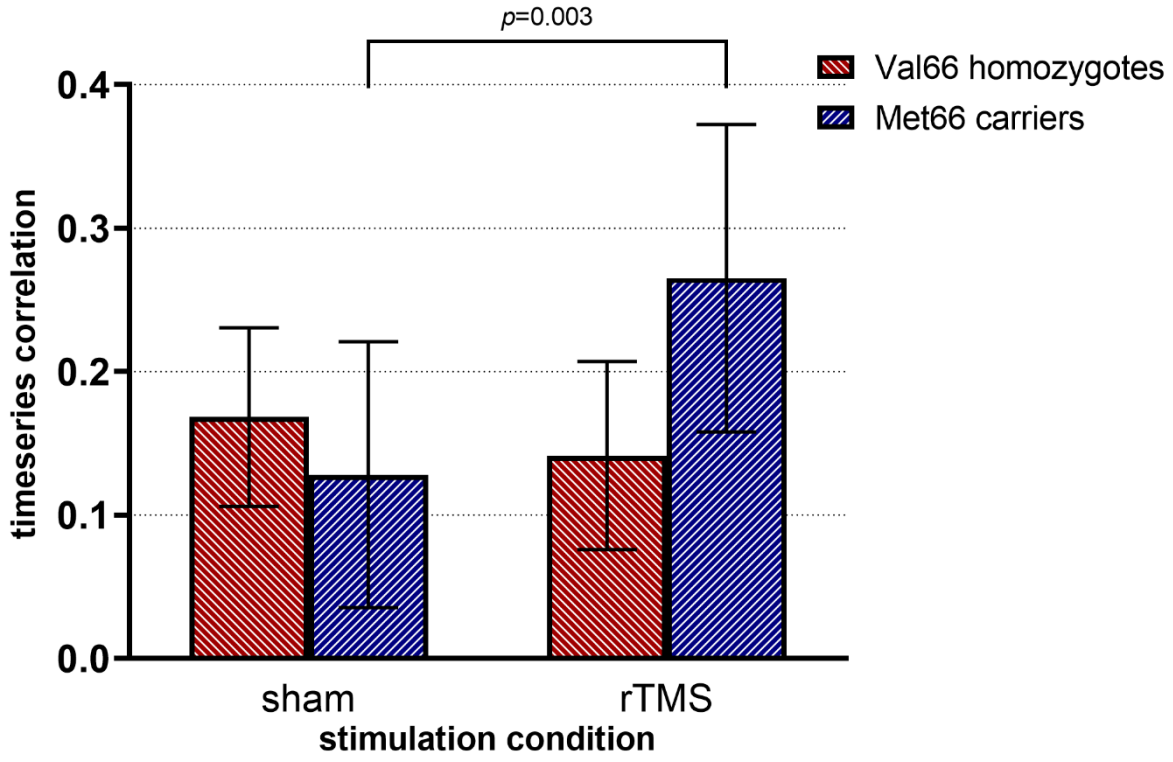

Fig 10: Bar chart of mean spDMN and lECN time series correlation for the stimulation condition (sham vs. rTMS) and genotype group (val^{66}val homozygotes vs. met^{66}-carriers). Error bars indicate 95% confidence interval. Abbreviations: spDMN, superior posterior default-mode network; lECN, left executive control network.

No other network pair showed an rTMS-by-genotype interaction effect.

For all remaining network pairs, main effects of stimulation condition and genotype group were determined from the mixed ANOVA.
A nominally significant main effect of rTMS stimulation was observed for the correlation between the ipDMN and the lECN, $F(1, 65) = 4.929$, $p = .030$, partial $\eta^2 = .070$, and for the correlation between the aDMN and the SLN, $F(1, 65) = 7.104$, $p = .010$, partial $\eta^2 = .099$. However, neither effect survived correction of the significance threshold to $p<0.003$, Bonferroni corrected for 15 multiple comparisons.
For completeness, the main effects of rTMS stimulation are shown in fig. 11 and fig. 12 in the appendix.

No significant main effect of genotype group was detected in any network pair.

See table 8 and table 9 in the appendix for an overview of interaction effects and main effects, respectively.

4. DISCUSSION

4.1. Identification of resting-state networks

Among the independent components generated via ICA, good matches for the three networks of interest of this investigation could be identified.
Regarding the DMN, all key nodes were covered by three ICs. The observation that the DMN is composed of three independent components matches descriptions in published studies that used ICA for resting-state fMRI data. Manoliu and colleagues, for instance, similarly reported the DMN to be composed of an anterior DMN, a superior posterior DMN and an inferior posterior DMN (Manoliu et al., 2013; Manoliu et al., 2014). Doll and colleagues reported an anterior component, a posterior dorsal component and a posterior ventral component (Doll et al., 2015), with the reported networks closely matching networks identified in this analysis.
The ECN was composed of two ICs in the current study. The observation of lateralized ECN sub-networks is frequently reported for ICA-based analysis of resting-state functional connectivity (Doll et al., 2015; Dong et al., 2019; W. Li et al., 2017; Manoliu et al., 2013; Manoliu et al., 2014).
The SLN was readily identified as one single network comprising all key network nodes.
Inter-network connectivity between the three DMN components was stronger than connectivity between DMN and ECN or SLN components, and connectivity between the two ECN components was greater than connectivity between ECN and DMN or SLN components (see: Table 8, section 3.2.4). This is expected since, despite splitting the DMN into three and the ECN into two ICs, connectivity of sub-networks belonging to the same resting-state network should be greater than the connectivity of these sub-networks with different networks. Overall, inter-network connectivity observed in this investigation closely matches reported data from an ICA-based study of resting-state functional connectivity with more than 600 subjects (Allen et al., 2011).

4.2. Main effect of rTMS

No main effects of 5Hz rTMS of the right DLPFC on inter-network connectivity were detected in this investigation. Two potential rTMS main effects of increased connectivity between the DMN and the ECN and between the DMN and the SLN did not survive correction of the significance threshold for multiple comparisons. The overall lack of a significant main effect of 5Hz rTMS of the right DLPFC aligns with published evidence.
Bilek and colleagues explored changes in resting-state functional connectivity after rTMS utilizing the same stimulation protocol as this investigation (Bilek et al., 2013). Their study employed seed-based analysis of connectivity between the right DLPFC and the hippocampus, which would be contained within the rECN and ipDMN respectively, and reported a lack of rTMS effect in line with the results of the ICA-based connectivity analysis.
The results of this investigation also match those published by Schluter and colleagues who also reported a lack of effect for rTMS of the right DLFPC on inter-network connectivity, albeit using a different rTMS protocol involving 10Hz stimulation above the active motor threshold (Schluter et al., 2018).

The findings of this thesis contrast with some published reports of rTMS effects on functional connectivity. Tik and colleagues reported an rTMS effect of increased connectivity between the anterior cingulate cortex, contained within this investigations' SLN, and a network containing the DLPFC, contained in this investigations' lECN and rECN (Tik et al., 2017). However, Tik and colleagues applied 10Hz rTMS to the left DLPFC, their rTMS-responsive meso-cortico-limbic network does not completely match the ECN and the connectivity changes were observed from a seed-voxel in the ACC rather than on a whole-network level. All these factors could contribute to explaining the discrepancies in the detected rTMS effects.
Other studies that have previously reported rTMS effects on inter-network connectivity also differ concerning stimulation site, stimulation protocol and/or sample characteristics: Shang and colleagues reported altered connectivity between ECN and DMN nodes after inhibitory continuous theta-burst rTMS over the left DLPFC (Shang et al., 2019). Liston and colleagues observed altered connectivity between the DMN and the ECN following 10Hz rTMS over the left DLPFC (Liston et al., 2014). Philip and colleagues described altered connectivity between DMN and SLN nodes after 5Hz rTMS of the left DLPFC in patients suffering from major depressive disorder and posttraumatic stress disorder (Philip et al., 2018). It should be noted that Schluter and colleagues reported a lack of effect on inter-network connectivity for 10 Hz rTMS both to the left and the right DLPFC (Schluter et al., 2018).

Overall, the findings of a lack of direct effects of 5Hz rTMS of the right DLPFC on resting-state inter-network connectivity concur with findings from one other study employing the same stimulation protocol and target, while utilizing an alternative method for connectivity analysis.
The discrepancy between the lack of an rTMS effect in this investigation and reports of rTMS effects in multiple publications could be attributed to the stimulation target, as all studies that reported an effect on inter-network connectivity applied rTMS to the left DLPFC. Furthermore, rTMS pulse frequency and intensity with respect to the active motor threshold should be considered as potential factors influencing stimulation effects on inter-network functional connectivity and warrant further systematic investigation.

4.3. Main effect of BDNF genotype

Significant effects of the BDNF val^{66}met genotype on inter-network connectivity between the DMN, the ECN, and the SLN were not observed in this investigation.
Wang and colleagues have reported increased resting-state functional connectivity between the DLPFC and the anterior insula in met^{66} carriers (C. Wang, Zhang, et al., 2014). No corresponding increase in connectivity between the ECN and the SLN in met^{66} carriers was observed in this investigation. A possible explanation for this discrepancy is that Wang and colleagues utilized a seed-based analysis, therefore focusing solely on the DLPFC and the anterior insula, while this investigation observed connectivity between the ECN and SLN on a whole-network level. Effects on the level of individual brain structures might have been obscured by a lack of or opposing effects between all other structures involved within the respective networks.
Other published research on BDNF val^{66}met genotype effects on functional connectivity either focused on intra-network connectivity (Thomason et al., 2009), involved a mental task instead of the resting-state (Fera et al., 2013; Mukherjee et al.,

2011; Schweiger et al., 2019) or investigated patients instead of healthy controls (Yin et al., 2015).

The findings of this thesis concerning BDNF genotype effects on inter-network functional connectivity to not align with the results of one study that investigated a similar hypothesis with a different approach to functional connectivity analysis. More research is needed to allow for a more conclusive assessment of possible BDNF genotype effects on between-network resting-state functional connectivity.

4.4. Interaction effect of rTMS and BDNF genotype

This study uncovered a significant interaction effect of BDNF val^{66}met genotype and rTMS stimulation on functional connectivity between the superior posterior DMN and the left ECN: rTMS of the right DLPFC resulted in greater inter-network functional connectivity than sham stimulation in met^{66} alleles carriers. This increase in connectivity was stronger in met^{66} carriers compared to val^{66}val homozygotes, which however did not survive correction for multiple comparisons.
To the best of my knowledge, no study has investigated interaction effects between rTMS of the right DLPFC and BDNF genotype on inter-network resting-state functional connectivity, preventing direct comparison with the literature.

A significant share of research concerning resting-state functional connectivity, rTMS, and the BDNF genotype has however been performed in individuals suffering from psychiatric disorders, motivated by the potential therapeutic relevance of discoveries. Some inferences regarding the implications of this investigations' findings can be drawn, based on published research performed in patients suffering from schizophrenia and major depressive disorder.

Increased connectivity between the DMN and the ECN has been observed in patients with schizophrenia and the increased connectivity between these networks was found to correlate with the severity of positive symptoms, namely hallucinations (Manoliu et al., 2014). The findings reported by Manoliu and colleagues involved increased connectivity between a right ventral sub-network of the ECN and both a superior posterior and an anterior sub-network of the DMN. There is some overlap in the brain regions grouped into the right ventral ECN by Manoliu and colleagues and those belonging to the lECN in this study.
A meta-analysis of randomized controlled trials performed in 2018 by Kennedy, Lee and Frangou explored the effects of non-invasive brain stimulation, including rTMS, on symptom dimensions in schizophrenia (Kennedy et al., 2018). A non-significant (p=0.13) overall worsening of positive symptoms was detected for rTMS compared to sham, with worsening reaching significance for high-frequency stimulation and stimulation of the DLPFC.
Synthesizing the above-mentioned published findings with the results of this investigation, a possible mechanism can be proposed that explains the worsening of positive symptoms in schizophrenia. rTMS of the right DLPFC resulted in increased connectivity between the DMN and the ECN in subjects carrying one or two copies of the met^{66} allele. If this stimulation effect of increased DMN-ECN connectivity is also present in met^{66}-carrying patients with schizophrenia, it could be associated with the worsening of positive symptoms following high-frequency DLPFC stimulation. Following this line of reasoning, the adverse effects of DLPFC rTMS in patients with schizophrenia would be associated with the BDNF genotype. No research

investigating genotype effects on rTMS treatment outcomes in has been published to date, preventing further evaluation of this theory.
It should be noted that the altered inter-network functional connectivity described by Manoliu and colleagues was present at baseline, in the absence of rTMS. More research would be needed to determine whether rTMS in these patients would result in even further increases in connectivity between the DMN and the ECN and whether the effect is still influenced by the BDNF genotype. The meta-analysis by Kennedy, Lee and Frangou (Kennedy et al., 2018) and other meta-analyses (Jiang et al., 2019; Osoegawa et al., 2018; Wagner et al., 2019) found overall positive effects of rTMS on symptoms in schizophrenia, highlighting the potential therapeutic applications in patients suffering from this condition and warranting further investigation. However, based on the results from this investigation, the BDNF genotype of subjects with schizophrenia included in rTMS studies should be determined, to allow for the detection of possible genotype-specific adverse effects with respect to psychotic symptoms.

Decreased connectivity between the DMN and the ECN has been reported to be present in major depressive disorder (Manoliu et al., 2013). In that study, patients with depression demonstrated a reduced correlation between a superior posterior DMN and a dorsal ECN in addition to reduced connectivity between an inferior posterior DMN and the dorsal ECN. Both the superior posterior and the inferior posterior DMN identified by Manoliu and colleagues match the spDMN and ipDMN identified in this thesis. The dorsal ECN, showing overlap with both the rECN and lECN identified in this thesis, was one of three ECN sub-networks, along a left ventral ECN and a right ventral ECN. The division of the ECN into three instead of two sub-networks could be explained as a consequence of the high-model-order ICA with 75 IC used by Manoliu and colleagues, which may have further subdivided the ECN. Decreased connectivity between the DMN and the ECN in major depressive disorder was also reported by Dong and colleagues, both in current and remitted patients (Dong et al., 2019).
It should be noted that the altered inter-network connectivity in MDD, between the DMN and the ECN, reported by Manoliu and colleagues as well as Dong and colleagues does not directly match observed alterations in connectivity between these networks in individuals suffering from late-life depression, reported by Li and colleagues (W. Li et al., 2017). The latter described reduced connectivity between bilateral ECN components and a subcortical DMN, involving striatal and thalamic regions not included in the DMN components of this investigation or by Manoliu and colleagues or Dong and colleagues, but also increased connectivity between the left ECN and the posterior DMN. These discrepancies could relate to the age of the subjects included by Li and colleagues, which were on average 67 years of age, compared to an average of 49 years in Manoliu's sample. Age has been shown to influence inter-network functional connectivity (Allen et al., 2011). Furthermore, Li and colleagues highlight that their results for inter-network connectivity were not corrected for multiple comparisons and based on a modest sample and therefore advise caution in the interpretation of their findings.
rTMS has a considerable therapeutic effect in major depressive disorder (Mutz, Edgcumbe, Brunoni, & Fu, 2018) and is an established treatment for the condition (Food and Drug Administration, 2011). Restoration of impaired inter-network functional connectivity could point towards a potential mechanism of action of rTMS in major depressive disorder. However, the effect of rTMS on inter-network resting-state functional connectivity was present only in individuals carrying a met^{66} allele

and was not observed in val^{66}val homozygous individuals. It must be noted that the sample of for this thesis was purposefully constituted of subjects not suffering from any psychiatric conditions, including major depressive disorder, that are detectable via screening with the Mini-DIPS. Baseline inter-network connectivity between the DMN and ECN was therefore unlikely to be lowered in the first place. A repetition of this thesis' study protocol in patients with major depressive disorder would be needed to determine whether increases in DMN-ECN inter-network functional connectivity persist in met^{66} carriers and appear in val^{66}val homozygotes if baseline DMN-ECN connectivity is impaired.
The observation, that met^{66} carriers may experience a potential antidepressant therapeutic effect of rTMS which is not detectable in val^{66}val homozygotes does not match published findings on the relationship between antidepressant effectiveness of rTMS and the BDNF val^{66}met genotype in patients with depression. Bocchio-Chiavetto and colleagues reported significantly greater antidepressant effects of rTMS in depressed patients with the val^{66}val homozygote genotype compared to met^{66} carriers (Bocchio-Chiavetto et al., 2008). However, in that study, patients received either high-frequency (17Hz) or low-frequency (1Hz) rTMS of the left DLPFC, compared to 5Hz rTMS of the right DLPFC in this investigation. While high-frequency rTMS of the left DLPFC and low-frequency rTMS of the right DLPFC have been shown to produce similar antidepressant effects in patients (Cao et al., 2018), variations in stimulation intensity and target site could result in both differential rTMS effects on functional connectivity and different impacts on rTMS effectiveness associated with the BDNF genotype.
Krstic and colleagues reported a somewhat better clinical response in val^{66}val homozygous patients with major depressive disorder to right DLPFC 1Hz rTMS combined with therapeutic sleep deprivation (Krstic et al., 2014). The genotype effect of treatment response was inferred by Krstic and colleagues from the fact that 4 out of 5 responders possessed the val^{66}val homozygous genotype. The study differed in the frequency used in the rTMS, 1Hz vs. 5Hz, and employed an additional antidepressant treatment in the form of sleep deprivation, again complicating comparisons between the reported outcomes and the rTMS and genotype effect observed in this investigation.
Thus, the published evidence of the interaction between the BDNF genotype and antidepressant treatment-effects of rTMS does not directly concur with the findings in this thesis, if one assumes an increase of connectivity between the DMN and ECN to be involved in the antidepressant effect of rTMS. However, especially due to discrepancies in methods and sample populations, further research into genotype-dependent inter-network connectivity alterations in response to rTMS, especially in individuals suffering from major depressive disorder, is warranted.

4.5. Limitations

Contamination with physiological noise:
It has been reported that ICA of fMRI data has difficulties in separating low-frequency neural signals from physiological noise related to respiration rates, especially with respect to the DMN (Birn, Murphy, & Bandettini, 2008). The authors recommended the monitoring of respiration during data collection to allow for more reliable identification of breathing-related artifacts. Motion contamination was also found to be present in IC of even high-model-order ICA, in the component time courses, as well as the component spatial maps (Allen et al., 2011). Datasets with excessive head movement were excluded in data analysis during the preprocessing step. Residual

effects of movement, however, cannot be ruled out. Respiration and head movements were not monitored directly as part of this study, a possible influence of these factors on the identified resting-state networks can therefore not be excluded.

ICA model-order:
This investigation utilized a low-model-order ICA for 26 independent components. The number of independent components was selected by performing a dimension analysis based on the minimum description length criterion. Low-model-order ICA using 20-25 independent components is an established approach for resting-state functional connectivity (Biswal et al., 2010; Damoiseaux et al., 2006; Greicius et al., 2007; Greicius, Srivastava, Reiss, & Menon, 2004). It has however been shown that high-model-order ICA with 70 to 100 components also yield stable independent components that match known functional and anatomical segmentations (Allen et al., 2011; Kiviniemi et al., 2009) and can be superior with respect to the detection of certain networks (Abou-Elseoud et al., 2010). Overestimation of independent components, i.e. the selection of an unnecessarily high number of IC, has been reported to decrease the stability of the IC estimates and to degrade the ability to estimate brain networks (Y. O. Li et al., 2007). The components selected to represent the DMN, ECN, and SLN in this investigation showed adequate spatial correlation and visual matching with corresponding components generated in studies using a high-model-order approach (Allen et al., 2011; Doll et al., 2015; Dong et al., 2019; Manoliu et al., 2013; Manoliu et al., 2014). Nevertheless, a high-model-order approach could conceivably result in independent components with a higher degree of segregation and network specificity, allowing for better detection of intra- and inter-network effects.

Sham paradigm:
In this study, sham stimulation was performed by rotating the rTMS-coil 180°, which, according to the manufacturer, resulted in at least an 80% reduction in the strength of the magnetic stimulus. The symmetry of the coil prevented subjects from being able to tell whether true stimulation took part by visual or tactile perception. The noise generated by the magnetic pulses was identical during true and sham stimulation, thus precluding auditory identification of the stimulation condition. However, the magnetic pulses applied during stimulation may result in local paresthesia in the scalp, thus allowing subjects to differentiate between true and sham stimulations. Furthermore, small but significant placebo responses for sham rTMS have been reported, in part influenced by the method for sham coil placement, with a 45° coil position causing the greatest effect sizes, potentially due to some form of actual stimulation of the cortex taking place (Dollfus, Lecardeur, Morello, & Etard, 2016). To minimize the size of the placebo effect, a sham coil, which produces identical sounds without any magnetic stimulation could have been used. However, this would not have dealt with the phenomenon of local paresthesia. It is possible, that the rTMS effect sizes in this study are influenced by insufficient blinding of the subjects to the verity of rTMS and/or low-level magnetic stimulation of the cortex taking place during sham stimulation.

rTMS protocol:
This investigation employed 5Hz rTMS to the right DLPFC. Published research features alternative stimulation frequencies, ranging from 1Hz to 200Hz, and alternative stimulation target sites, most commonly the left DLPFC. The effects of rTMS on functional connectivity vary considerably according to stimulation frequency

and stimulation sites, up to opposite effects resulting from 20Hz and 200Hz stimulation (Watanabe et al., 2014) and from stimulation of the right and left DLPFC (Schluter et al., 2018). The possibility that alternative stimulation protocols would lead to significantly different effects on resting-state functional connectivity can therefore not be discounted. While the inclusion of all possible permutations of stimulation frequency and stimulation target site would necessitate a prohibitively high number of data collection sessions, further studies should consider including at least a selection of different rTMS protocols, in addition to corresponding sham stimulations.

Resting-state task and duration of rTMS effect:
During fMRI scanning, subjects performed a flanker task immediately before the resting-state period which was analyzed in this investigation. Residual effects of the prior task could be present, i.e. if the subject still reflects on the working-memory task, and could alter resting-state functional connectivity. Furthermore, rTMS effects detectable by resting-state functional connectivity analysis have been shown to persist for up to 30 minutes, with stronger effects 15 minutes post-stimulation (Tik et al., 2017). With the resting-state scan taking place from approximately 11 minutes to 16 minutes after stimulation, rTMS effects should still be present. rTMS effects were indeed found in the inter-network connectivity analysis. Nevertheless, rTMS effects on functional connectivity are likely to be strongest immediately after stimulation and the timespan between rTMS and resting-state data collection was lengthened due to the flanker task. Ideally, subjects would not have performed any specific task before the resting-state data collection to limit both possible task-related effects on functional connectivity and possible time-related reductions in rTMS effects.

Genotype distribution:
While the sample population was in Hardy-Weinberg equilibrium for the BDNF val^{66}met genotype, only two individuals possessed a met^{66}met homozygous genotype. Consequently, the analysis for genotype groups was based on val^{66}val homozygotes versus met^{66} carriers. There is evidence of dose-dependent effects of the met^{66}-allele on functional connectivity, with met^{66}met homozygotes showing greater alterations than val^{66}met heterozygotes (Lin et al., 2016; C. Wang, Zhang, et al., 2014). A larger sample population, including more met^{66}met homozygotes, would have allowed for analysis of dose-dependent effects of the polymorphism on the measures of intra- and inter-network functional connectivity and the interaction between rTMS and genotype effect.

Statistical power:
Regarding the statistical sensitivity of this investigation to detect rTMS effects and rTMS by genotype interaction effects, a power of 80% to detect standardized effect sizes of $f \geq .24$ reflects an inability to detect small effects at the Type I error rate of $\alpha = .003$. For the genotype effects, a power of 80% to detect standardized effect sizes of $f \geq .42$ implies that only large effects were detectable at the Type I error rate of $\alpha = .003$. A larger study population would have allowed the detection of smaller effects for both rTMS and genotype. Alternatively, a study seeking only to observe the connectivity between two networks would not have involved Bonferroni correction of the Type I error rate for multiple comparisons and would have been able to detect small and medium effects, respectively, for rTMS and genotype at an $\alpha = .05$.

5. CONCLUSION

This thesis studied the interaction of neural stimulation and genotype on functional connectivity in 67 healthy subjects. Neural stimulation was performed using repetitive transcranial magnetic stimulation of the right dorsolateral prefrontal cortex. The effect of genotype was studied for a well-known polymorphism in the brain-derived neurotrophic factor, which is implicated in neuronal plasticity. Functional connectivity was assessed as the degree of correlation between well-established functional networks during resting-state. In short, this thesis investigated the effect of repetitive transcranial magnetic stimulation and the genotype for a polymorphism in the brain-derived neurotrophic factor on the connectivity between resting-state functional connectivity networks in 67 healthy subjects.

Functional connectivity networks represent reproducible patterns of temporally correlated hemodynamic signal fluctuations in the human brain, which are involved in fundamental neurocognitive processes and show alterations in psychiatric disorders such as schizophrenia and depression. Repetitive transcranial magnetic stimulation of the right dorsolateral prefrontal cortex has been shown to produce lasting effects on functional connectivity and has emerged as an effective treatment in these disorders. Another mechanism affecting functional connectivity is the valine^{66}methionine polymorphism in the gene for the brain-derived neurotrophic factor. Both mechanisms have been linked to neuronal plasticity. However, the combined effect of brain-derived neurotrophic factor genotype and repetitive transcranial magnetic stimulation on functional connectivity is not known. To fill this gap, this thesis studied the interaction of repetitive transcranial magnetic stimulation and genotype on functional connectivity in a sample of 67 healthy subjects. Subjects received 5Hz stimulation of the right dorsolateral prefrontal cortex during one data collection session and sham stimulation of the identical stimulation site during the other session. Following both true and sham stimulation, a resting-state functional magnetic resonance imaging scan was performed. Subjects were genotyped for the valine^{66}methionine single-nucleotide polymorphism (rs6265) in the 5' proregion of the gene for the brain-derived neurotrophic factor. Methionine^{66}methionine homozygotes and valine^{66}methionine heterozygotes were grouped as methionine^{66} carriers for further analysis, due to the low number of homozygotes. The sample population consisted of 26 methionine^{66} allele carriers and 41 valine^{66} homozygotes.

Independent component analysis was used to generate independent components from the resting-state functional magnetic resonance imaging data. These independent components were spatially correlated with canonical samples of resting-state networks to determine best matches for the default-mode network, executive control network and salience network. The default-mode network was represented by three independent components, comprising predominantly superior posterior, inferior posterior and anterior nodes respectively. The executive control network was split into two components, corresponding to left-hemispheric and right-hemispheric network nodes, respectively. The salience network was covered by a single independent component. Functional connectivity between the networks was measured by the correlation of their voxel time series. Statistical analysis of the networks' Fisher r-to-z-transformed correlation coefficients was performed using a mixed analysis of variance approach.

The results of this study are as follows: Repetitive transcranial magnetic stimulation did not result in significant changes in inter-network connectivity compared to sham

stimulation. This concurs with published studies, which also reported a lack of effect of repetitive transcranial stimulation of the right dorsolateral prefrontal cortex on inter-network connectivity. There was also no effect of the brain-derived neurotrophic factor polymorphism on connectivity between the networks of interest, which contrasts with a publication, utilizing a different approach to functional connectivity analysis, that reported altered connectivity between nodes of two networks in methionine^{66} carriers. However, an interaction effect emerged which suggests that repetitive transcranial magnetic stimulation effects are influenced by the brain-derived neurotrophic factor genotype. Following stimulation, methionine^{66} allele carriers showed stronger connectivity between superior posterior parts of the default-mode network and left-hemispheric parts of the executive control network compared to the sham condition. This finding remained significant after correction for multiple comparisons and the effect was not observed in valine^{66} homozygote individuals.

This is the first study to demonstrate that the brain-derived neurotrophic factor valine^{66}methionine genotype modulates repetitive transcranial magnetic stimulation effects on inter-network functional connectivity. A tentative interpretation could be that the observed stimulation effect may be implicated in previously observed adverse effects of repetitive transcranial magnetic stimulation in patients with schizophrenia involving increased severity of hallucinations, as it mirrors functional connectivity abnormalities observed in schizophrenic patients that correlate with symptom intensity. Variations in the therapeutic effectiveness of repetitive transcranial magnetic stimulation in major depressive disorder could also conceivably be associated to genotype-associated differences in functional connectivity modulation, although the observed effects did not align with published findings concerning the influence of this genotype on presumed therapeutic mechanisms of action of repetitive transcranial magnetic stimulation involving functional connectivity.

The results from this investigation should be used to guide further research into the mechanisms of action underlying the therapeutic, and adverse, effects of repetitive transcranial magnetic stimulation and into the genotype for brain-derived neurotrophic factor as a potential cause for interindividual differences in therapeutic response. These results also suggest that the brain-derived neurotrophic factor valine^{66}methionine genotype of subjects should be routinely determined in repetitive transcranial magnetic stimulation studies, especially in those observing therapeutic effects of repetitive transcranial magnetic stimulation in patients suffering from major depressive disorder and schizophrenia.

6. REFERENCES

Abou-Elseoud, A., Starck, T., Remes, J., Nikkinen, J., Tervonen, O., & Kiviniemi, V. (2010). The effect of model order selection in group PICA. *Hum Brain Mapp, 31*(8), 1207-1216. doi:10.1002/hbm.20929

Ahmed, A. O., Mantini, A. M., Fridberg, D. J., & Buckley, P. F. (2015). Brain-derived neurotrophic factor (BDNF) and neurocognitive deficits in people with schizophrenia: a meta-analysis. *Psychiatry Res, 226*(1), 1-13. doi:10.1016/j.psychres.2014.12.069

Allen, E. A., Erhardt, E. B., Damaraju, E., Gruner, W., Segall, J. M., Silva, R. F., . . . Calhoun, V. D. (2011). A baseline for the multivariate comparison of resting-state networks. *Front Syst Neurosci, 5*, 2. doi:10.3389/fnsys.2011.00002

Amassian, V. E., Cracco, R. Q., Maccabee, P. J., Cracco, J. B., Rudell, A., & Eberle, L. (1989). Suppression of visual perception by magnetic coil stimulation of human occipital cortex. *Electroencephalogr Clin Neurophysiol, 74*(6), 458-462. doi:10.1016/0168-5597(89)90036-1

Anticevic, A., Cole, M. W., Murray, J. D., Corlett, P. R., Wang, X. J., & Krystal, J. H. (2012). The role of default network deactivation in cognition and disease. *Trends Cogn Sci, 16*(12), 584-592. doi:10.1016/j.tics.2012.10.008

Anticevic, A., Repovs, G., & Barch, D. M. (2013). Working memory encoding and maintenance deficits in schizophrenia: neural evidence for activation and deactivation abnormalities. *Schizophr Bull, 39*(1), 168-178. doi:10.1093/schbul/sbr107

Anticevic, A., Repovs, G., Shulman, G. L., & Barch, D. M. (2010). When less is more: TPJ and default network deactivation during encoding predicts working memory performance. *Neuroimage, 49*(3), 2638-2648. doi:10.1016/j.neuroimage.2009.11.008

Arfanakis, K., Cordes, D., Haughton, V. M., Moritz, C. H., Quigley, M. A., & Meyerand, M. E. (2000). Combining independent component analysis and correlation analysis to probe interregional connectivity in fMRI task activation datasets. *Magn Reson Imaging, 18*(8), 921-930. doi:10.1016/s0730-725x(00)00190-9

Baker, J. T., Holmes, A. J., Masters, G. A., Yeo, B. T., Krienen, F., Buckner, R. L., & Ongur, D. (2014). Disruption of cortical association networks in schizophrenia and psychotic bipolar disorder. *JAMA Psychiatry, 71*(2), 109-118. doi:10.1001/jamapsychiatry.2013.3469

Ballarin, M., Ernfors, P., Lindefors, N., & Persson, H. (1991). Hippocampal damage and kainic acid injection induce a rapid increase in mRNA for BDNF and NGF in the rat brain. *Exp Neurol, 114*(1), 35-43. doi:10.1016/0014-4886(91)90082-n

Barahona-Correa, J. B., Velosa, A., Chainho, A., Lopes, R., & Oliveira-Maia, A. J. (2018). Repetitive Transcranial Magnetic Stimulation for Treatment of Autism Spectrum Disorder: A Systematic Review and Meta-Analysis. *Frontiers in integrative neuroscience, 12*, 27. doi:10.3389/fnint.2018.00027

Barbacid, M. (1995). Neurotrophic factors and their receptors. *Current Opinion in Cell Biology, 7*(2), 148-155. doi:10.1016/0955-0674(95)80022-0

Barde, Y. A., Edgar, D., & Thoenen, H. (1982). Purification of a new neurotrophic factor from mammalian brain. *EMBO J, 1*(5), 549-553. doi:10.1002/j.1460-2075.1982.tb01207.x

Barker, A. T., Jalinous, R., & Freeston, I. L. (1985). Non-invasive magnetic stimulation of human motor cortex. *Lancet, 1*(8437), 1106-1107. doi:10.1016/s0140-6736(85)92413-4

Bath, K. G., Jing, D. Q., Dincheva, I., Neeb, C. C., Pattwell, S. S., Chao, M. V., . . . Ninan, I. (2012). BDNF Val66Met impairs fluoxetine-induced enhancement of adult hippocampus plasticity. *Neuropsychopharmacology, 37*(5), 1297-1304. doi:10.1038/npp.2011.318

Beckers, G., & Zeki, S. (1995). The consequences of inactivating areas V1 and V5 on visual motion perception. *Brain, 118 (Pt 1)*(1), 49-60. doi:10.1093/brain/118.1.49

Beckmann, C. F., DeLuca, M., Devlin, J. T., & Smith, S. M. (2005). Investigations into resting-state connectivity using independent component analysis. *Philos Trans R Soc Lond B Biol Sci, 360*(1457), 1001-1013. doi:10.1098/rstb.2005.1634

Bell, A. J., & Sejnowski, T. J. (1995). An information-maximization approach to blind separation and blind deconvolution. *Neural Comput, 7*(6), 1129-1159. doi:10.1162/neco.1995.7.6.1129

Bilek, E., Schafer, A., Ochs, E., Esslinger, C., Zangl, M., Plichta, M. M., . . . Tost, H. (2013). Application of high-frequency repetitive transcranial magnetic stimulation to the DLPFC alters human prefrontal-hippocampal functional interaction. *J Neurosci, 33*(16), 7050-7056. doi:10.1523/JNEUROSCI.3081-12.2013

Birn, R. M., Murphy, K., & Bandettini, P. A. (2008). The effect of respiration variations on independent component analysis results of resting state functional connectivity. *Hum Brain Mapp, 29*(7), 740-750. doi:10.1002/hbm.20577

Biswal, B. B., Kylen, J. V., & Hyde, J. S. (1997). Simultaneous assessment of flow and BOLD signals in resting-state functional connectivity maps NMR in Biomedicine Volume 10, Issue 4-5. *NMR in Biomedicine, 10*(4-5), 165-170. Retrieved from http://onlinelibrary.wiley.com/doi/10.1002/(SICI)1099-1492(199706/08)10:4/5<165::AID-NBM454>3.0.CO;2-7/abstract

Biswal, B. B., Mennes, M., Zuo, X. N., Gohel, S., Kelly, C., Smith, S. M., . . . Milham, M. P. (2010). Toward discovery science of human brain function. *Proc Natl Acad Sci U S A, 107*(10), 4734-4739. doi:10.1073/pnas.0911855107

Biswal, B. B., Yetkin, F. Z., Haughton, V. M., & Hyde, J. S. (1995). Functional connectivity in the motor cortex of resting human brain using echo-planar mri Magnetic Resonance in Medicine Volume 34, Issue 4. *Magnetic Resonance in Medicine, 34*(4), 537-541. Retrieved from http://onlinelibrary.wiley.com/doi/10.1002/mrm.1910340409/abstract

Bocchio-Chiavetto, L., Miniussi, C., Zanardini, R., Gazzoli, A., Bignotti, S., Specchia, C., & Gennarelli, M. (2008). 5-HTTLPR and BDNF Val66Met polymorphisms and response to rTMS treatment in drug resistant depression. *Neurosci Lett, 437*(2), 130-134. doi:10.1016/j.neulet.2008.04.005

Brown, C. A., Schmitt, F. A., Smith, C. D., & Gold, B. T. (2019). Distinct patterns of default mode and executive control network circuitry contribute to present and future executive function in older adults. *Neuroimage, 195*, 320-332. doi:10.1016/j.neuroimage.2019.03.073

Brunholzl, C., & Claus, D. (1994). Central motor conduction time to upper and lower limbs in cervical cord lesions. *Arch Neurol, 51*(3), 245-249. doi:10.1001/archneur.1994.00540150039013

Buckner, R. L., Andrews-Hanna, J. R., & Schacter, D. L. (2008). The brain's default network: anatomy, function, and relevance to disease. *Ann N Y Acad Sci, 1124*, 1-38. doi:10.1196/annals.1440.011

Buckner, R. L., & Vincent, J. L. (2007). Unrest at rest: default activity and spontaneous network correlations. *Neuroimage, 37*(4), 1091-1096; discussion 1097-1099. doi:10.1016/j.neuroimage.2007.01.010

Calhoun, V. D., Adali, T., Pearlson, G. D., & Pekar, J. J. (2001). A method for making group inferences from functional MRI data using independent component analysis. *Hum Brain Mapp, 14*(3), 140-151. doi:10.1002/hbm.1048

Cao, X., Deng, C., Su, X., & Guo, Y. (2018). Response and Remission Rates Following High-Frequency vs. Low-Frequency Repetitive Transcranial Magnetic Stimulation (rTMS) Over Right DLPFC for Treating Major Depressive Disorder (MDD): A Meta-Analysis of Randomized, Double-Blind Trials. *Frontiers in psychiatry, 9*, 413. doi:10.3389/fpsyt.2018.00413

Castren, E., Pitkanen, M., Sirvio, J., Parsadanian, A., Lindholm, D., Thoenen, H., & Riekkinen, P. J. (1993). The induction of LTP increases BDNF and NGF mRNA but decreases NT-3 mRNA in the dentate gyrus. *NeuroReport, 4*(7), 895-898. doi:10.1097/00001756-199307000-00014

Castren, E., Thoenen, H., & Lindholm, D. (1995). Brain-derived neurotrophic factor messenger RNA is expressed in the septum, hypothalamus and in adrenergic brain stem nuclei of adult rat brain and is increased by osmotic stimulation in the paraventricular nucleus. *Neuroscience, 64*(1), 71-80. doi:10.1016/0306-4522(94)00386-j

Castren, E., Zafra, F., Thoenen, H., & Lindholm, D. (1992). Light regulates expression of brain-derived neurotrophic factor mRNA in rat visual cortex. *Proc Natl Acad Sci U S A, 89*(20), 9444-9448. doi:10.1073/pnas.89.20.9444

Cathomas, F., Vogler, C., Euler-Sigmund, J. C., de Quervain, D. J., & Papassotiropoulos, A. (2010). Fine-mapping of the brain-derived neurotrophic factor (BDNF) gene supports an association of the Val66Met polymorphism with episodic memory. *Int J Neuropsychopharmacol, 13*(8), 975-980. doi:10.1017/S1461145710000519

Chan, R. C., Chen, E. Y., & Law, C. W. (2006). Specific executive dysfunction in patients with first-episode medication-naive schizophrenia. *Schizophr Res, 82*(1), 51-64. doi:10.1016/j.schres.2005.09.020

Cheeran, B., Talelli, P., Mori, F., Koch, G., Suppa, A., Edwards, M., . . . Rothwell, J. C. (2008). A common polymorphism in the brain-derived neurotrophic factor gene (BDNF) modulates human cortical plasticity and the response to rTMS. *J Physiol, 586*(23), 5717-5725. doi:10.1113/jphysiol.2008.159905

Chen, Z. Y., Jing, D., Bath, K. G., Ieraci, A., Khan, T., Siao, C. J., . . . Lee, F. S. (2006). Genetic variant BDNF (Val66Met) polymorphism alters anxiety-related behavior. *Science, 314*(5796), 140-143. doi:10.1126/science.1129663

Chen, Z. Y., Patel, P. D., Sant, G., Meng, C. X., Teng, K. K., Hempstead, B. L., & Lee, F. S. (2004). Variant brain-derived neurotrophic factor (BDNF) (Met66) alters the intracellular trafficking and activity-dependent secretion of wild-type BDNF in neurosecretory cells and cortical neurons. *J Neurosci, 24*(18), 4401-4411. doi:10.1523/JNEUROSCI.0348-04.2004

Cirillo, P., Gold, A. K., Nardi, A. E., Ornelas, A. C., Nierenberg, A. A., Camprodon, J., & Kinrys, G. (2019). Transcranial magnetic stimulation in anxiety and trauma-related disorders: A systematic review and meta-analysis. *Brain and behavior, 9*(6), e01284. doi:10.1002/brb3.1284

Cohen, J. (2013). *Statistical power analysis for the behavioral sciences*: Routledge.

Cole, J., Weinberger, D. R., Mattay, V. S., Cheng, X., Toga, A. W., Thompson, P. M., . . . Fu, C. H. (2011). No effect of 5HTTLPR or BDNF Val66Met polymorphism

on hippocampal morphology in major depression. *Genes Brain Behav, 10*(7), 756-764. doi:10.1111/j.1601-183X.2011.00714.x

Cordes, D., Haughton, V. M., Arfanakis, K., Carew, J. D., Turski, P. A., Moritz, C. H., . . . Meyerand, M. E. (2001). Frequencies contributing to functional connectivity in the cerebral cortex in "resting-state" data. *AJNR Am J Neuroradiol, 22*(7), 1326-1333. Retrieved from https://www.ncbi.nlm.nih.gov/pubmed/11498421

Cordes, D., Haughton, V. M., Arfanakis, K., Wendt, G. J., Turski, P. A., Moritz, C. H., . . . Meyerand, M. E. (2000). Mapping functionally related regions of brain with functional connectivity MR imaging. *AJNR Am J Neuroradiol, 21*(9), 1636-1644. Retrieved from https://www.ncbi.nlm.nih.gov/pubmed/11039342

Critchley, H. D., Wiens, S., Rotshtein, P., Ohman, A., & Dolan, R. J. (2004). Neural systems supporting interoceptive awareness. *Nat Neurosci, 7*(2), 189-195. doi:10.1038/nn1176

Damoiseaux, J. S., Rombouts, S. A., Barkhof, F., Scheltens, P., Stam, C. J., Smith, S. M., & Beckmann, C. F. (2006). Consistent resting-state networks across healthy subjects. *Proc Natl Acad Sci U S A, 103*(37), 13848-13853. doi:10.1073/pnas.0601417103

Dang, T., Avery, D. H., & Russo, J. (2007). Within-session mood changes from TMS in depressed patients. *J Neuropsychiatry Clin Neurosci, 19*(4), 458-463. doi:10.1176/jnp.2007.19.4.458

de Araujo, C. M., Zugman, A., Swardfager, W., Belangero, S. I. N., Ota, V. K., Spindola, L. M., . . . Jackowski, A. P. (2018). Effects of the brain-derived neurotropic factor variant Val66Met on cortical structure in late childhood and early adolescence. *Journal of psychiatric research, 98*, 51-58. doi:10.1016/j.jpsychires.2017.12.008

de Leeuw, M., Kahn, R. S., Zandbelt, B. B., Widschwendter, C. G., & Vink, M. (2013). Working memory and default mode network abnormalities in unaffected siblings of schizophrenia patients. *Schizophr Res, 150*(2-3), 555-562. doi:10.1016/j.schres.2013.08.016

De Luca, M., Beckmann, C. F., De Stefano, N., Matthews, P. M., & Smith, S. M. (2006). fMRI resting state networks define distinct modes of long-distance interactions in the human brain. *Neuroimage, 29*(4), 1359-1367. doi:10.1016/j.neuroimage.2005.08.035

Doll, A., Holzel, B. K., Boucard, C. C., Wohlschlager, A. M., & Sorg, C. (2015). Mindfulness is associated with intrinsic functional connectivity between default mode and salience networks. *Front Hum Neurosci, 9*(461), 461. doi:10.3389/fnhum.2015.00461

Dollfus, S., Lecardeur, L., Morello, R., & Etard, O. (2016). Placebo Response in Repetitive Transcranial Magnetic Stimulation Trials of Treatment of Auditory Hallucinations in Schizophrenia: A Meta-Analysis. *Schizophr Bull, 42*(2), 301-308. doi:10.1093/schbul/sbv076

Dong, D., Ming, Q., Zhong, X., Pu, W., Zhang, X., Jiang, Y., . . . Yao, S. (2019). State-independent alterations of intrinsic brain network in current and remitted depression. *Prog Neuropsychopharmacol Biol Psychiatry, 89*, 475-480. doi:10.1016/j.pnpbp.2018.08.031

Dugich-Djordjevic, M. M., Tocco, G., Lapchak, P. A., Pasinetti, G. M., Najm, I., Baudry, M., & Hefti, F. (1992). Regionally specific and rapid increases in brain-derived neurotrophic factor messenger RNA in the adult rat brain following seizures induced by systemic administration of kainic acid. *Neuroscience, 47*(2), 303-315. doi:10.1016/0306-4522(92)90246-x

Egan, M. F., Kojima, M., Callicott, J. H., Goldberg, T. E., Kolachana, B. S., Bertolino, A., . . . Weinberger, D. R. (2003). The BDNF val66met polymorphism affects activity-dependent secretion of BDNF and human memory and hippocampal function. *Cell, 112*(2), 257-269. doi:10.1016/s0092-8674(03)00035-7

Erhardt, E. B., Rachakonda, S., Bedrick, E. J., Allen, E. A., Adali, T., & Calhoun, V. D. (2011). Comparison of multi-subject ICA methods for analysis of fMRI data. *Hum Brain Mapp, 32*(12), 2075-2095. doi:10.1002/hbm.21170

Ernfors, P., Bengzon, J., Kokaia, Z., Persson, H., & Lindvall, O. (1991). Increased levels of messenger RNAs for neurotrophic factors in the brain during kindling epileptogenesis. *Neuron, 7*(1), 165-176. doi:10.1016/0896-6273(91)90084-d

Esslinger, C., Schuler, N., Sauer, C., Gass, D., Mier, D., Braun, U., . . . Meyer-Lindenberg, A. (2014). Induction and quantification of prefrontal cortical network plasticity using 5 Hz rTMS and fMRI. *Hum Brain Mapp, 35*(1), 140-151. doi:10.1002/hbm.22165

Ettinger, G. J., Leventon, M. E., Grimson, W. E., Kikinis, R., Gugino, L., Cote, W., . . . Alexander, E. (1998). Experimentation with a transcranial magnetic stimulation system for functional brain mapping. *Med Image Anal, 2*(2), 133-142. doi:10.1016/s1361-8415(98)80008-x

Faul, F., Erdfelder, E., Buchner, A., & Lang, A. G. (2009). Statistical power analyses using G*Power 3.1: tests for correlation and regression analyses. *Behav Res Methods, 41*(4), 1149-1160. doi:10.3758/BRM.41.4.1149

Fera, F., Passamonti, L., Cerasa, A., Gioia, M. C., Liguori, M., Manna, I., . . . Quattrone, A. (2013). The BDNF Val66Met polymorphism has opposite effects on memory circuits of multiple sclerosis patients and controls. *PLoS One, 8*(4), e61063. doi:10.1371/journal.pone.0061063

Fitzgerald, P. B., Fountain, S., & Daskalakis, Z. J. (2006). A comprehensive review of the effects of rTMS on motor cortical excitability and inhibition. *Clin Neurophysiol, 117*(12), 2584-2596. doi:10.1016/j.clinph.2006.06.712

Fitzgerald, P. B., Hoy, K., McQueen, S., Maller, J. J., Herring, S., Segrave, R., . . . Daskalakis, Z. J. (2009). A randomized trial of rTMS targeted with MRI based neuro-navigation in treatment-resistant depression. *Neuropsychopharmacology, 34*(5), 1255-1262. doi:10.1038/npp.2008.233

Food and Drug Administration. (2011). Class II special controls guidance document: Repetitive Transcranial Magnetic Stimulation (rTMS) Systems–Guidance for industry and FDA staff. In *Maryland: US Department of Health and Human Service*.

Fox, M. D., & Raichle, M. E. (2007). Spontaneous fluctuations in brain activity observed with functional magnetic resonance imaging. *Nat Rev Neurosci, 8*(9), 700-711. doi:10.1038/nrn2201

Fox, M. D., Snyder, A. Z., Vincent, J. L., Corbetta, M., Van Essen, D. C., & Raichle, M. E. (2005). The human brain is intrinsically organized into dynamic, anticorrelated functional networks. *Proc Natl Acad Sci U S A, 102*(27), 9673-9678. doi:10.1073/pnas.0504136102

Fox, M. D., Zhang, D., Snyder, A. Z., & Raichle, M. E. (2009). The global signal and observed anticorrelated resting state brain networks. *J Neurophysiol, 101*(6), 3270-3283. doi:10.1152/jn.90777.2008

Fransson, P. (2006). How default is the default mode of brain function? Further evidence from intrinsic BOLD signal fluctuations. *Neuropsychologia, 44*(14), 2836-2845. doi:10.1016/j.neuropsychologia.2006.06.017

Fregni, F., & Pascual-Leone, A. (2007). Technology insight: noninvasive brain stimulation in neurology-perspectives on the therapeutic potential of rTMS and tDCS. *Nat Clin Pract Neurol, 3*(7), 383-393. doi:10.1038/ncpneuro0530

Friston, K. J. (1994). Functional and effective connectivity in neuroimaging A synthesis, Human Brain Mapping Volume 2, Issue 1-2. *Human Brain Mapping, 2*(1-2), 56-78. Retrieved from http://onlinelibrary.wiley.com/doi/10.1002/hbm.460020107/abstract

Friston, K. J., Frith, C. D., Liddle, P. F., & Frackowiak, R. S. (1993). Functional connectivity: the principal-component analysis of large (PET) data sets. *J Cereb Blood Flow Metab, 13*(1), 5-14. doi:10.1038/jcbfm.1993.4

Fukunaga, M., Horovitz, S. G., van Gelderen, P., de Zwart, J. A., Jansma, J. M., Ikonomidou, V. N., . . . Duyn, J. H. (2006). Large-amplitude, spatially correlated fluctuations in BOLD fMRI signals during extended rest and early sleep stages. *Magn Reson Imaging, 24*(8), 979-992. doi:10.1016/j.mri.2006.04.018

Gangitano, M., Valero-Cabre, A., Tormos, J. M., Mottaghy, F. M., Romero, J. R., & Pascual-Leone, A. (2002). Modulation of input-output curves by low and high frequency repetitive transcranial magnetic stimulation of the motor cortex. *Clin Neurophysiol, 113*(8), 1249-1257. doi:10.1016/s1388-2457(02)00109-8

Garrity, A. G., Pearlson, G. D., McKiernan, K., Lloyd, D., Kiehl, K. A., & Calhoun, V. D. (2007). Aberrant "default mode" functional connectivity in schizophrenia. *Am J Psychiatry, 164*(3), 450-457. doi:10.1176/ajp.2007.164.3.450

Geller, B., Badner, J. A., Tillman, R., Christian, S. L., Bolhofner, K., & Cook, E. H., Jr. (2004). Linkage disequilibrium of the brain-derived neurotrophic factor Val66Met polymorphism in children with a prepubertal and early adolescent bipolar disorder phenotype. *Am J Psychiatry, 161*(9), 1698-1700. doi:10.1176/appi.ajp.161.9.1698

Geng, H., Li, X., Chen, J., Li, X., & Gu, R. (2015). Decreased Intra- and Inter-Salience Network Functional Connectivity is Related to Trait Anxiety in Adolescents. *Front Behav Neurosci, 9*, 350. doi:10.3389/fnbeh.2015.00350

Gerloff, C., Corwell, B., Chen, R., Hallett, M., & Cohen, L. G. (1997). Stimulation over the human supplementary motor area interferes with the organization of future elements in complex motor sequences. *Brain, 120 (Pt 9)*(9), 1587-1602. doi:10.1093/brain/120.9.1587

Giambra, L. M. (1995). A laboratory method for investigating influences on switching attention to task-unrelated imagery and thought. *Conscious Cogn, 4*(1), 1-21. doi:10.1006/ccog.1995.1001

Goulden, N., Khusnulina, A., Davis, N. J., Bracewell, R. M., Bokde, A. L., McNulty, J. P., & Mullins, P. G. (2014). The salience network is responsible for switching between the default mode network and the central executive network: replication from DCM. *Neuroimage, 99*, 180-190. doi:10.1016/j.neuroimage.2014.05.052

Gourion, D., Goldberger, C., Leroy, S., Bourdel, M. C., Olie, J. P., & Krebs, M. O. (2005). Age at onset of schizophrenia: interaction between brain-derived neurotrophic factor and dopamine D3 receptor gene variants. *NeuroReport, 16*(12), 1407-1410. doi:10.1097/01.wnr.0000175245.58708.6b

Gratacos, M., Gonzalez, J. R., Mercader, J. M., de Cid, R., Urretavizcaya, M., & Estivill, X. (2007). Brain-derived neurotrophic factor Val66Met and psychiatric disorders: meta-analysis of case-control studies confirm association to substance-related disorders, eating disorders, and schizophrenia. *Biol Psychiatry, 61*(7), 911-922. doi:10.1016/j.biopsych.2006.08.025

Greicius, M. D. (2008). Resting-state functional connectivity in neuropsychiatric disorders. *Curr Opin Neurol, 21*(4), 424-430. doi:10.1097/WCO.0b013e328306f2c5

Greicius, M. D., Flores, B. H., Menon, V., Glover, G. H., Solvason, H. B., Kenna, H., . . . Schatzberg, A. F. (2007). Resting-state functional connectivity in major depression: abnormally increased contributions from subgenual cingulate cortex and thalamus. *Biol Psychiatry, 62*(5), 429-437. doi:10.1016/j.biopsych.2006.09.020

Greicius, M. D., Krasnow, B., Reiss, A. L., & Menon, V. (2003). Functional connectivity in the resting brain: a network analysis of the default mode hypothesis. *Proc Natl Acad Sci U S A, 100*(1), 253-258. doi:10.1073/pnas.0135058100

Greicius, M. D., & Menon, V. (2004). Default-mode activity during a passive sensory task: uncoupled from deactivation but impacting activation. *J Cogn Neurosci, 16*(9), 1484-1492. doi:10.1162/0898929042568532

Greicius, M. D., Srivastava, G., Reiss, A. L., & Menon, V. (2004). Default-mode network activity distinguishes Alzheimer's disease from healthy aging: evidence from functional MRI. *Proc Natl Acad Sci U S A, 101*(13), 4637-4642. doi:10.1073/pnas.0308627101

Greicius, M. D., Supekar, K., Menon, V., & Dougherty, R. F. (2009). Resting-state functional connectivity reflects structural connectivity in the default mode network. *Cereb Cortex, 19*(1), 72-78. doi:10.1093/cercor/bhn059

Grimm, S., Boesiger, P., Beck, J., Schuepbach, D., Bermpohl, F., Walter, M., . . . Northoff, G. (2009). Altered negative BOLD responses in the default-mode network during emotion processing in depressed subjects. *Neuropsychopharmacology, 34*(4), 932-943. doi:10.1038/npp.2008.81

Gusnard, D. A., Akbudak, E., Shulman, G. L., & Raichle, M. E. (2001). Medial prefrontal cortex and self-referential mental activity: relation to a default mode of brain function. *Proc Natl Acad Sci U S A, 98*(7), 4259-4264. doi:10.1073/pnas.071043098

Gusnard, D. A., Raichle, M. E., & Raichle, M. E. (2001). Searching for a baseline: functional imaging and the resting human brain. *Nat Rev Neurosci, 2*(10), 685-694. doi:10.1038/35094500

Habas, C., Kamdar, N., Nguyen, D., Prater, K., Beckmann, C. F., Menon, V., & Greicius, M. D. (2009). Distinct cerebellar contributions to intrinsic connectivity networks. *J Neurosci, 29*(26), 8586-8594. doi:10.1523/JNEUROSCI.1868-09.2009

Hallett, M. (2000). Transcranial magnetic stimulation and the human brain. *Nature, 406*(6792), 147-150. doi:10.1038/35018000

Hare, S. M., Ford, J. M., Mathalon, D. H., Damaraju, E., Bustillo, J., Belger, A., . . . Turner, J. A. (2019). Salience-Default Mode Functional Network Connectivity Linked to Positive and Negative Symptoms of Schizophrenia. *Schizophr Bull, 45*(4), 892-901. doi:10.1093/schbul/sby112

Hariri, A. R., Goldberg, T. E., Mattay, V. S., Kolachana, B. S., Callicott, J. H., Egan, M. F., & Weinberger, D. R. (2003). Brain-derived neurotrophic factor val66met polymorphism affects human memory-related hippocampal activity and predicts memory performance. *J Neurosci, 23*(17), 6690-6694. Retrieved from https://www.ncbi.nlm.nih.gov/pubmed/12890761

Harrison, B. J., Yucel, M., Pujol, J., & Pantelis, C. (2007). Task-induced deactivation of midline cortical regions in schizophrenia assessed with fMRI. *Schizophr Res, 91*(1-3), 82-86. doi:10.1016/j.schres.2006.12.027

Hattiangady, B., Rao, M. S., Shetty, G. A., & Shetty, A. K. (2005). Brain-derived neurotrophic factor, phosphorylated cyclic AMP response element binding protein and neuropeptide Y decline as early as middle age in the dentate gyrus and CA1 and CA3 subfields of the hippocampus. *Exp Neurol, 195*(2), 353-371. doi:10.1016/j.expneurol.2005.05.014

Hauer, L., Sellner, J., Brigo, F., Trinka, E., Sebastianelli, L., Saltuari, L., . . . Nardone, R. (2019). Effects of Repetitive Transcranial Magnetic Stimulation over Prefrontal Cortex on Attention in Psychiatric Disorders: A Systematic Review. *Journal of clinical medicine, 8*(4), 416. doi:10.3390/jcm8040416

Hawi, Z., Straub, R. E., O'Neill, A., Kendler, K. S., Walsh, D., & Gill, M. (1998). No linkage or linkage disequilibrium between brain-derived neurotrophic factor (BDNF) dinucleotide repeat polymorphism and schizophrenia in Irish families. *Psychiatry Research, 81*(2), 111-116. doi:10.1016/s0165-1781(98)00076-6

Himberg, J., Hyvarinen, A., & Esposito, F. (2004). Validating the independent components of neuroimaging time series via clustering and visualization. *Neuroimage, 22*(3), 1214-1222. doi:10.1016/j.neuroimage.2004.03.027

Ho, B. C., Milev, P., O'Leary, D. S., Librant, A., Andreasen, N. C., & Wassink, T. H. (2006). Cognitive and magnetic resonance imaging brain morphometric correlates of brain-derived neurotrophic factor Val66Met gene polymorphism in patients with schizophrenia and healthy volunteers. *Arch Gen Psychiatry, 63*(7), 731-740. doi:10.1001/archpsyc.63.7.731

Hofer, M., Pagliusi, S. R., Hohn, A., Leibrock, J., & Barde, Y. A. (1990). Regional distribution of brain-derived neurotrophic factor mRNA in the adult mouse brain. *EMBO J, 9*(8), 2459-2464. doi:10.1002/j.1460-2075.1990.tb07423.x

Hong, C. J., Liou, Y. J., & Tsai, S. J. (2011). Effects of BDNF polymorphisms on brain function and behavior in health and disease. *Brain Res Bull, 86*(5-6), 287-297. doi:10.1016/j.brainresbull.2011.08.019

Horovitz, S. G., Fukunaga, M., de Zwart, J. A., van Gelderen, P., Fulton, S. C., Balkin, T. J., & Duyn, J. H. (2008). Low frequency BOLD fluctuations during resting wakefulness and light sleep: a simultaneous EEG-fMRI study. *Hum Brain Mapp, 29*(6), 671-682. doi:10.1002/hbm.20428

Hsu, C. W., Wang, L. J., & Lin, P. Y. (2018). Efficacy of repetitive transcranial magnetic stimulation for Tourette syndrome: A systematic review and meta-analysis. *Brain Stimul, 11*(5), 1110-1118. doi:10.1016/j.brs.2018.06.002

Huerta, P. T., & Volpe, B. T. (2009). Transcranial magnetic stimulation, synaptic plasticity and network oscillations. *J Neuroeng Rehabil, 6*(1), 7. doi:10.1186/1743-0003-6-7

Hwang, J. M., Kim, Y. H., Yoon, K. J., Uhm, K. E., & Chang, W. H. (2015). Different responses to facilitatory rTMS according to BDNF genotype. *Clin Neurophysiol, 126*(7), 1348-1353. doi:10.1016/j.clinph.2014.09.028

Iimori, T., Nakajima, S., Miyazaki, T., Tarumi, R., Ogyu, K., Wada, M., . . . Noda, Y. (2019). Effectiveness of the prefrontal repetitive transcranial magnetic stimulation on cognitive profiles in depression, schizophrenia, and Alzheimer's disease: A systematic review. *Prog Neuropsychopharmacol Biol Psychiatry, 88*, 31-40. doi:10.1016/j.pnpbp.2018.06.014

Itoh, K., Hashimoto, K., Kumakiri, C., Shimizu, E., & Iyo, M. (2004). Association between brain-derived neurotrophic factor 196 G/A polymorphism and personality traits in healthy subjects. *Am J Med Genet B Neuropsychiatr Genet, 124B*(1), 61-63. doi:10.1002/ajmg.b.20078

Jafri, M. J., Pearlson, G. D., Stevens, M., & Calhoun, V. D. (2008). A method for functional network connectivity among spatially independent resting-state

components in schizophrenia. *Neuroimage, 39*(4), 1666-1681. doi:10.1016/j.neuroimage.2007.11.001

Jiang, Y., Guo, Z., Xing, G., He, L., Peng, H., Du, F., . . . Mu, Q. (2019). Effects of High-Frequency Transcranial Magnetic Stimulation for Cognitive Deficit in Schizophrenia: A Meta-Analysis. *Frontiers in psychiatry, 10*, 135. doi:10.3389/fpsyt.2019.00135

Jones, K. R., Fariñas, I., Backus, C., & Reichardt, L. F. (1994). Targeted disruption of the BDNF gene perturbs brain and sensory neuron development but not motor neuron development. *Cell, 76*(6), 989-999. doi:10.1016/0092-8674(94)90377-8

Kaiser, R. H., Andrews-Hanna, J. R., Wager, T. D., & Pizzagalli, D. A. (2015). Large-Scale Network Dysfunction in Major Depressive Disorder: A Meta-analysis of Resting-State Functional Connectivity. *JAMA Psychiatry, 72*(6), 603-611. doi:10.1001/jamapsychiatry.2015.0071

Kanazawa, T., Glatt, S. J., Kia-Keating, B., Yoneda, H., & Tsuang, M. T. (2007). Meta-analysis reveals no association of the Val66Met polymorphism of brain-derived neurotrophic factor with either schizophrenia or bipolar disorder. *Psychiatr Genet, 17*(3), 165-170. doi:10.1097/YPG.0b013e32801da2e2

Katoh-Semba, R., Takeuchi, I. K., Semba, R., & Kato, K. (1997). Distribution of brain-derived neurotrophic factor in rats and its changes with development in the brain. *J Neurochem, 69*(1), 34-42. doi:10.1046/j.1471-4159.1997.69010034.x

Kelly, A. M., Uddin, L. Q., Biswal, B. B., Castellanos, F. X., & Milham, M. P. (2008). Competition between functional brain networks mediates behavioral variability. *Neuroimage, 39*(1), 527-537. doi:10.1016/j.neuroimage.2007.08.008

Kennedy, N. I., Lee, W. H., & Frangou, S. (2018). Efficacy of non-invasive brain stimulation on the symptom dimensions of schizophrenia: A meta-analysis of randomized controlled trials. *Eur Psychiatry, 49*, 69-77. doi:10.1016/j.eurpsy.2017.12.025

Kiers, L., Cros, D., Chiappa, K. H., & Fang, J. (1993). Variability of motor potentials evoked by transcranial magnetic stimulation. *Electroencephalogr Clin Neurophysiol, 89*(6), 415-423. doi:10.1016/0168-5597(93)90115-6

Kim, S. W., Lee, J. Y., Kang, H. J., Kim, S. Y., Bae, K. Y., Kim, J. M., . . . Yoon, J. S. (2016). Gender-specific Associations of the Brain-derived Neurotrophic Factor Val66Met Polymorphism with Neurocognitive and Clinical Features in Schizophrenia. *Clin Psychopharmacol Neurosci, 14*(3), 270-278. doi:10.9758/cpn.2016.14.3.270

Kiviniemi, V., Kantola, J. H., Jauhiainen, J., Hyvarinen, A., & Tervonen, O. (2003). Independent component analysis of nondeterministic fMRI signal sources. *Neuroimage, 19*(2 Pt 1), 253-260. doi:10.1016/s1053-8119(03)00097-1

Kiviniemi, V., Starck, T., Remes, J., Long, X., Nikkinen, J., Haapea, M., . . . Tervonen, O. (2009). Functional segmentation of the brain cortex using high model order group PICA. *Hum Brain Mapp, 30*(12), 3865-3886. doi:10.1002/hbm.20813

Kleim, J. A., Chan, S., Pringle, E., Schallert, K., Procaccio, V., Jimenez, R., & Cramer, S. C. (2006). BDNF val66met polymorphism is associated with modified experience-dependent plasticity in human motor cortex. *Nat Neurosci, 9*(6), 735-737. doi:10.1038/nn1699

Korte, M., Carroll, P., Wolf, E., Brem, G., Thoenen, H., & Bonhoeffer, T. (1995). Hippocampal long-term potentiation is impaired in mice lacking brain-derived neurotrophic factor. *Proc Natl Acad Sci U S A, 92*(19), 8856-8860. doi:10.1073/pnas.92.19.8856

Krstic, J., Buzadzic, I., Milanovic, S. D., Ilic, N. V., Pajic, S., & Ilic, T. V. (2014). Low-frequency repetitive transcranial magnetic stimulation in the right prefrontal cortex combined with partial sleep deprivation in treatment-resistant depression: a randomized sham-controlled trial. *J ECT, 30*(4), 325-331. doi:10.1097/YCT.0000000000000099

Kunugi, H., Iijima, Y., Tatsumi, M., Yoshida, M., Hashimoto, R., Kato, T., . . . Yoshikawa, T. (2004). No association between the Val66Met polymorphism of the brain-derived neurotrophic factor gene and bipolar disorder in a Japanese population: a multicenter study. *Biol Psychiatry, 56*(5), 376-378. doi:10.1016/j.biopsych.2004.06.017

Lee, L., Siebner, H., & Bestmann, S. (2006). Rapid modulation of distributed brain activity by Transcranial Magnetic Stimulation of human motor cortex. *Behavioural neurology, 17*(3-4), 135-148. doi:10.1155/2006/287276

Leech, R., Kamourieh, S., Beckmann, C. F., & Sharp, D. J. (2011). Fractionating the default mode network: distinct contributions of the ventral and dorsal posterior cingulate cortex to cognitive control. *J Neurosci, 31*(9), 3217-3224. doi:10.1523/JNEUROSCI.5626-10.2011

Li, C. L., Deng, Y. J., He, Y. H., Zhai, H. C., & Jia, F. C. (2019). The development of brain functional connectivity networks revealed by resting-state functional magnetic resonance imaging. *Neural regeneration research, 14*(8), 1419-1429. doi:10.4103/1673-5374.253526

Li, M., Chang, H., & Xiao, X. (2016). BDNF Val66Met polymorphism and bipolar disorder in European populations: A risk association in case-control, family-based and GWAS studies. *Neurosci Biobehav Rev, 68*, 218-233. doi:10.1016/j.neubiorev.2016.05.031

Li, W., Wang, Y., Ward, B. D., Antuono, P. G., Li, S. J., & Goveas, J. S. (2017). Intrinsic inter-network brain dysfunction correlates with symptom dimensions in late-life depression. *Journal of psychiatric research, 87*, 71-80. doi:10.1016/j.jpsychires.2016.12.011

Li, X., Nahas, Z., Kozel, F. A., Anderson, B., Bohning, D. E., & George, M. S. (2004). Acute left prefrontal transcranial magnetic stimulation in depressed patients is associated with immediately increased activity in prefrontal cortical as well as subcortical regions. *Biol Psychiatry, 55*(9), 882-890. doi:10.1016/j.biopsych.2004.01.017

Li, Y. O., Adali, T., & Calhoun, V. D. (2007). Estimating the number of independent components for functional magnetic resonance imaging data. *Hum Brain Mapp, 28*(11), 1251-1266. doi:10.1002/hbm.20359

Lin, P. H., Tsai, S. J., Huang, C. W., Mu-En, L., Hsu, S. W., Lee, C. C., . . . Chang, C. C. (2016). Dose-dependent genotype effects of BDNF Val66Met polymorphism on default mode network in early stage Alzheimer's disease. *Oncotarget, 7*(34), 54200-54214. doi:10.18632/oncotarget.11027

Lindvall, O., Ernfors, P., Bengzon, J., Kokaia, Z., Smith, M. L., Siesjo, B. K., & Persson, H. (1992). Differential regulation of mRNAs for nerve growth factor, brain-derived neurotrophic factor, and neurotrophin 3 in the adult rat brain following cerebral ischemia and hypoglycemic coma. *Proc Natl Acad Sci U S A, 89*(2), 648-652. doi:10.1073/pnas.89.2.648

Liston, C., Chen, A. C., Zebley, B. D., Drysdale, A. T., Gordon, R., Leuchter, B., . . . Dubin, M. J. (2014). Default mode network mechanisms of transcranial magnetic stimulation in depression. *Biol Psychiatry, 76*(7), 517-526. doi:10.1016/j.biopsych.2014.01.023

Liu, H., Kaneko, Y., Ouyang, X., Li, L., Hao, Y., Chen, E. Y., . . . Liu, Z. (2012). Schizophrenic patients and their unaffected siblings share increased resting-state connectivity in the task-negative network but not its anticorrelated task-positive network. *Schizophr Bull, 38*(2), 285-294. doi:10.1093/schbul/sbq074

Lowe, M. J., Dzemidzic, M., Lurito, J. T., Mathews, V. P., & Phillips, M. D. (2000). Correlations in low-frequency BOLD fluctuations reflect cortico-cortical connections. *Neuroimage, 12*(5), 582-587. doi:10.1006/nimg.2000.0654

Lu, W., Zhang, C., Yi, Z., Li, Z., Wu, Z., & Fang, Y. (2012). Association between BDNF Val66Met polymorphism and cognitive performance in antipsychotic-naive patients with schizophrenia. *J Mol Neurosci, 47*(3), 505-510. doi:10.1007/s12031-012-9750-4

Maisonpierre, P. C., Belluscio, L., Friedman, B., Alderson, R. F., Wiegand, S. J., Furth, M. E., . . . Yancopoulos, G. D. (1990). NT-3, BDNF, and NGF in the developing rat nervous system: Parallel as well as reciprocal patterns of expression. *Neuron, 5*(4), 501-509. doi:10.1016/0896-6273(90)90089-x

Manoliu, A., Meng, C., Brandl, F., Doll, A., Tahmasian, M., Scherr, M., . . . Sorg, C. (2013). Insular dysfunction within the salience network is associated with severity of symptoms and aberrant inter-network connectivity in major depressive disorder. *Front Hum Neurosci, 7*(930), 930. doi:10.3389/fnhum.2013.00930

Manoliu, A., Riedl, V., Zherdin, A., Muhlau, M., Schwerthoffer, D., Scherr, M., . . . Sorg, C. (2014). Aberrant dependence of default mode/central executive network interactions on anterior insular salience network activity in schizophrenia. *Schizophr Bull, 40*(2), 428-437. doi:10.1093/schbul/sbt037

Margraf, J. (1994). Mini-DIPS: Diagnostic short interview on mental disorders. In: Berlin, Germany: Springer.

Martin, D. M., McClintock, S. M., Forster, J. J., Lo, T. Y., & Loo, C. K. (2017). Cognitive enhancing effects of rTMS administered to the prefrontal cortex in patients with depression: A systematic review and meta-analysis of individual task effects. *Depress Anxiety, 34*(11), 1029-1039. doi:10.1002/da.22658

MATLAB 8.0 and Statistics Toolbox 8.1. (2013). Natick, Massachusetts, United States: The MathWorks, Inc.

Mattson, M. P., & Magnus, T. (2006). Ageing and neuronal vulnerability. *Nat Rev Neurosci, 7*(4), 278-294. doi:10.1038/nrn1886

Mayer, J. S., Roebroeck, A., Maurer, K., & Linden, D. E. (2010). Specialization in the default mode: Task-induced brain deactivations dissociate between visual working memory and attention. *Hum Brain Mapp, 31*(1), 126-139. doi:10.1002/hbm.20850

Mazoyer, B., Zago, L., Mellet, E., Bricogne, S., Etard, O., Houde, O., . . . Tzourio-Mazoyer, N. (2001). Cortical networks for working memory and executive functions sustain the conscious resting state in man. *Brain Res Bull, 54*(3), 287-298. doi:10.1016/s0361-9230(00)00437-8

McKiernan, K. A., Kaufman, J. N., Kucera-Thompson, J., & Binder, J. R. (2003). A parametric manipulation of factors affecting task-induced deactivation in functional neuroimaging. *J Cogn Neurosci, 15*(3), 394-408. doi:10.1162/089892903321593117

Menon, V. (2011). Large-scale brain networks and psychopathology: a unifying triple network model. *Trends Cogn Sci, 15*(10), 483-506. doi:10.1016/j.tics.2011.08.003

Menon, V., & Uddin, L. Q. (2010). Saliency, switching, attention and control: a network model of insula function. *Brain Struct Funct, 214*(5-6), 655-667. doi:10.1007/s00429-010-0262-0

Mezquida, G., Penades, R., Cabrera, B., Savulich, G., Lobo, A., Gonzalez-Pinto, A., . . . group, P. E. (2016). Association of the brain-derived neurotrophic factor Val66Met polymorphism with negative symptoms severity, but not cognitive function, in first-episode schizophrenia spectrum disorders. *Eur Psychiatry, 38*, 61-69. doi:10.1016/j.eurpsy.2016.04.011

Morse, J. K., Wiegand, S. J., Anderson, K., You, Y., Cai, N., Carnahan, J., . . . et al. (1993). Brain-derived neurotrophic factor (BDNF) prevents the degeneration of medial septal cholinergic neurons following fimbria transection. *J Neurosci, 13*(10), 4146-4156. doi:10.1523/jneurosci.13-10-04146.1993

Mukherjee, P., Whalley, H. C., McKirdy, J. W., McIntosh, A. M., Johnstone, E. C., Lawrie, S. M., & Hall, J. (2011). Effects of the BDNF Val66Met polymorphism on neural responses to facial emotion. *Psychiatry Res, 191*(3), 182-188. doi:10.1016/j.pscychresns.2010.10.001

Mutz, J., Edgcumbe, D. R., Brunoni, A. R., & Fu, C. H. Y. (2018). Efficacy and acceptability of non-invasive brain stimulation for the treatment of adult unipolar and bipolar depression: A systematic review and meta-analysis of randomised sham-controlled trials. *Neurosci Biobehav Rev, 92*, 291-303. doi:10.1016/j.neubiorev.2018.05.015

Nahas, Z., Lomarev, M., Roberts, D. R., Shastri, A., Lorberbaum, J. P., Teneback, C., . . . Bohning, D. E. (2001). Unilateral left prefrontal transcranial magnetic stimulation (TMS) produces intensity-dependent bilateral effects as measured by interleaved BOLD fMRI. *Biological Psychiatry, 50*(9), 712-720. doi:10.1016/s0006-3223(01)01199-4

Nakata, K., Ujike, H., Sakai, A., Uchida, N., Nomura, A., Imamura, T., . . . Kuroda, S. (2003). Association study of the brain-derived neurotrophic factor (BDNF) gene with bipolar disorder. *Neurosci Lett, 337*(1), 17-20. doi:10.1016/s0304-3940(02)01292-2

Neeper, S. A., Gomez-Pinilla, F., Choi, J., & Cotman, C. (1995). Exercise and brain neurotrophins. *Nature, 373*(6510), 109. doi:10.1038/373109a0

Neves-Pereira, M., Mundo, E., Muglia, P., King, N., Macciardi, F., & Kennedy, J. L. (2002). The brain-derived neurotrophic factor gene confers susceptibility to bipolar disorder: evidence from a family-based association study. *Am J Hum Genet, 71*(3), 651-655. doi:10.1086/342288

Nikolac Perkovic, M., Nedic Erjavec, G., Zivkovic, M., Sagud, M., Uzun, S., Mihaljevic-Peles, A., . . . Pivac, N. (2014). Association between the brain-derived neurotrophic factor Val66Met polymorphism and therapeutic response to olanzapine in schizophrenia patients. *Psychopharmacology (Berl), 231*(18), 3757-3764. doi:10.1007/s00213-014-3515-4

Ohta, M., Nakataki, M., Takeda, T., Numata, S., Tominaga, T., Kameoka, N., . . . Ohmori, T. (2018). Structural equation modeling approach between salience network dysfunction, depressed mood, and subjective quality of life in schizophrenia: an ICA resting-state fMRI study. *Neuropsychiatric disease and treatment, 14*, 1585-1597. doi:10.2147/NDT.S163132

Oldehinkel, M., Mennes, M., Marquand, A., Charman, T., Tillmann, J., Ecker, C., . . . group, E.-A. L. (2019). Altered Connectivity Between Cerebellum, Visual, and Sensory-Motor Networks in Autism Spectrum Disorder: Results from the EU-AIMS Longitudinal European Autism Project. *Biological psychiatry. Cognitive*

neuroscience and neuroimaging, 4(3), 260-270. doi:10.1016/j.bpsc.2018.11.010

Osoegawa, C., Gomes, J. S., Grigolon, R. B., Brietzke, E., Gadelha, A., Lacerda, A. L. T., . . . Trevizol, A. P. (2018). Non-invasive brain stimulation for negative symptoms in schizophrenia: An updated systematic review and meta-analysis. *Schizophr Res, 197*, 34-44. doi:10.1016/j.schres.2018.01.010

Pascual-Leone, A., Gates, J. R., & Dhuna, A. (1991). Induction of speech arrest and counting errors with rapid-rate transcranial magnetic stimulation. *Neurology, 41*(5), 697-702. doi:10.1212/wnl.41.5.697

Pascual-Leone, A., Rubio, B., Pallardo, F., & Catala, M. D. (1996). Rapid-rate transcranial magnetic stimulation of left dorsolateral prefrontal cortex in drug-resistant depression. *Lancet, 348*(9022), 233-237. doi:10.1016/s0140-6736(96)01219-6

Patterson, S. L., Abel, T., Deuel, T. A., Martin, K. C., Rose, J. C., & Kandel, E. R. (1996). Recombinant BDNF rescues deficits in basal synaptic transmission and hippocampal LTP in BDNF knockout mice. *Neuron, 16*(6), 1137-1145. doi:10.1016/s0896-6273(00)80140-3

Patterson, S. L., Grover, L. M., Schwartzkroin, P. A., & Bothwell, M. (1992). Neurotrophin expression in rat hippocampal slices: a stimulus paradigm inducing LTP in CA1 evokes increases in BDNF and NT-3 mRNAs. *Neuron, 9*(6), 1081-1088. doi:10.1016/0896-6273(92)90067-n

Peinemann, A., Reimer, B., Loer, C., Quartarone, A., Munchau, A., Conrad, B., & Siebner, H. R. (2004). Long-lasting increase in corticospinal excitability after 1800 pulses of subthreshold 5 Hz repetitive TMS to the primary motor cortex. *Clin Neurophysiol, 115*(7), 1519-1526. doi:10.1016/j.clinph.2004.02.005

Peltier, S. J., Kerssens, C., Hamann, S. B., Sebel, P. S., Byas-Smith, M., & Hu, X. (2005). Functional connectivity changes with concentration of sevoflurane anesthesia. *NeuroReport, 16*(3), 285-288. doi:10.1097/00001756-200502280-00017

Pezawas, L., Verchinski, B. A., Mattay, V. S., Callicott, J. H., Kolachana, B. S., Straub, R. E., . . . Weinberger, D. R. (2004). The brain-derived neurotrophic factor val66met polymorphism and variation in human cortical morphology. *J Neurosci, 24*(45), 10099-10102. doi:10.1523/JNEUROSCI.2680-04.2004

Philip, N. S., Barredo, J., van 't Wout-Frank, M., Tyrka, A. R., Price, L. H., & Carpenter, L. L. (2018). Network Mechanisms of Clinical Response to Transcranial Magnetic Stimulation in Posttraumatic Stress Disorder and Major Depressive Disorder. *Biol Psychiatry, 83*(3), 263-272. doi:10.1016/j.biopsych.2017.07.021

Piccoli, T., Valente, G., Linden, D. E., Re, M., Esposito, F., Sack, A. T., & Di Salle, F. (2015). The default mode network and the working memory network are not anti-correlated during all phases of a working memory task. *PLoS One, 10*(4), e0123354. doi:10.1371/journal.pone.0123354

Pruunsild, P., Kazantseva, A., Aid, T., Palm, K., & Timmusk, T. (2007). Dissecting the human BDNF locus: bidirectional transcription, complex splicing, and multiple promoters. *Genomics, 90*(3), 397-406. doi:10.1016/j.ygeno.2007.05.004

Raichle, M. E. (1998). Behind the scenes of functional brain imaging: a historical and physiological perspective. *Proc Natl Acad Sci U S A, 95*(3), 765-772. doi:10.1073/pnas.95.3.765

Raichle, M. E., MacLeod, A. M., Snyder, A. Z., Powers, W. J., Gusnard, D. A., & Shulman, G. L. (2001). A default mode of brain function. *Proc Natl Acad Sci U S A, 98*(2), 676-682. doi:10.1073/pnas.98.2.676

Raine, A. (1991). The SPQ: a scale for the assessment of schizotypal personality based on DSM-III-R criteria. *Schizophr Bull, 17*(4), 555-564. doi:10.1093/schbul/17.4.555

Rehn, S., Eslick, G. D., & Brakoulias, V. (2018). A Meta-Analysis of the Effectiveness of Different Cortical Targets Used in Repetitive Transcranial Magnetic Stimulation (rTMS) for the Treatment of Obsessive-Compulsive Disorder (OCD). *Psychiatr Q, 89*(3), 645-665. doi:10.1007/s11126-018-9566-7

Reithler, J., Peters, J. C., & Sack, A. T. (2011). Multimodal transcranial magnetic stimulation: using concurrent neuroimaging to reveal the neural network dynamics of noninvasive brain stimulation. *Prog Neurobiol, 94*(2), 149-165. doi:10.1016/j.pneurobio.2011.04.004

Rizzo, V., Siebner, H. R., Modugno, N., Pesenti, A., Munchau, A., Gerschlager, W., . . . Rothwell, J. C. (2004). Shaping the excitability of human motor cortex with premotor rTMS. *J Physiol, 554*(Pt 2), 483-495. doi:10.1113/jphysiol.2003.048777

Robinson, S., Basso, G., Soldati, N., Sailer, U., Jovicich, J., Bruzzone, L., . . . Moser, E. (2009). A resting state network in the motor control circuit of the basal ganglia. *BMC neuroscience, 10*, 137. doi:10.1186/1471-2202-10-137

Rothwell, J. C., Hallett, M., Berardelli, A., Eisen, A., Rossini, P., & Paulus, W. (1999). Magnetic stimulation: motor evoked potentials. The International Federation of Clinical Neurophysiology. *Electroencephalogr Clin Neurophysiol Suppl, 52*, 97-103. Retrieved from https://www.ncbi.nlm.nih.gov/pubmed/10590980

Rounis, E., Stephan, K. E., Lee, L., Siebner, H. R., Pesenti, A., Friston, K. J., . . . Frackowiak, R. S. (2006). Acute changes in frontoparietal activity after repetitive transcranial magnetic stimulation over the dorsolateral prefrontal cortex in a cued reaction time task. *J Neurosci, 26*(38), 9629-9638. doi:10.1523/JNEUROSCI.2657-06.2006

Rybakowski, J. K., Borkowska, A., Czerski, P. M., Skibinska, M., & Hauser, J. (2003). Polymorphism of the brain-derived neurotrophic factor gene and performance on a cognitive prefrontal test in bipolar patients. *Bipolar Disord, 5*(6), 468-472. doi:10.1046/j.1399-5618.2003.00071.x

Rybakowski, J. K., Borkowska, A., Skibinska, M., & Hauser, J. (2006). Illness-specific association of val66met BDNF polymorphism with performance on Wisconsin Card Sorting Test in bipolar mood disorder. *Mol Psychiatry, 11*(2), 122-124. doi:10.1038/sj.mp.4001765

Rybakowski, J. K., Borkowska, A., Skibinska, M., Szczepankiewicz, A., Kapelski, P., Leszczynska-Rodziewicz, A., . . . Hauser, J. (2006). Prefrontal cognition in schizophrenia and bipolar illness in relation to Val66Met polymorphism of the brain-derived neurotrophic factor gene. *Psychiatry Clin Neurosci, 60*(1), 70-76. doi:10.1111/j.1440-1819.2006.01462.x

Salvador, R., Sarro, S., Gomar, J. J., Ortiz-Gil, J., Vila, F., Capdevila, A., . . . Pomarol-Clotet, E. (2010). Overall brain connectivity maps show cortico-subcortical abnormalities in schizophrenia. *Hum Brain Mapp, 31*(12), 2003-2014. doi:10.1002/hbm.20993

Sanchez, M. M., Das, D., Taylor, J. L., Noda, A., Yesavage, J. A., & Salehi, A. (2011). BDNF polymorphism predicts the rate of decline in skilled task performance and hippocampal volume in healthy individuals. *Transl Psychiatry, 1*, e51. doi:10.1038/tp.2011.47

Sasaki, T., Dai, X. Y., Kuwata, S., Fukuda, R., Kunugi, H., Hattori, M., & Nanko, S. (1997). Brain-derived neurotrophic factor gene and schizophrenia in Japanese

subjects. *Am J Med Genet, 74*(4), 443-444. Retrieved from https://www.ncbi.nlm.nih.gov/pubmed/9259382

Schluter, R. S., Jansen, J. M., van Holst, R. J., van den Brink, W., & Goudriaan, A. E. (2018). Differential Effects of Left and Right Prefrontal High-Frequency Repetitive Transcranial Magnetic Stimulation on Resting-State Functional Magnetic Resonance Imaging in Healthy Individuals. *Brain Connect, 8*(2), 60-67. doi:10.1089/brain.2017.0542

Schweiger, J. I., Bilek, E., Schafer, A., Braun, U., Moessnang, C., Harneit, A., . . . Tost, H. (2019). Effects of BDNF Val(66)Met genotype and schizophrenia familial risk on a neural functional network for cognitive control in humans. *Neuropsychopharmacology, 44*(3), 590-597. doi:10.1038/s41386-018-0248-9

Seeley, W. W., Menon, V., Schatzberg, A. F., Keller, J., Glover, G. H., Kenna, H., . . . Greicius, M. D. (2007). Dissociable intrinsic connectivity networks for salience processing and executive control. *J Neurosci, 27*(9), 2349-2356. doi:10.1523/JNEUROSCI.5587-06.2007

Seminowicz, D. A., de Martino, E., Schabrun, S. M., & Graven-Nielsen, T. (2018). Left dorsolateral prefrontal cortex repetitive transcranial magnetic stimulation reduces the development of long-term muscle pain. *PAIN, 159*(12), 2486-2492. doi:10.1097/j.pain.0000000000001350

Sevinc, G., Gurvit, H., & Spreng, R. N. (2017). Salience network engagement with the detection of morally laden information. *Social cognitive and affective neuroscience, 12*(7), 1118-1127. doi:10.1093/scan/nsx035

Shang, Y., Chang, D., Zhang, J., Peng, W., Song, D., Gao, X., & Wang, Z. (2019). Theta-burst transcranial magnetic stimulation induced functional connectivity changes between dorsolateral prefrontal cortex and default-mode-network. *Brain Imaging Behav*. doi:10.1007/s11682-019-00139-y

Sheline, Y. I., Barch, D. M., Price, J. L., Rundle, M. M., Vaishnavi, S. N., Snyder, A. Z., . . . Raichle, M. E. (2009). The default mode network and self-referential processes in depression. *Proc Natl Acad Sci U S A, 106*(6), 1942-1947. doi:10.1073/pnas.0812686106

Shulman, G. L., Fiez, J. A., Corbetta, M., Buckner, R. L., Miezin, F. M., Raichle, M. E., & Petersen, S. E. (1997). Common Blood Flow Changes across Visual Tasks: II. Decreases in Cerebral Cortex. *J Cogn Neurosci, 9*(5), 648-663. doi:10.1162/jocn.1997.9.5.648

Siskind, D., Honarparvar, F., Hasan, A., Wagner, E., Sinha, S., Orr, S., & Kisely, S. (2019). rTMS for clozapine refractory schizophrenia - A systematic review and pairwise meta-analysis. *Schizophr Res, 211*, 113-114. doi:10.1016/j.schres.2019.07.004

Sklar, P., Gabriel, S. B., McInnis, M. G., Bennett, P., Lim, Y., Tsan, G., . . . Lander, E. S. (2002). Family-based association study of 76 candidate genes in bipolar disorder: BDNF is a potential risk locus. Brain-derived neutrophic factor. *Mol Psychiatry, 7*(6), 579-593. doi:10.1038/sj.mp.4001058

Smith, M. A., Makino, S., Kvetnansky, R., & Post, R. M. (1995). Effects of stress on neurotrophic factor expression in the rat brain. *Ann N Y Acad Sci, 771*(1 Stress), 234-239. doi:10.1111/j.1749-6632.1995.tb44684.x

Smith, S. M., Fox, P. T., Miller, K. L., Glahn, D. C., Fox, P. M., Mackay, C. E., . . . Beckmann, C. F. (2009). Correspondence of the brain's functional architecture during activation and rest. *Proc Natl Acad Sci U S A, 106*(31), 13040-13045. doi:10.1073/pnas.0905267106

Smith, S. M., Miller, K. L., Moeller, S., Xu, J., Auerbach, E. J., Woolrich, M. W., . . . Ugurbil, K. (2012). Temporally-independent functional modes of spontaneous

brain activity. *Proc Natl Acad Sci U S A, 109*(8), 3131-3136. doi:10.1073/pnas.1121329109

Song, S., Zilverstand, A., Gui, W., Li, H. J., & Zhou, X. (2019). Effects of single-session versus multi-session non-invasive brain stimulation on craving and consumption in individuals with drug addiction, eating disorders or obesity: A meta-analysis. *Brain Stimul, 12*(3), 606-618. doi:10.1016/j.brs.2018.12.975

Soppet, D., Escandon, E., Maragos, J., Middlemas, D. S., Reid, S. W., Blair, J., . . . Parada, L. F. (1991). The neurotrophic factors brain-derived neurotrophic factor and neurotrophin-3 are ligands for the trkB tyrosine kinase receptor. *Cell, 65*(5), 895-903. doi:10.1016/0092-8674(91)90396-g

Squinto, S. P., Stitt, T. N., Aldrich, T. H., Davis, S., Blanco, S. M., RadzieJewski, C., . . . Yancopoulos, G. D. (1991). trkB encodes a functional receptor for brain-derived neurotrophic factor and neurotrophin-3 but not nerve growth factor. *Cell, 65*(5), 885-893. doi:10.1016/0092-8674(91)90395-f

Sridharan, D., Levitin, D. J., & Menon, V. (2008). A critical role for the right fronto-insular cortex in switching between central-executive and default-mode networks. *Proc Natl Acad Sci U S A, 105*(34), 12569-12574. doi:10.1073/pnas.0800005105

Supekar, K., Musen, M., & Menon, V. (2009). Development of large-scale functional brain networks in children. *PLoS Biol, 7*(7), e1000157. doi:10.1371/journal.pbio.1000157

Supekar, K., Uddin, L. Q., Prater, K., Amin, H., Greicius, M. D., & Menon, V. (2010). Development of functional and structural connectivity within the default mode network in young children. *Neuroimage, 52*(1), 290-301. doi:10.1016/j.neuroimage.2010.04.009

Thomason, M. E., Yoo, D. J., Glover, G. H., & Gotlib, I. H. (2009). BDNF genotype modulates resting functional connectivity in children. *Front Hum Neurosci, 3*, 55. doi:10.3389/neuro.09.055.2009

Tik, M., Hoffmann, A., Sladky, R., Tomova, L., Hummer, A., Navarro de Lara, L., . . . Windischberger, C. (2017). Towards understanding rTMS mechanism of action: Stimulation of the DLPFC causes network-specific increase in functional connectivity. *Neuroimage, 162*, 289-296. doi:10.1016/j.neuroimage.2017.09.022

Tost, H., Alam, T., Geramita, M., Rebsch, C., Kolachana, B., Dickinson, D., . . . Marenco, S. (2013). Effects of the BDNF Val66Met polymorphism on white matter microstructure in healthy adults. *Neuropsychopharmacology, 38*(3), 525-532. doi:10.1038/npp.2012.214

TReNDS. (2019). TReNDS Center for Translational Research in Neuroimaging and Data Science. Retrieved from http://trendscenter.org/wp/wp-content/uploads/2019/06/RSN_HC_unthresholded_tmaps.zip

Tu, P. C., Lee, Y. C., Chen, Y. S., Li, C. T., & Su, T. P. (2013). Schizophrenia and the brain's control network: aberrant within- and between-network connectivity of the frontoparietal network in schizophrenia. *Schizophr Res, 147*(2-3), 339-347. doi:10.1016/j.schres.2013.04.011

van der Werf, Y. D., Sanz-Arigita, E. J., Menning, S., & van den Heuvel, O. A. (2010). Modulating spontaneous brain activity using repetitive transcranial magnetic stimulation. *BMC neuroscience, 11*, 145. doi:10.1186/1471-2202-11-145

Ventriglia, M., Bocchio Chiavetto, L., Benussi, L., Binetti, G., Zanetti, O., Riva, M. A., & Gennarelli, M. (2002). Association between the BDNF 196 A/G polymorphism and sporadic Alzheimer's disease. *Mol Psychiatry, 7*(2), 136-137. doi:10.1038/sj.mp.4000952

Verhagen, M., van der Meij, A., van Deurzen, P. A., Janzing, J. G., Arias-Vasquez, A., Buitelaar, J. K., & Franke, B. (2010). Meta-analysis of the BDNF Val66Met polymorphism in major depressive disorder: effects of gender and ethnicity. *Mol Psychiatry, 15*(3), 260-271. doi:10.1038/mp.2008.109

Vincent, J. L., Patel, G. H., Fox, M. D., Snyder, A. Z., Baker, J. T., Van Essen, D. C., . . . Raichle, M. E. (2007). Intrinsic functional architecture in the anaesthetized monkey brain. *Nature, 447*(7140), 83-86. doi:10.1038/nature05758

Vyas, N. S., & Puri, B. K. (2012). Evidence for an association between brain-derived neurotrophic factor Val66Met gene polymorphism and general intellectual ability in early-onset schizophrenia. *The Israel journal of psychiatry and related sciences, 49*(2), 137-142.

Wagner, E., Wobrock, T., Kunze, B., Langguth, B., Landgrebe, M., Eichhammer, P., . . . Hasan, A. (2019). Efficacy of high-frequency repetitive transcranial magnetic stimulation in schizophrenia patients with treatment-resistant negative symptoms treated with clozapine. *Schizophr Res, 208*, 370-376. doi:10.1016/j.schres.2019.01.021

Wang, C., Zhang, Y., Liu, B., Long, H., Yu, C., & Jiang, T. (2014). Dosage effects of BDNF Val66Met polymorphism on cortical surface area and functional connectivity. *J Neurosci, 34*(7), 2645-2651. doi:10.1523/JNEUROSCI.3501-13.2014

Wang, H., Wang, X., & Scheich, H. (1996). LTD and LTP induced by transcranial magnetic stimulation in auditory cortex. *NeuroReport, 7*(2), 521-525. doi:10.1097/00001756-199601310-00035

Wang, Z., Li, Z., Gao, K., & Fang, Y. (2014). Association between brain-derived neurotrophic factor genetic polymorphism Val66Met and susceptibility to bipolar disorder: a meta-analysis. *BMC Psychiatry, 14*, 366. doi:10.1186/s12888-014-0366-9

Wassermann, E. M. (1998). Risk and safety of repetitive transcranial magnetic stimulation: report and suggested guidelines from the International Workshop on the Safety of Repetitive Transcranial Magnetic Stimulation, June 5-7, 1996. *Electroencephalogr Clin Neurophysiol, 108*(1), 1-16. doi:10.1016/s0168-5597(97)00096-8

Watanabe, T., Hanajima, R., Shirota, Y., Ohminami, S., Tsutsumi, R., Terao, Y., . . . Ohtomo, K. (2014). Bidirectional effects on interhemispheric resting-state functional connectivity induced by excitatory and inhibitory repetitive transcranial magnetic stimulation. *Hum Brain Mapp, 35*(5), 1896-1905. doi:10.1002/hbm.22300

Webster, M. J., Herman, M. M., Kleinman, J. E., & Shannon Weickert, C. (2006). BDNF and trkB mRNA expression in the hippocampus and temporal cortex during the human lifespan. *Gene Expr Patterns, 6*(8), 941-951. doi:10.1016/j.modgep.2006.03.009

Webster, M. J., Weickert, C. S., Herman, M. M., & Kleinman, J. E. (2002). BDNF mRNA expression during postnatal development, maturation and aging of the human prefrontal cortex. *Brain Res Dev Brain Res, 139*(2), 139-150. doi:10.1016/s0165-3806(02)00540-0

Weiß, R. H. (2008). *Grundintelligenztest Skala 2: CFT 20-R, Revision*: Hogrefe.

Weissman-Fogel, I., Moayedi, M., Taylor, K. S., Pope, G., & Davis, K. D. (2010). Cognitive and default-mode resting state networks: do male and female brains "rest" differently? *Hum Brain Mapp, 31*(11), 1713-1726. doi:10.1002/hbm.20968

White, T. P., Gilleen, J., & Shergill, S. S. (2013). Dysregulated but not decreased salience network activity in schizophrenia. *Front Hum Neurosci, 7*, 65. doi:10.3389/fnhum.2013.00065

White, T. P., Jansen, M., Doege, K., Mullinger, K. J., Park, S. B., Liddle, E. B., . . . Liddle, P. F. (2013). Theta power during encoding predicts subsequent-memory performance and default mode network deactivation. *Hum Brain Mapp, 34*(11), 2929-2943. doi:10.1002/hbm.22114

Whitfield-Gabrieli, S., Thermenos, H. W., Milanovic, S., Tsuang, M. T., Faraone, S. V., McCarley, R. W., . . . Seidman, L. J. (2009). Hyperactivity and hyperconnectivity of the default network in schizophrenia and in first-degree relatives of persons with schizophrenia. *Proc Natl Acad Sci U S A, 106*(4), 1279-1284. doi:10.1073/pnas.0809141106

Yin, Y., Hou, Z., Wang, X., Sui, Y., & Yuan, Y. (2015). The BDNF Val66Met polymorphism, resting-state hippocampal functional connectivity and cognitive deficits in acute late-onset depression. *J Affect Disord, 183*, 22-30. doi:10.1016/j.jad.2015.04.050

Zhang, J. P., Lencz, T., Geisler, S., DeRosse, P., Bromet, E. J., & Malhotra, A. K. (2013). Genetic variation in BDNF is associated with antipsychotic treatment resistance in patients with schizophrenia. *Schizophr Res, 146*(1-3), 285-288. doi:10.1016/j.schres.2013.01.020

Zhang, R., & Volkow, N. D. (2019). Brain default-mode network dysfunction in addiction. *Neuroimage, 200*, 313-331. doi:10.1016/j.neuroimage.2019.06.036

Zhang, X. Y., Chen, D. C., Xiu, M. H., Haile, C. N., Luo, X., Xu, K., . . . Kosten, T. R. (2012). Cognitive and serum BDNF correlates of BDNF Val66Met gene polymorphism in patients with schizophrenia and normal controls. *Hum Genet, 131*(7), 1187-1195. doi:10.1007/s00439-012-1150-x

Zhao, Y. J., Tor, P. C., Khoo, A. L., Teng, M., Lim, B. P., & Mok, Y. M. (2018). Cost-Effectiveness Modeling of Repetitive Transcranial Magnetic Stimulation Compared to Electroconvulsive Therapy for Treatment-Resistant Depression in Singapore. *Neuromodulation, 21*(4), 376-382. doi:10.1111/ner.12723

Zhou, Y., Liang, M., Tian, L., Wang, K., Hao, Y., Liu, H., . . . Jiang, T. (2007). Functional disintegration in paranoid schizophrenia using resting-state fMRI. *Schizophr Res, 97*(1-3), 194-205. doi:10.1016/j.schres.2007.05.029

Zhu, X., Wang, X., Xiao, J., Liao, J., Zhong, M., Wang, W., & Yao, S. (2012). Evidence of a dissociation pattern in resting-state default mode network connectivity in first-episode, treatment-naive major depression patients. *Biol Psychiatry, 71*(7), 611-617. doi:10.1016/j.biopsych.2011.10.035

Ziemann, U., Lonnecker, S., Steinhoff, B. J., & Paulus, W. (1996). Effects of antiepileptic drugs on motor cortex excitability in humans: a transcranial magnetic stimulation study. *Ann Neurol, 40*(3), 367-378. doi:10.1002/ana.410400306

Zuo, N., Salami, A., Yang, Y., Yang, Z., Sui, J., & Jiang, T. (2019). Activation-based association profiles differentiate network roles across cognitive loads. *Hum Brain Mapp, 40*(9), 2800-2812. doi:10.1002/hbm.24561

7. APPENDIX

Figure 1: **Scatter plot of low-frequency (LF) to high-frequency (HF) power ratio versus dynamic range (arbitrary units) for all independent components**. Independent components selected to represent the default-mode network (DMN), executive control network (ECN) and salience network (SLN) are highlighted in green, other resting-state networks are highlighted in yellow. Independent components that failed quality control criteria of power ratio <4 or dynamic range <0.025 are highlighted in red.

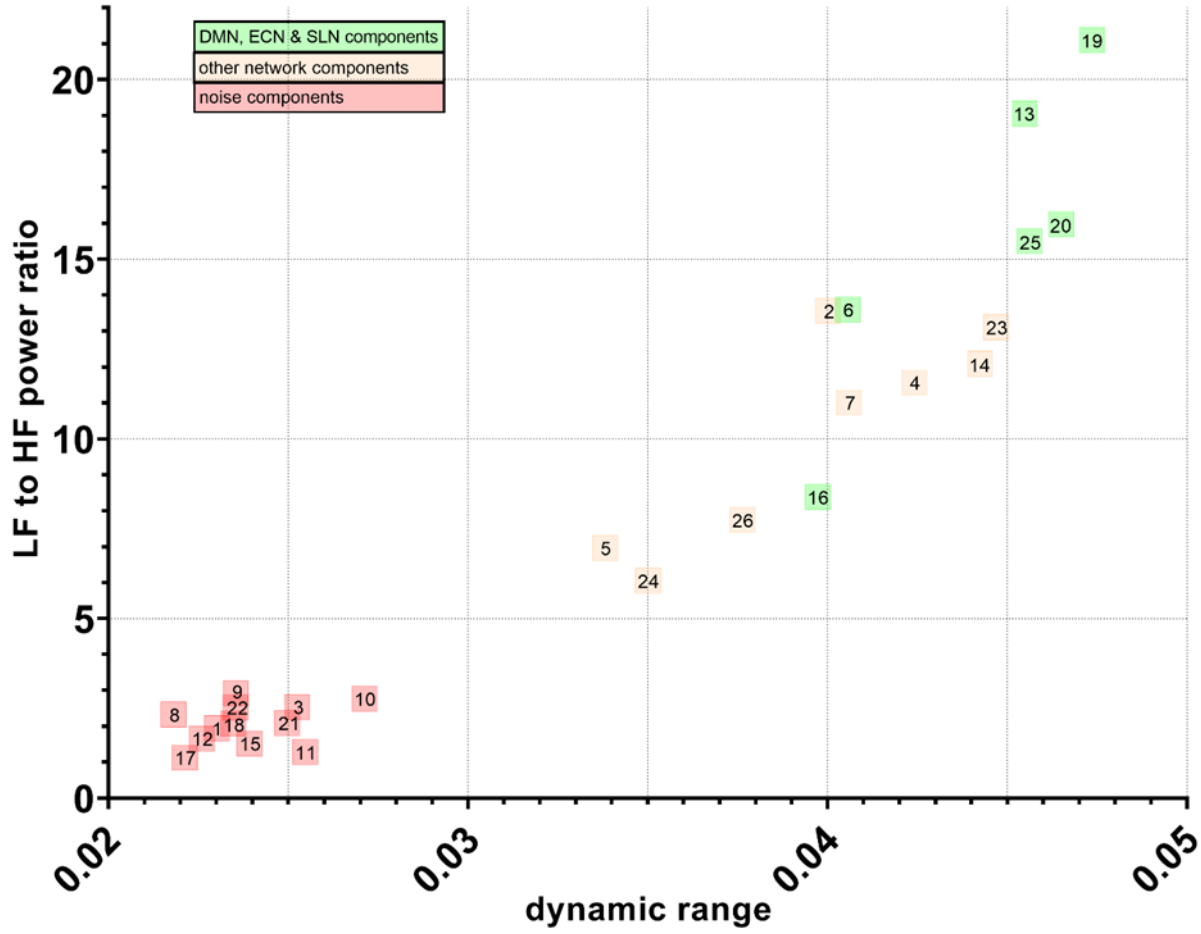

Table 7: **Mean and standard deviation (SD) of Pearson correlation coefficients across all 67 subjects for the sham stimulation and rTMS conditions and the BDNF val^{66}met genotype.** Abbreviations: SD, standard deviation; spDMN, superior posterior default-mode network; ipDMN, inferior posterior default-mode network; aDMN, anterior default-mode network; lECN, left executive control network; rECN, right executive control network; SLN, salience network.

Network pair	**sham stimulation**			
	val^{66} homozygotes		met^{66} carriers	
	Mean	SD	Mean	SD
spDMN/ipDMN	0.349	0.189	0.328	0.144
spDMN/aDMN	0.335	0.175	0.295	0.157
spDMN/lECN	0.161	0.188	0.120	0.215
spDMN/rECN	0.206	0.229	0.232	0.137
spDMN/SLN	0.001	0.220	0.033	0.247
ipDMN/aDMN	0.211	0.160	0.140	0.197
ipDMN/lECN	0.023	0.178	0.026	0.193
ipDMN/rECN	0.014	0.209	-0.007	0.174
ipDMN/SLN	-0.066	0.240	-0.097	0.214
aDMN/lECN	0.219	0.231	0.213	0.184
aDMN/rECN	0.060	0.245	0.053	0.205
aDMN/SLN	-0.265	0.278	-0.272	0.199
lECN/rECN	0.353	0.183	0.313	0.212
lECN/SLN	-0.175	0.184	-0.147	0.199
rECN/SLN	0.104	0.190	0.116	0.240
Network pair	**rTMS**			
	val^{66} homozygotes		met^{66} carriers	
	Mean	SD	Mean	SD
spDMN/ipDMN	0.340	0.179	0.374	0.197
spDMN/aDMN	0.324	0.178	0.328	0.143
spDMN/lECN	0.135	0.198	0.244	0.238
spDMN/rECN	0.192	0.167	0.230	0.191
spDMN/SLN	0.022	0.262	0.031	0.184
ipDMN/aDMN	0.153	0.159	0.133	0.147
ipDMN/lECN	0.044	0.193	0.123	0.190
ipDMN/rECN	-0.004	0.173	-0.033	0.233
ipDMN/SLN	-0.091	0.223	-0.079	0.220
aDMN/lECN	0.218	0.213	0.300	0.192
aDMN/rECN	0.080	0.198	0.093	0.191
aDMN/SLN	-0.182	0.281	-0.211	0.200
lECN/rECN	0.372	0.161	0.392	0.142
lECN/SLN	-0.210	0.206	-0.169	0.181
rECN/SLN	0.071	0.190	0.115	0.199

Table 8: **Interaction effects and associated errors for all network pairs for all subjects, for the stimulation condition (sham vs. rTMS) and genotype group (val^{66}val homozygotes vs. met^{66}-carriers).** Abbreviations: spDMN, superior posterior default-mode network; ipDMN, inferior posterior DMN; aDMN, anterior default-mode network; lECN, left executive control network; rECN, right executive control network; SLN, salience network.

Effect of stimulation condition by genotype group interaction

Network pair	Type III Sum of Squares	df	Mean Square	F	Sig.	partial η²
spDMN/ipDMN	0.043	1	0.043	1.932	0.169	0.029
spDMN/aDMN	0.020	1	0.020	1.018	0.317	0.015
spDMN/lECN	0.214	1	0.214	9.331	0.003	0.126
spDMN/rECN	0.004	1	0.004	0.111	0.741	0.002
spDMN/SLN	0.004	1	0.004	0.137	0.712	0.002
ipDMN/aDMN	0.022	1	0.022	1.261	0.266	0.019
ipDMN/lECN	0.046	1	0.046	1.846	0.179	0.028
ipDMN/rECN	0.000	1	0.000	0.012	0.915	0.000
ipDMN/SLN	0.016	1	0.016	0.406	0.526	0.006
aDMN/lECN	0.074	1	0.074	2.271	0.137	0.034
aDMN/rECN	0.003	1	0.003	0.095	0.759	0.001
aDMN/SLN	0.004	1	0.004	0.148	0.701	0.002
lECN/rECN	0.029	1	0.029	0.918	0.342	0.014
lECN/SLN	0.002	1	0.002	0.042	0.838	0.001
rECN/SLN	0.007	1	0.007	0.209	0.649	0.003

Error for stimulation condition

Network pair	Type III Sum of Squares	df	Mean Square
spDMN/ipDMN	1.460	65	0.022
spDMN/aDMN	1.274	65	0.020
spDMN/lECN	1.488	65	0.023
spDMN/rECN	2.287	65	0.035
spDMN/SLN	1.808	65	0.028
ipDMN/aDMN	1.153	65	0.018
ipDMN/lECN	1.610	65	0.025
ipDMN/rECN	2.302	65	0.035
ipDMN/SLN	2.555	65	0.039
aDMN/lECN	2.106	65	0.032
aDMN/rECN	2.028	65	0.031
aDMN/SLN	1.952	65	0.030
lECN/rECN	2.040	65	0.031
lECN/SLN	2.545	65	0.039
rECN/SLN	2.203	65	0.034

Table 9: **Main effects for all network pairs for all subjects, for the stimulation condition (sham vs. rTMS) and for the genotype group (val^{66}val homozygotes vs. met^{66}-carriers).** Abbreviations: spDMN, superior posterior default-mode network; ipDMN, inferior posterior default-mode network; aDMN, anterior default-mode network; lECN, left executive control network; rECN, right executive control network; SLN, salience network.

Main effect of stimulation condition

Network pair	Type III Sum of Squares	df	Mean Square	F	Sig.	partial η²
spDMN/ipDMN	0.017	1	0.017	0.763	0.385	0.012
spDMN/aDMN	0.004	1	0.004	0.217	0.643	0.003
spDMN/lECN	0.097	1	0.097	4.232	0.044	0.061
spDMN/rECN	0.004	1	0.004	0.106	0.746	0.002
spDMN/SLN	0.003	1	0.003	0.096	0.758	0.001
ipDMN/aDMN	0.042	1	0.042	2.342	0.131	0.035
ipDMN/lECN	0.122	1	0.122	4.929	0.030	0.070
ipDMN/rECN	0.017	1	0.017	0.483	0.490	0.007
ipDMN/SLN	0.001	1	0.001	0.015	0.903	0.000
aDMN/lECN	0.068	1	0.068	2.103	0.152	0.031
aDMN/rECN	0.029	1	0.029	0.945	0.335	0.014
aDMN/SLN	0.213	1	0.213	7.104	0.010	0.099
lECN/rECN	0.079	1	0.079	2.524	0.117	0.037
lECN/SLN	0.027	1	0.027	0.700	0.406	0.011
rECN/SLN	0.010	1	0.010	0.294	0.589	0.005

Main effect of genotype group

Network pair	Type III Sum of Squares	df	Mean Square	F	Sig.	partial η²
spDMN/ipDMN	0.001	1	0.001	0.017	0.895	0.000
spDMN/aDMN	0.018	1	0.018	0.341	0.561	0.005
spDMN/lECN	0.056	1	0.056	0.742	0.392	0.011
spDMN/rECN	0.032	1	0.032	0.655	0.421	0.010
spDMN/SLN	0.014	1	0.014	0.149	0.701	0.002
ipDMN/aDMN	0.073	1	0.073	1.675	0.200	0.025
ipDMN/lECN	0.059	1	0.059	1.147	0.288	0.017
ipDMN/rECN	0.021	1	0.021	0.423	0.518	0.006
ipDMN/SLN	0.005	1	0.005	0.070	0.793	0.001
aDMN/lECN	0.046	1	0.046	0.635	0.428	0.010
aDMN/rECN	5.28E-05	1	5.28E-05	0.001	0.978	0.000
aDMN/SLN	0.008	1	0.008	0.063	0.802	0.001
lECN/rECN	0.002	1	0.002	0.029	0.865	0.000
lECN/SLN	0.047	1	0.047	1.044	0.311	0.016
rECN/SLN	0.028	1	0.028	0.485	0.489	0.007

Figure 11: **ipDMN/lECN stimulation condition main effect**

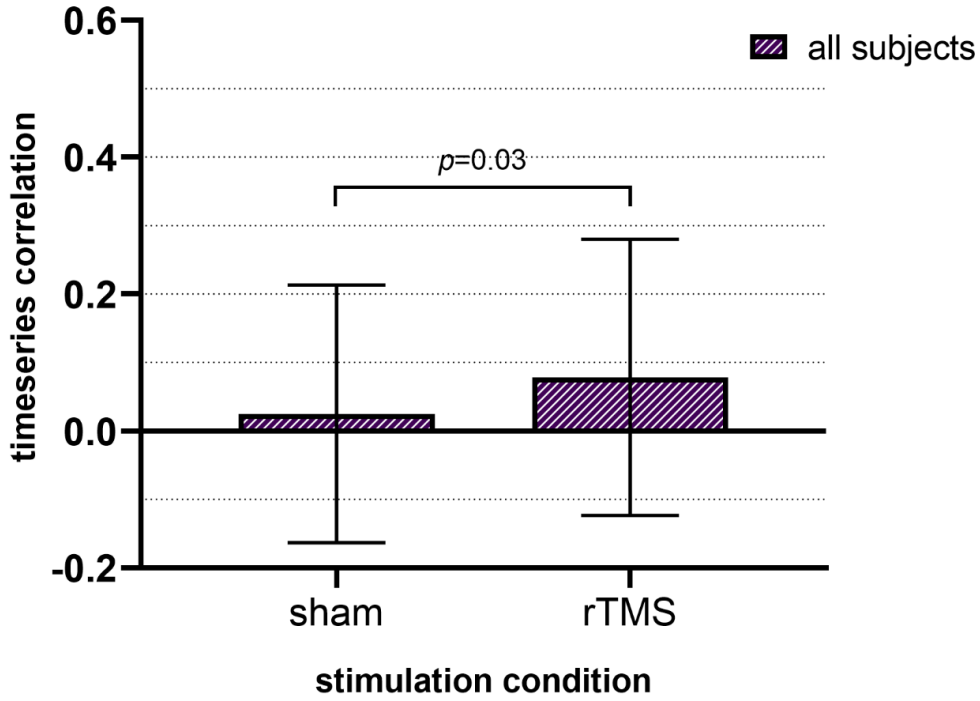

Fig 11: Bar chart of mean ipDMN and lECN time series correlation for the stimulation condition (sham vs. rTMS) across all subjects. Error bars indicate 95% confidence interval. Abbreviations: ipDMN, inferior posterior default-mode network; lECN, left executive control network.

Figure 12: **aDMN/SLN stimulation condition main effect**

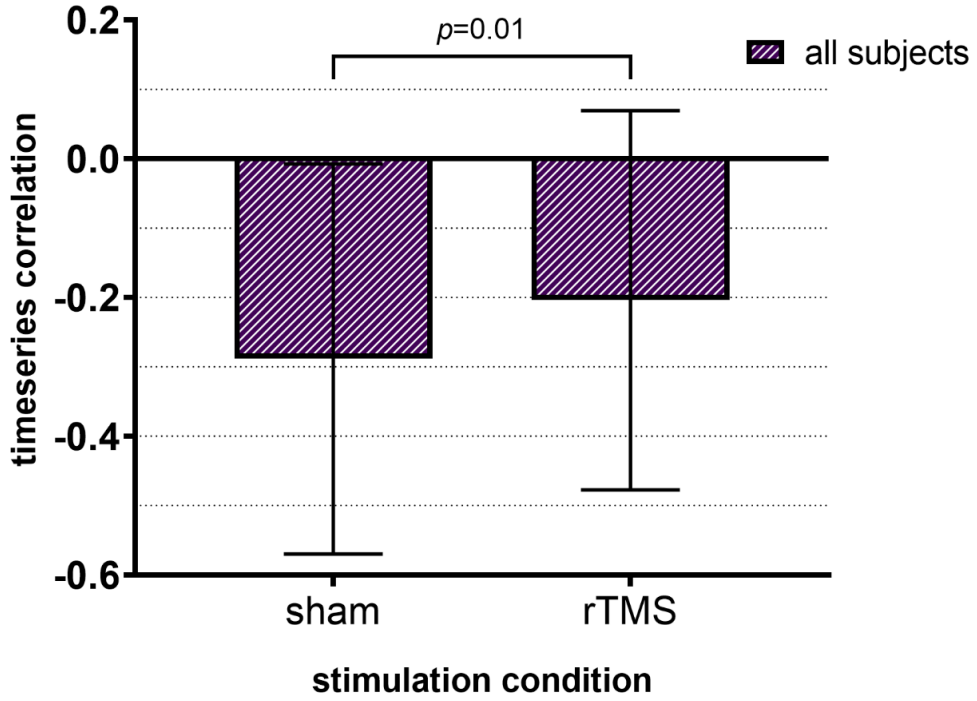

Fig 12: Bar chart of mean aDMN and SLN time series correlation for the stimulation condition (sham vs. rTMS) across all subjects. Error bars indicate 95% confidence interval. Abbreviations: aDMN, anterior default-mode network; SLN, salience network.

8. EIGENANTEIL AN DATENERHEBUNG UND -AUSWERTUNG UND EIGENE VERÖFFENTLICHUNGEN

Diese Arbeit wurde im Rahmen des SFB-Projekts SFB636-B7 durchgeführt. Die rTMS Anwendungen und die anschließenden fMRI Bildgebung wurden zu gleichen Teilen gemeinsam von meiner Co-Doktorandin Frau Schweiger und mir durchgeführt, unterstützt durch eine MTRA und supervidiert durch Hr. Dr. Schäfer aus der Arbeitsgruppe SNiP des ZI Mannheim. Die Auswertung der Daten des resting-state Scans wurde vollständig von mir durchgeführt und ist das zentrale Ergebnis dieser Dissertation. Frau Schweiger führte eine Auswertung der fMRI Daten, die während dem flanker-task Scans erhoben wurden, durch. Ihre Ergebnisse, aus der u.g. Publikation, werden in Kapitel 1.3.5 aufgezeigt, um die Einordnung in den Gesamtkontext zu ermöglichen.

(Teil-)ergebnisse der vorliegenden Arbeit wurden bisher nicht publiziert:

Die Ergebnisse der Auswertung der fMRI Daten aus dem flanker-task wurden von Frau Schweiger in folgender Arbeit publiziert:

> Schweiger, J. I., Bilek, E., Schafer, A., Braun, U., Moessnang, C., Harneit, A., Post, P., Otto, K., Romanczuk-Seiferth, N., Erk, S., Wackerhagen, C., Mattheisen, M., Muhleisen, T. W., Cichon, S., Nothen, M. M., Frank, J., Witt, S. H., Rietschel, M., Heinz, A., Walter, H., Meyer-Lindenberg, A., Tost, H.. (2019). Effects of BDNF Val(66)Met genotype and schizophrenia familial risk on a neural functional network for cognitive control in humans. Neuropsychopharmacology, 44(3), 590-597. doi:10.1038/s41386-018-0248-9

9. CURRICULUM VITAE

Name	Philip Post
Date of birth	03.08.1990
Place of birth	Heidelberg

EDUCATION

2000 – 2006	Moll Gymnasium, Mannheim, Germany
2006 – 2007	Glens Falls High School, Glens Falls, NY, USA
2007 – 2009	Salem International College, Überlingen, Germany
05.07.2009	International Baccalaureate (IB) Diploma (final score: 41)
2009 – 2016	Medical studies Medizinische Fakultät Mannheim der Ruprecht-Karls-Universität Heidelberg, Mannheim, Germany
08.09.2011	Erster Abschnitt der Ärztlichen Prüfung (M1), grade 3.0
09.10.2014	Zweiter Abschnitt der Ärztlichen Prüfung (M2), grade 3.0
08.06.2016	Dritter Abschnitt der Ärztlichen Prüfung (M3), grade 2.0
10.06.2016	Licensure as a physician
2012 – 2016	Studies of Health Economics M.Sc. Medizinische Fakultät Mannheim der Ruprecht-Karls-Universität Heidelberg, Mannheim, Germany
18.04.2016	M.Sc. in Health Economics, grade 1.5 Master thesis: “The effect of G-DRG introduction on length of stay and treatment outcomes for orthopedic joint replacement surgeries.”

PROFESSIONAL CAREER

Since 2016	Assistenzarzt at the department of General Psychiatry at the Central Institute of Mental Health, Mannheim, Germany

10. DANKSAGUNG

Ich danke Herrn Prof. Dr. med. Andreas Meyer-Lindenberg und Frau Prof. Dr. Dr. Heike Tost für die Betreuung dieser Arbeit, sowie für die Bereitstellung des Themas und die Möglichkeiten dieses zu bearbeiten.

Besonderer Dank gilt Dr. Carolin Mößnang für ihre unabdingbare Unterstützung mit methodischem Fachwissen bei der Datenauswertung und die wiederholte Durchsicht der Arbeit. Ich danke Dr. Axel Schäfer für seine umfangreiche Unterstützung bei der Durchführung der Stimulationen und Messungen und bei der Bearbeitung der Bildgebungsdaten.

Ich möchte mich auch ausdrücklich bei den Studienteilnehmern bedanken, ohne deren Bereitschaft die Durchführung dieser Studie nicht möglich gewesen wäre.

Ebenso bedanke ich mich bei meinen Eltern und meinem Bruder, die immer ein offenes Ohr in anstrengenden Phasen meiner Arbeit hatten und mir den Rücken stärkten.
Frau Nora Küppers danke für die Durchsicht meiner Arbeit unter sprachlichen Gesichtspunkten und für die wertvollen Hinweise zur Verbesserung derselben.

Abschließend möchte ich mich von Herzen bei meiner Ehefrau Carina bedanken: Du hast mir mit unseren Töchtern das schönste Geschenk meines Lebens gemacht und mich bei der Fertigstellung dieser Dissertation stets in vollem Maße unterstützt.